Studies on Inorganic Electrochemical Reactions by the Derivative Voltammetry

by

Nobuaki OGAWA

Osaka University

1986

Contents

List of symbols and abbreviations

A	electrode area
a_i	activity of species i
C	differential capacity of the electrical double layer
C_f	equivalent-series-capacitive component of faradaic impedance
C_i	concentration of species i
C^*	initial(bulk) concentration
$E°$	standard redox potential
$E^r_{1/2}$	reversible half-wave potential
$E(t)$	instantaneous applied potential
E_{dc} or E	dc component of potential
ΔE_{ac} or ΔE	amplitude of applied alternating potential
$[E_{dc}]_{max}$	dc potential of maximum cot ϕ
$[E_{dc}]_{peak}$ or E_p	dc potential of maximum alternating current
F	Faraday's constant
f	frequency
f_i	activity coefficient of species i
D_i	diffusion coefficient of species i
I_d or i_d	dc current or dc diffusion current
I_p or i_p	peak faradaic alternating current

$I(\omega t)$	fundamental harmonic faradaic alternating current
$I(n\omega t)$	nth-harmonic faradaic alternating current
$i(t)$	total faradaic current
k	(first-order) chemical reaction rate constant
k_s	heterogeneous rate constant for charge transfer at E°
n	number of electrons transferred in heterogeneous charge transfer step
R	ideal-gas constant
R_f	equivalent-series-resistance component of faradaic impedance
R_Ω or R_s	uncompensated ohmic resistance or solution resistance
T	absolute temparature
t	time
u	auxiliary variable of integration
v	dc potential scan rate
x	distance from electrode surface
Z_f	faradaic impedance(absolute value)
z_i	charge on species i
α	charge-transfer coefficient for reduction
β	charge-transfer coefficient for oxidation ($\alpha + \beta = 1$)
Γ	surface concentration

ψ_i	current relative to applied alternating potential
ϕ_i or ϕ	phase angle of alternating current relative to applied alternating potential
ϕ_2	potential at outer Helmholtz plane relative to potential in bulk solution
ω	angular frequency($\omega = 2\pi f$)
C.E.	counter electrode
CPE	cotrolled potential electrolysis
CV	cyclic voltammetry
DME	dropping mercury electrode
HMDE	hanging mercury drop electrode
R.E.	reference electrode
W.E.	working electrode

Chapter 1. General introduction

Oxidation and reduction of chemical species are utilized very often in the course of the study of the method for the chemical analysis of inorganic materials and the analysis of electron transfer mechanism in the redox systems is one of the major areas in analytical chemistry. Although many brilliant works have been performed to elucidate those mechanism of inorganic species in aqueous media and succeeded, most of multiple steps of oxidation or reduction of a single ion still remained under the controversy. CrO_4^{2-} is one of those ions whose kinetic character in reduction process have not been cleared yet. Various techniques have been introduced to observe kinetically the redox reaction of inorganic ions in aqueous solution.

Voltammetry is the most widely used electrochemical technique for the chemical analysis of inorganic ions in aqueous medium. And the technique is very useful for the determination of micro-amounts of chemical species. One can also get by this method various informations related to the electron transfer between chemical species and the electrode.

Direct current(dc) polarography is one of the oldest and most popular method in voltammetry. One of its major assets is its ability to the simultaneous determinations of various ions at low concentration in liquid medium, while the major limitation of this technique is located to the difficulty in the separation of non-faradaic current, that is a charging current to an electrochemical double layer, from the faradaic current developed by the electrode reaction of chemical species to be interested. This makes rather inadequate to apply dc polarography to the kinetic analysis of multistep electron transfer systems.

Differential pulse(DP) polarography is the modified method of dc polarography and can reduce the charging current in the observed signal. But it is not applicable to the kinetic study of the fast reaction, unfortunately.

Although cyclic voltammetry can control the scanning rate of applied voltage to the electrolytic circuit and is useful to observe the electrode reaction with a large rate constant, it can not distinguish the phase shift of the faradaic and non-faradaic components of current at the onset of the applied voltage.

The differential capacity for investigating on the vicinity of electrode cannot be isolated by those methods above described.

In the mathematical expression, the faradaic

alternating current through the electrochemical cell is developed nonlinearly in the power series[1]. In other words, the equivalent circuit of the cell cannot be expressed by the linear combination of the electric parameters such as a resistance and capacitance. The fundamental harmonic(1f) mode(the current component of the same frequency as the input ac voltage, that is to say, the first developed term of the power series of output ac signal) is, conventionally, called as the ac polarography. In this sence, the ac polarography can be called one of the nonlinear analyses[2-15]. The ac polarography[16-20] is available to the analysis of the comparatively fast electrochemical reaction. The use of the phase selective mode could reduce the charging current, too[16-33]. Unless the reaction is reversible in process, however, the polarogram in the 1f mode is not a real first derivative form of the dc polarogram in the second harmonic(2f) mode (the current component which have twice as high frequency as the input, e.g., the second term of the output power series) is again not the derivative form of 1f mode. However, these modes are the extreme function of the kinetic character of the electrochemical reactions.

Though the phase selective mode may be useful for the electrochemistry, only 1f(0°)(0° means the same phase angle as the input ac voltage) and 2f(90°) have been mainly

utilized for analytical purposes so far, e.g., the quantitative analyses[34-41], studies on kinetics[42-44] and determination of reversible half-wave potentials for organic compounds[45-47]. And the phase angle component other than 1f(0°) and 2f(90°) modes have never been employed. The differential capacity can be also obtained by the use of the phase selective mode. Therefore, the ac polarography could be widely applied to the studies on reaction kinetics and to the chemical analyses.

In the present work, therefore, special instruments designed for the derivative voltmmetry were constructed, and phase angle components of 1f(45°), 1f(90°), 2f(0°) and 2f(45°) in addition to the 1f(0°) and 2f(90°) components to elucidate the kinetic character of CrO_4^{2-}, catalytic reduction of NO_3^- to establish the kinetic electrochemical analysis by means of non-linear methods. And some new applications developed by the phase selective ac polarographic technique were performed.

1-1. Properties of some phase angle components

According to the theoretical analysis, the reversible process is carried out at the phase angle of 45° in 1f mode and in a quasi-reversible or an irreversible process, it changes from 0° to 45° depending on the dc potential and other kinetic parameters such as k_s(heterogeneous rate

constant for charge transfer step) and α(charge transfer coefficient for reduction). When the reaction process is reversible, the current amplitude of 45° component is highest in all phase angle components. Therefore, the 1f(45°) is the highest sensitive component in order to elucidate the rate determining step for the electrochemical reaction including successive multi-step charge transfers.

Since Cakenberghe[53] has tried basically to the second harmonic mode, the 2f mode has come into use for kinetic and analytical applications[25,37-44,47-49,54] and determination of reversible half-wave pootentials for many organic compounds[50-52].

Though all phase angle components in 2f mode are reduced in the charging current as compared with those in 1f mode, only the 2f(90°)(compared with 1f(0°)) has been generally utilized for the analytical purpose. The phase angle for the reversible process, in the 2f mode, is -45° or 135° and that for the quasi-reversible or irreversible process changes from 0° to 360° depending on the dc potential and other kinetic parameters. For example, if the reaction process is reversible, 45° component in 2f mode gives zero in its current amplitude. If the process is quasi-reversible or irreversible, the current amplitude of this component is not zero. From this principle, 2f(45°) can be used for the separation analyses of two species

having similar redox potentials and having different reaction rates with each other.

Except for the faradaic current, the charging current to the electrochemical double layer flows through the electrochemical cell. The differential capacity of the adsorption of chemical species on electrode and for the structure of the vicinity of electrode[55-59]. An ac bridge method can be employed in these purposes, but the technical treatment is troublesome. Therefore, the differential capacity has not been obtained in complicated systems so far. The phase selective ac polarography is a very useful technique for these purposes. The differential capacity is calculated easily from the observed current values of 1f(0°) and 1f(90°) modes. The techniques are applied in the present work, to the analysis for the vicinity of the electrode of zirconium(IV)-nitrate system.

1-2. Utilization of 1f(45°) component for chromium(VI) system

The oxidation and reduction of chemical species have been one of the interesting subjects to the chemist. As the reaction of such a multivalent species involves a multi-step electron transfer process, the understanding of such reaction mechanism is one of the purposes of this research.

A chromium(VI) has been known as one of these elements

[60-68]. The existence of chromium(V)[60,61] and chromium(IV)[62-68] were certified as the reduction products and as the intermediates, respectively. The kinetic mechanism for the reduction of chromium(VI) also changed with the property of reductant employed.

The electrode reduction of chromium(VI) in alkaline solution has also been investigated by the dc polarography and by other electrochemical techniques[69-75], but the rate determining step for total reaction of chromium(VI) to chromium(III) has never been determined and the kinetics has not been investigated quantitatively by those studies. The dc polarogram of this system shows only single reduction wave. However, from the ac polarographic data in the 1f(45°) mode observed in this work, it was clearly shown that the reaction is two step mechanism.

1-3. Application of differential capacity measurement to zirconium(IV)-nitrate ion system

Though the oxidation capacity of nitric acid has been well-known[76,77], the nitrate anion is hardly reduced electrochemically in univalent supporting electrolytes [78,82]. The nitrate ion is, however, reduced at a more positive reduction potential when a multi-valent cation is present than when it is absent[78-82].

The reduction potential of nitrate ion shifts 1.3 V to

the more positive potential in the presence of zirconium(IV) than that in its absence(in the presence of a univalent supporting electrolyte)[83,84]. The kinetic mechanism has not been fully clarified, especially because of the lackin of the data concerning the structure in the vicinity of the electrode. In this work, a role of zirconium(IV) in this system was discussed from the measurement of the differential capacities by using 1f(0°) and 1f(90°) components and from some other electrochemical and spectral

1-4. Application of 2f(45°) and 2f(0°) to chemical analyses

In the chemical analysis, the problem of elimination of interference should be settled in any case.

In electroanalytical methods, it is well known that cadmium(II) usually interferes in the analysis of indium(III)[the half-wave potential($E_{1/2}$) difference is 45 mV], and that nickel(II) also interferes in the analysis of zinc(II)(the $E_{1/2}$ difference is 60 mV). In the present work, the usefullness of the phase selective ac polarogram even in the quantitative analysis was shown again. The quantitative analises of indium(III) and zinc(II) in large excess of cadmium(II) and of nickel(II) solutions respectively, can be performed even without any pretreatments by the phase selective ac polarographic technique.

Consequently, the purpose of this work is to utilize the validity of various phase angle components in the ac polarography: (1) 1f(45°), for analyzing the kinetic mechanism of the Cr(VI)/Cr(III) in alkaline solution; (2) 1f(0°) and 1f(90°), for investigating on the role of zirconium(IV) in the reduction of nitrate ion from the data of the differential capacity obtained from these components and by other electrochemical and spectral techniques; (3) 2f(45°) and 2f(0°), for applying to the chemical analysis of one of two metal ions having similar reduction potentials by considering the difference between reduction mechaniss of these ions.

1-5. References

1 R.H. Muller, R.L. Garman, M.E. Droz and J. Petras, Ind. Eng. Chem., 10(1938)339.

2 C. MacAleavy, Belgian Pat., 443(1941)003.

3 B. Breyer and F. Gutmann, Aust. J. Sci., 8(1945)21.

4 B. Breyer and F. Gutmann, Trans. Faraday Soc., 42(1946)645,650.

5 B. Breyer and F. Gutmann, Trans. Faraday Soc., 43(1947)785.

6 B. Beryer and F. Gutmann, Disc. Faraday Soc., 1(1947)19.

7 D.C. Grahame, J. Am. Chem. Soc., 63(1941)1207.

8 B. Ershler, Disc. Faraday Soc., 1(1947)269.

9 J.E.B. Randles, Disc. Faraday Soc., 1(1947)11,47.

10 P. Delahay, Anal. Chem., 34(1962)1161.

11 M. Senda and I. Tachi, Bull. Chem. Soc. Jpn, 28(1955)632.

12 R. Neeb, Z. Anal. Chem., 188(1962)401.

13 H. Matsuda, Z. Elektrochem., 59(1955)494.

14 H. Matsuda, Z. Elektrochem., 61(1957)489.

15 H.H. Bauer, J. Electroanal. Chem., 1(1960)256.

16 T. Fujinaga and M. Maruyama(Eds.), Polarography Dai-isshu(First Collection for Polarography), Nanko-do, Tokyo, 1962.

17 B. Breyer and H.H. Bauer, Alternating Current

Polarography and Tensammetry, Wiley, New York, 1963.

18 D.E. Smith, in A.J. Bard(Ed.), Electroanalytical Chemistry, Vol. 1, Dekker, New York, 1966, p. 1.

19 B. Breyer, Pure Appl. Chem., 15(1967)313.

20 D.E. Smith, Crit. Rev. Anal. Chem., 2(1971)247.

21 W.L. Underkofler and I. Shain, Anal. Chem., 37(1965)218.

22 D.E. Smith, Anal. Chem., 35(1963)1811.

23 G. Jessop, British Pat., 640,768(1950).

24 G. Jessop, British Pat., 776,543(1957).

25 D.J. Ferrett, G.W.C. Milner, H.I. Shalgosky and L.J. Slee, Analyst, 81(1956)506.

26 L.A. Balchin and D.I. Williams, Analyst, 85(1960)503.

27 J.W. Hayes and H.H. Bauer, J. Electroanal. Chem., 3(1962)336.

28 E. Niki, Rev. Polarogr.(Kyoto), 3(1955)41.

29 E. Niki, Kagaku no Ryoiki, 10(1956)203.

30 E. Niki, Denki Kagaku(J. Electrochemical. Soc. Jpn.), 23(1955)526.

31 T. Takahashi and E. Niki, Talanta, 1(1958)245.

32 D.E. Smith and W.H. Reinmuth, Anal. Chem., 32(1960)1892.

33 H. Blutstein, A.M. Bond and A. Norris, Anal. Chem., 46(1974)1754.

34 R. Neeb, Fresenius' Z. Anal. Chem., 186(1962)53.

35 D. Saur and R. Need, Fresenius' Z. Anal. Chem., 290(1978)220.

36 H.H. Bauer, Aust. J. Chem., 17(1964)715; correction to 17(1964)715.

37 J. Devay, T. Grarai, L. Meszaros and B. Palagri-Fenyes, Hung. Sci. Instrum., 15(1968)1.

38 F. Fajioli, F. Dondi and C. Bighi, Ann. Chim. (Rome), 68(1978)111.

39 S. Fujiwara, M. Hirota, K. Sawatari, Y. Umezawa and H. Kojima, Bull. Chem. Soc. Jpn., 47(1974)499.

40 M. Kasagi and C.V. Banks, Anal. Chim. Acta, 30(1964)248.

41 E. Jacobsen and G. Tandberg, Anal. Chim. Acta, 47(1969)285.

42 T.G. McCord and D.E. Smith, Anal. Chem., 42(1970)126.

43 M. Hirota, Y. Umezawa, H. Kojima and S. Fujiwara, Bull. Chem. Soc. Jpn., 47(1974)2486.

44 M. Hirota, Y. Umezawa and S. Fujiwara, Bull. Chem. Soc. Jpn., 48(1975)1053.

45 A.M. Bond and D.E. Smith, Anal. Chem., 46(1974)1946.

46 R. Breslow and J.L. Grant, J. Am. Chem. Soc., 99(1977)7745.

47 E. Alberg and V.D. Parker, Acta Chem. Scand., B34(1980)91.

48 J. van Cakenberghe, Bull. Soc. Chem. Belges, 60(1951)3.

49 H.H. Bauer and P.J. Elving, Anal. Chem., 30(1958)341.

50 D.C. Grahame, Chem. Rev., 41(1947)441.

51 R. Parsons, in J.O'M. Bockris and B.E. Conway(Eds.),

Modern Aspects of Electrochemistry, Vol. 1, Butterworth, London, 1954.

52 R. Parsons, in P. Delahay(Ed.), Advances in Electrochemistry and Electrochemical Engineering, Vol. 1, Interscience, New York, 1961, p. 1.

53 P. Delahay, Double Layer and Electrode Kinetics, Interscience, New York, 1965.

54 E. Laviron, in A.J. Bard(Ed.), Electroanalytical Chemistry, Vol. 12, Dekker, New York, 1982, p. 53.

55 M. Krumpolc and J. Rocek, J. Am. Chem. Soc., 101(1979)3206.

56 N. Matsuura and M. Nishikawa, Inorganic Chemistry, II, Morikita Book Co., Tokyo, 1973, p. 147.

57 K. Yamamoto and K. Ohashi, Bull. Chem. Soc. Jpn., 49(1976)2433.

58 M.T. Beck and D.A. Durham, J. Inorg. Nucl. Chem., 32(1970)1971.

59 J. Rocek and A.E. Radkowsky, J. Am. Chem. Soc., 90(1968)2896; 95(1973)7123.

60 K.B. Wiberg and S.K. Mukherjee, J. Am. Chem. Soc., 93(1973)2543.

61 P.M. Nave and W.S. Trahanovsky, J. Am. Chem. Soc., 92(1970)1120.

62 M. Rahman and J. Rocek, J. Am. Chem. Soc., 93(1971)5455, 5462.

63 M. Doyle, R.J. Swedo and J. Rocek, J. Am. Chem. Soc., 95(1973)8352.

64 J.J. Lingane and I.M. Kolthoff, J. Am. Chem. Soc., 62(1940)852.

65 J.J. Tondeur, A. Dombret and L. Gierst, J. Electroanal. Chem., 3(1962)225.

66 I.R. Miller, J. Electroanal. Chem., 15(1967)49.

67 T. Berzins and P. Delahay, J. Am. Chem. Soc., 75(1953)5716.

68 P. Delahay and C.C. Mattax, J. Am. Chem. Soc., 76(1954)874.

69 A. Saito, Nippon Kagaku Zasshi, 82(1961)718.

70 P.F. Urone, M.L. Drushel and H.K. Anders, Anal. Chem., 22(1950)472.

71 D.M. Yost and H. Russell, Jr., Systematic Inorganic Chemistry of the Fifth-and-Sixth-Group Nonmetallic Elements, Prentice-Hall, New York, 1944.

72 K. Sone, Sanka to Kangen(Oxidation and Reduction)(in Japanese), Baifu-kan, Tokyo, 1978, p. 85.

73 M. Tokuda, Collect. Czech. Chem. Commun., 4(1932)444.

74 J.W. Collat and J.J. Lingane, J. Am. Chem. Soc., 76(1954)4214.

75 M. Tokuda and J. Ruzicka, Collect. Czeck. Chem. Commun., 6(1934)339.

76 L. Holleck, Z. Physik. Chem(Leipzig)., 194(1944)140.

77 I.M. Kolthoff and J.J. Lingane, Polarography, 2nd. Ed., Interscience Publishers, New York, 1952, p. 533.

78 Ph. Mechelynck and C. Mechelynck-David, Anal. Chim. Acta, 21(1959)432.

79 H.W. Wharton, J. Electroanal. Chem., 9(1965)134.

Chapter 2. Experimental and theory

2-1. Experimental device

A block diagram of the experimental device for the dc and phase-selective ac polarographies used in this work, is given in Fig. 2-1. A hand-made function generator produces a dc lamp wave(sawtooth or triangular). An oscillator (Kikusui Electronics Corp., RC Oscillator Model 4045) was used as a generator of sine wave ac voltage. The dc lamp wave(typically 1 mVs^{-1}) and the sine wave are fed to a hand-made potentiostat. This potentiostat has a positive feedback for iR compensation circuit(Fig. 2-2)[1,2]. All amplifiers used for its construction were of Burr-Brown 3507J (fast slewing OP AMP). The fundamental and second harmonic alternating currents were detected by employing a lock-in amplifier(NF Circuit Design Block Co., Model LI 507). The ac polarogram was recorded by using an X-Y recorder (Yokogawa Type 3086).

The iR compensation at the potential where the faradaic alternating current was not detected, was attained by adjusting the variable resistance of the compensator(R3

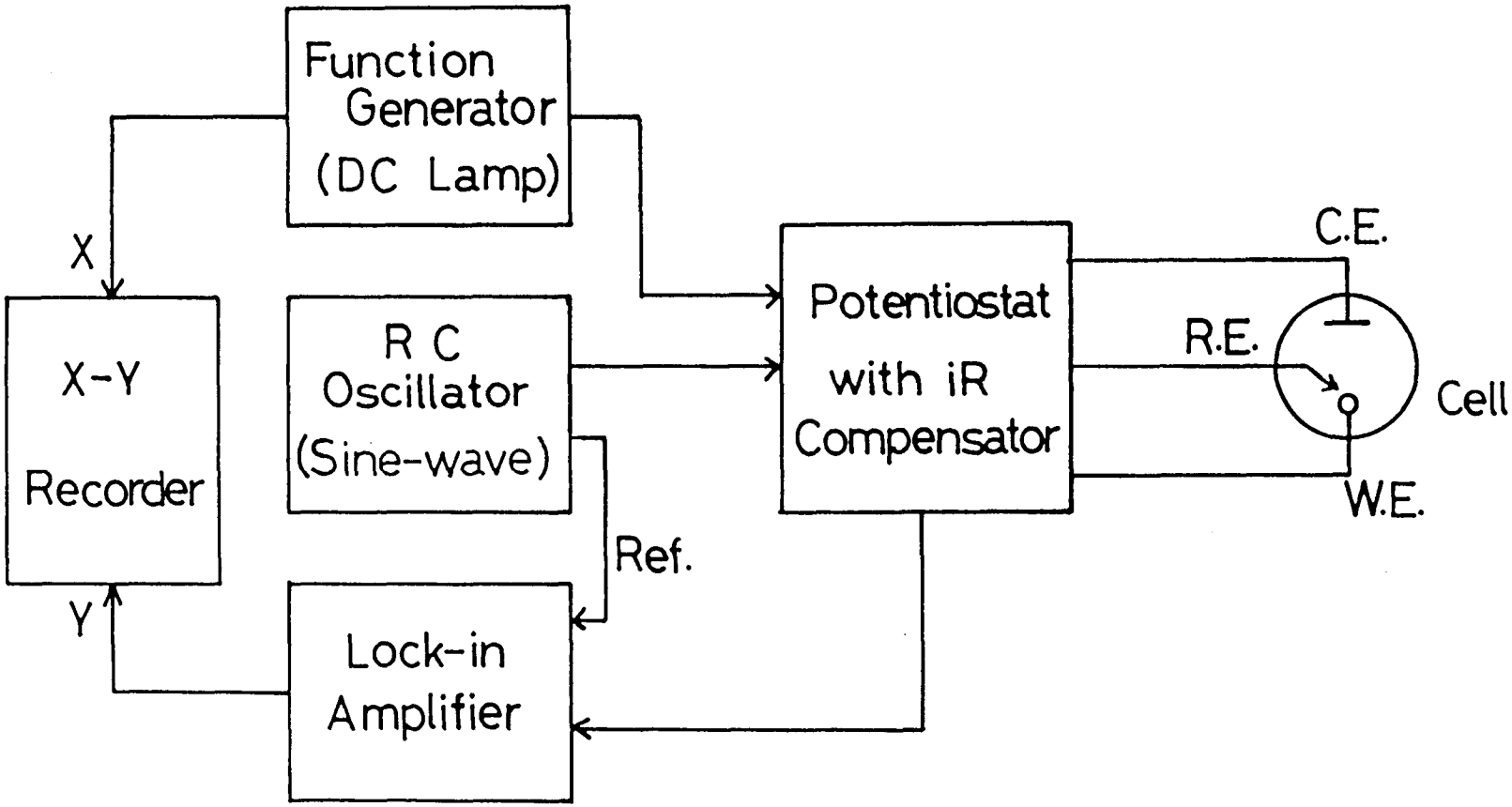

Fig. 2-1. Block diagram of experimental device for the phase-selective ac polarography.

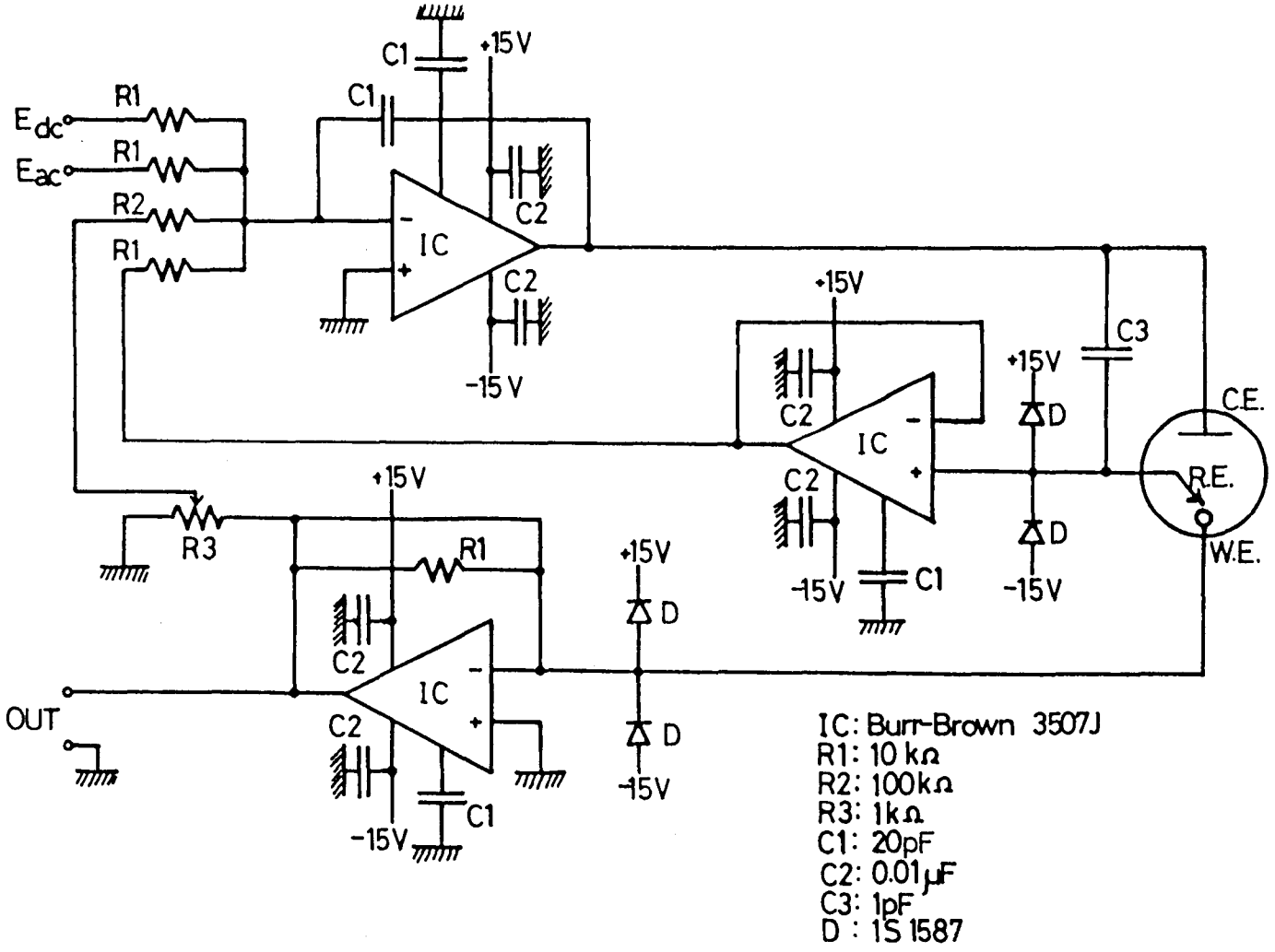

Fig. 2-2. The circuit diagram of the potentiostat with positive feedback iR compensation.

voltage(E_{ac}) is given by the equation: $E_{ac} = \Delta E_{ac} \cos \omega t$, and i_{ac} can be expressed as:

$$i_{ac} = a_1 \Delta E_{ac} \cos \omega t + a_2 \Delta E_{ac}^2 \cos^2 \omega t + a_3 \Delta E_{ac}^3 \cos^3 \omega t + \text{--------}. \quad (2\text{-}2)$$

And using the relations: $\cos^2 x = (1 + \cos 2x)/2$, $\cos^3 x = (3\cos x + \cos 3x)/4$, $\cos^4 x = (3 + 4\cos 2x + \cos 4x)/8$, -----, Eq. (2-2) can be rewritten:

$$i_{ac} = [(a_2/2)\Delta E_{ac}^2 + (3a_4/8)\Delta E_{ac}^4 + ---] + [a_1 \Delta E_{ac} + (3a_3/4)\Delta E_{ac}^3 + ---]\cos \omega t + [(a_2/2)\Delta E_{ac}^2 + (a_4/2)\Delta E_{ac}^4 + ---]\cos 2\omega t + [(a_3/4)\Delta E_{ac}^3 + ---]\times \cos 3\omega t + [(a_4/8)\Delta E_{ac}^4 + ---]\cos 4\omega t + \text{-----}, \quad (2\text{-}3)$$

where the phase difference of the output current replied to the input voltage is not included in this equation so that the relationship between them is simply expressed.

And when the input amplitude ΔE_{ac} is small, the leading term in each square bracket is significant. Namely, the amplitude of cos ωt (fundamental harmonic) is proportinal to ΔE_{ac}, that of cos $2\omega t$ (second harmonic) to ΔE_{ac}^2, that of cos $3\omega t$ (third harmonic) to ΔE_{ac}^3 and so on. In other words, the amplitude of cos $n\omega t$ (nth harmonic) varies in proportion to the nth power term developed the total alternating current. This procedure will be explained in detail later(cf. Appendix I,II).

For the simple electrode reaction, $Ox + ne^- \rightleftharpoons Red$,

in Fig. 2-2), until the alternating current amplitude of the 1f(0°) component vanished or reached minimum amount. At the potential, the chargeing current of the electric double layer should be detected only in the 1f(90°) component, provided the resistance of the solution is 0 ohm. Figure 2-3 shows the effect on the iR compensation. If there is no compensation, the 1f(90°) suffers a significant loss of amplitude.

The iR compensation circuit was tested with a Zn(II)/Zn(Hg) system in 1 M potassium chloride solution. The potentiostat gave theoretical phase angle in the frequency range 9-500 Hz[3].

When the dc polarogram is recorded, the oscillator and lock-in amplifier are disconnected from the circuit, while the potentiostat output signal of the direct current was directly fed to the X-Y recorder.

The polarograms were obtained with a conventional three-electrode system. The working electrode was a dropping mercury electrode(DME). A hanging mercury drop electrode(HMDE)(Metrohm AG., EA 290) was also used for a cyclic voltammetry(CV): drop diameter was 0.84 mm, drop surface area was 2.20±0.05 mm^2. The counter electrode was a platinum spiral wire. The reference electrode was a saturated silver silver chloride electrode(SSE) (Ag/AgCl[sat. KCl]).

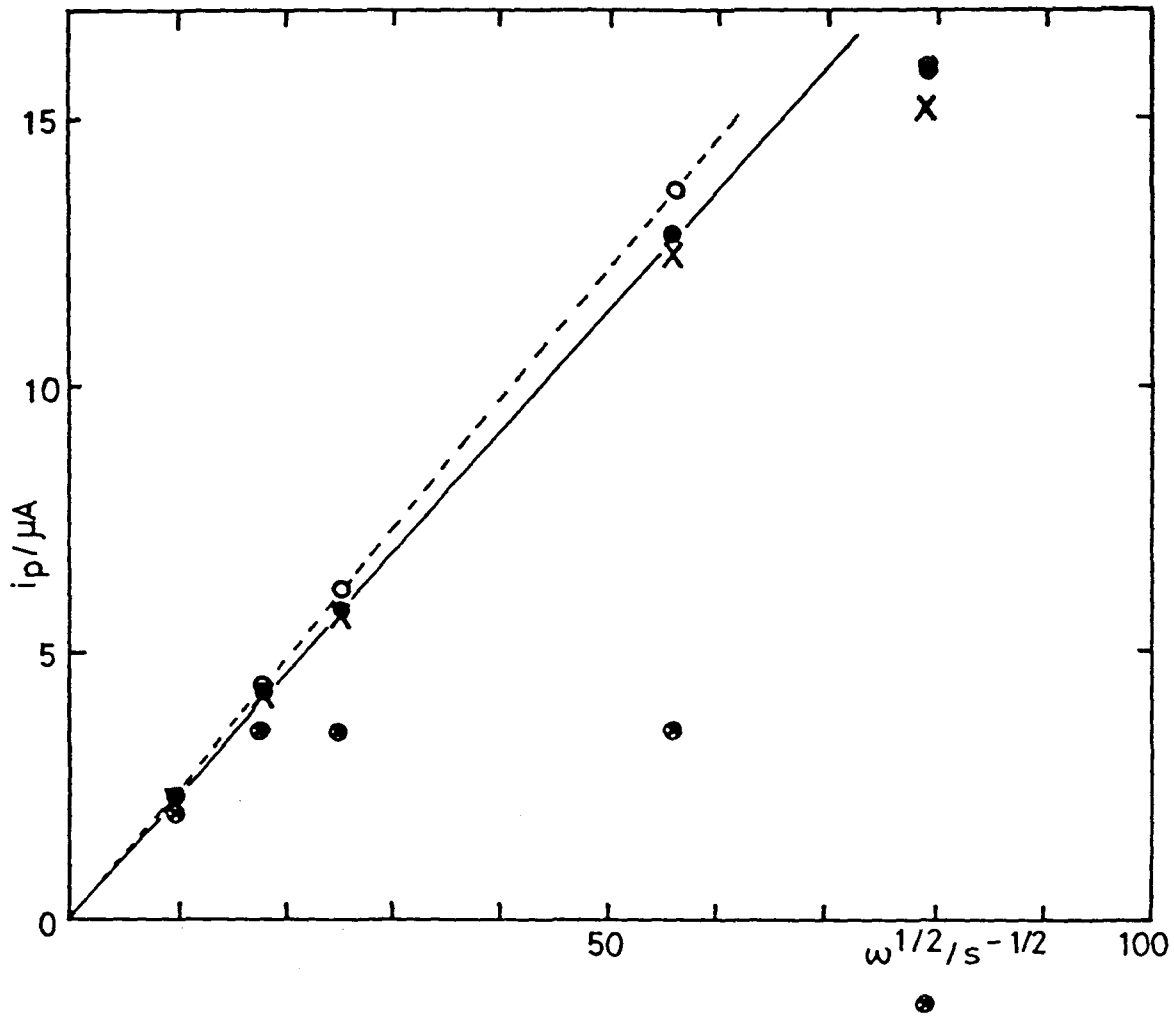

Fig. 2-3. Plots of peak current(i_p) of fundamental harmonic ac polarogram vs. $\omega^{1/2}$. (○) 1f(0°), (⊗) 1f(90°) without iR compensation, and (●) 1f(0°), (X) 1f(90°) with iR compensation. 0.2 mM cadmium chloride in 1 M potassium chroride(pH 2). ΔE_{ac} = 2 mV(r.m.s.).

2-2. Reagents

All chemicals were of analytical-reagent grade and used without further purification. Deionized-distilled water was used for the preparation of all solutions. A stock solution of cadmium(II) was prepared from $CdCl_2 \cdot 21/2H_2O$. Other reagents used for studies in later chapters will be shown in the experimental sections of these chapters. Temperture of the solutions were regurated at 25±0.5 °C. Dissolved oxygen was removed from the sample solution for 15-20 min prior to recording of polarograms or voltamograms.

2-3. Phase angle adjustment

The phase angle of the lock-in amplifier was calibrated by the use of a dummy cell[4]. A resistance was used as a dummy cell for the fundamental alternating current. The phase shifter of the lock-in amplifier are adjusted so that the lock-in amplifier output is maximized (in-phase(0°) current), and then a quadrature(90°) current amplitude vanished.

For the second-harmonic alternating current, an output signal of the potentiostat is fed to a full wave rectifier (the resistance was used as the dummy cell). The phase angle of the output current is determined by the following relationship,

input signal: $y = A\sin x$,

output signal: $y = (2A/\pi)[1 - (2\cos 2x)/3 - (2\cos 4x)/3\cdot5 - (2\cos 6x)/5\cdot7 \cdots]$. (2-1)

The circuit diagram of the full wave rectifier is given in Fig. 2-4. As is found from Eq. (2-1), the phase angle in the 2f mode becomes -90° when the maximum signal is detected in the lock-in amplifier.

If one wants to obtain the 45° component of the fundamental harmonic alternating current[1f(45°)], the phase shifter of the lock-in amplifier should be ajusted to the point so that the output current is $I_{1f(0°)}\cos 45° = I_{1f(0°)}/\sqrt{2}$.

2-4. Theoretical background

The total alternating current(i_{ac}) through a nonlinear circuit element such as an electrochemical cell is developed nonlinearly the power series. When the input

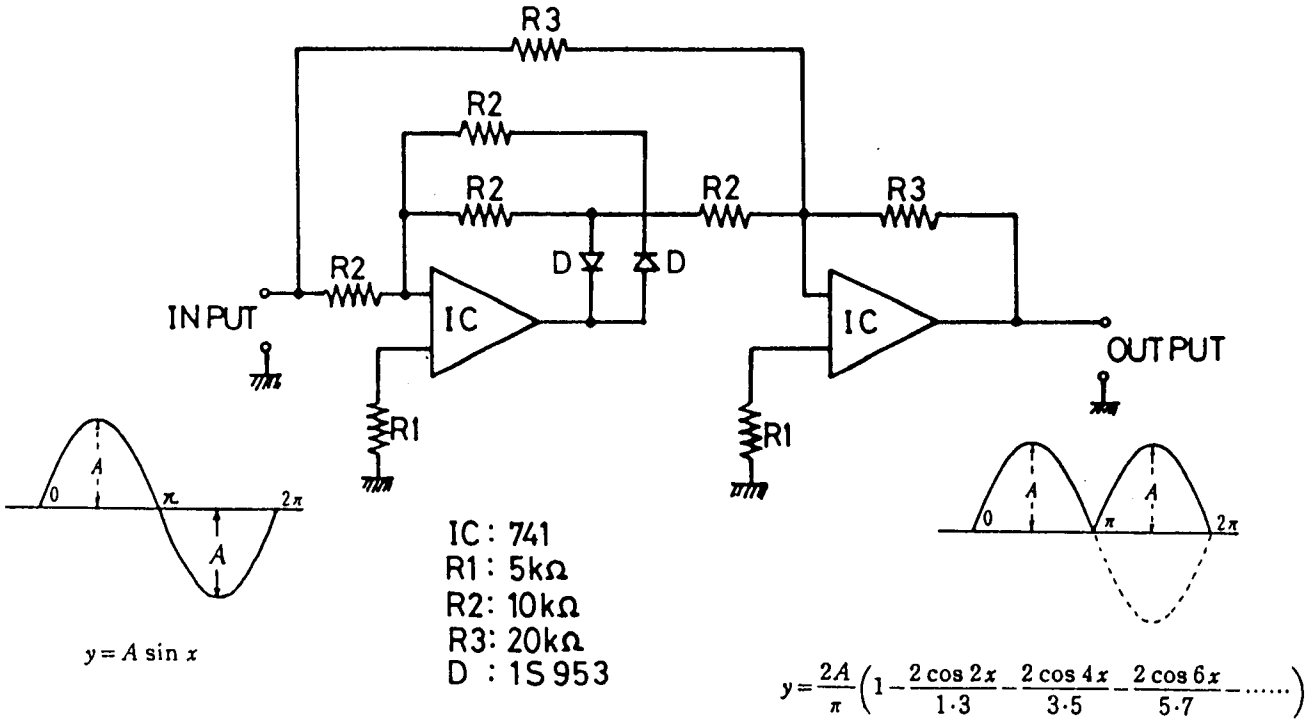

Fig. 2-4. The circuit diagram of the full wave rectifier used as the phase adjuster of 2f mode in lock-in amplifier.

where the rate is controlled by diffusion and/or heterogeneous charge transfer kinetics, the fundamental and second harmonic alternating currents are given by the following equations[5,6](Appendix I,II):

$$I(\omega t) = I(\omega t)_{rev} F_1(t) G_1(\omega) \sin(\omega t + \phi_1), \quad (2\text{-}4)$$

$$I(2\omega t) = I(2\omega t)_{rev} F_2(t) G_2(\omega) \sin(2\omega t + \phi_2), \quad (2\text{-}5)$$

where

$$I(\omega t)_{rev} = (nF)^2 A C_0^* (\omega D_0)^{1/2} \Delta E_{ac} [4RT\cosh^2(j/2)]^{-1}, \quad (2\text{-}6)$$

$$I(2\omega t)_{rev} = (nF)^3 A C_0^* (2\omega D_0)^{1/2} \Delta E_{ac}^2 [16R^2T^2\cosh^3(j/2)]^{-1}, \quad (2\text{-}7)$$

$$\phi_1 = \cot^{-1}[1 + (2\omega)^{1/2}/\lambda], \quad (2\text{-}8)$$

$$\phi_2 = \cot^{-1}\{[L(2\omega^{1/2}/\lambda + 1) + P]/[L - P(2\omega^{1/2}/\lambda + 1)]\}, \quad (2\text{-}9)$$

where

$$j = nF(RT)^{-1}(E_{dc} - E_{1/2}^r); \quad \lambda = (k_s f_a/RT)(e^{-\alpha j} + e^{\beta j}). \quad (2\text{-}10)$$

The current component $I(\theta)$ at a phase angle, θ is given by the following equation,

$$I(\theta) = I_{total} \cos(\phi - \theta), \quad (2\text{-}11)$$

where the I_{total} is the amplitude of Eq. (2-4) or (2-5).

Appendix I. The reversible ac polarographic wave[5]

For the system presented by the reaction scheme Ox + $ne^- \rightleftharpoons$ Red, the partial-differential equations, initial and boudary conditions for diffusion to a stationary planar electrode are:

$$dC_O/dt = D_O d^2C_O/dx^2, \quad \text{(I-1)}$$

$$dC_R/dt = D_R d^2C_R/dx^2. \quad \text{(I-2)}$$

For t = 0, any x,

$$C_O = C_O^*, \quad \text{(I-3)}$$

$$C_R = C_R^*. \quad \text{(I-4)}$$

For t > 0, x $\rightarrow \infty$,

$$C_O \longrightarrow C_O^*, \quad \text{(I-5)}$$

$$C_R \longrightarrow C_R^*. \quad \text{(I-6)}$$

For t > 0, x = 0,

$$D_O dC_O/dx = -D_R dC_R/dx = i(t)/nFA, \quad \text{(I-7)}$$

$$C_O = C_R(D_R/D_O)^{1/2}\exp[(nF/RT)[E(t) - E^r_{1/2}]]. \quad \text{(I-8)}$$

The assumptions that Fick's law is applicable to each species independently, that coupled chemical reactions exert to no influence, and that electrode curvature and motion relative to the solution have a negative effect are incorporated in Eqs. (I-1) and (I-2). Equation (I-7) assumes that each reacting species is soluble either in the solution or electrode phase, that is, there is no accumulation of electroactive material at the interface.

Equation (I-8) states the Nernst equation in terms of the reversible dc polarographic half-wave potential, $E^r_{1/2}$, where

$$E^r_{1/2} = E^\circ - (RT/nF)\ln (f_R/f_O)(D_O/D_R)^{1/2}. \qquad \text{(I-9)}$$

The assumption of nernstian behavior is obeyed if heterogeneous charge transfer kinetics are very rapid.

Application of the method of Laplace transformation to Eqs. (I-1) through (I-7) yields, for surface concetrations,

$$C_{Ox=0} = C^*_O - \int_0^t i(t-u)du/nFA(D_O\pi u)^{1/2}, \qquad \text{(I-10)}$$

$$C_{Rx=0} = C^*_R + \int_0^t i(t-u)du/nFA(D_R\pi u)^{1/2}. \qquad \text{(I-11)}$$

Derivation of Eqs. (I-10) and (I-11) is well known and contains no features specific to ac polarography. For simplicity, we shall assume at this stage that the reduced form is initially absent from the solution; that is, $C^*_R = 0$. Substituting Eq. (I-10) and (I-11) in Eq. (I-8) and rearranging yields the integral expression(given in a form most convenient for subsequent steps):

$$e^{-j(t)} - e^{-j(t)}\int_0^t \psi(t-u)du/(\pi u)^{1/2} = \int_0^t \psi(t-u)du/(\pi u)^{1/2}, \qquad \text{(I-12)}$$

where

$$\psi(t) = i(t)/nFAC^*_O D^{1/2}, \qquad \text{(I-13)}$$

$$j(t) = (nF/RT)[E(t) - E^r_{1/2}]. \qquad \text{(I-14)}$$

In ac polarography the applied potential is given by

$$E(t) = E_{dc} - \Delta E_{ac}\sin \omega t. \qquad \text{(I-15)}$$

The dc potential term is considered constant. This assumes

the rate of scan is slow relative to the rate of change of alternating potential and that the dc potential does not change significantly over the life of a single mercury drop. The latter restriction applies also to dc polarography. Substitution of Eq. (I-15) in the exponential term gives as:

$$e^{-j(t)} = e^{-j} \exp\left[(nF\Delta E_{ac}/RT)\sin \omega t\right], \qquad \text{(I-16)}$$

where

$$j = (nF/RT)(E_{dc} - E^{r}_{1/2}) \qquad \text{(I-17)}$$

One then develops the power series:

$$\exp\left[(nF\Delta E_{ac}/RT)\sin \omega t\right] = (nF\Delta E_{ac}/RT)^{p}(\sin \omega t)^{p}/p!, \qquad \text{(I-18)}$$

$$\psi(t) = \sum_{p=0}^{\infty} \psi_{p}(t)(nF\Delta E_{ac}/RT)^{p}, \qquad \text{(I-19)}$$

$$p = 0,1,2,3 \text{ ---}. \qquad \text{(I-20)}$$

Substituting Eqs. (I-18) and (I-19) in Eq. (I-12) and equating coefficients of equal powers of $(nF\Delta E_{ac}/RT)^{p}$, one obtains a system of integral equations:

$$e^{-j}(\sin \omega t)^{p}/p! - \sum_{r=0}^{p} \{[e^{-j}(\sin \omega t)^{r}/r!] \times \int_{0}^{t} \psi_{p-r}(t-u)\,du/(\pi u)^{1/2}]\} = \int_{0}^{t} \psi_{p}(t-u)\,du/(\pi u)^{1/2}. \qquad \text{(I-21)}$$

Solutions of Eq. (I-21) for different values of p represent the various faradaic current components in the following manner. If k is the order of the current harmonic(k = 0 for dc, k = 1 for fundamental-harmonic ac, etc.), contributions to a particular harmonic k are obtained from values of p given by

$$p = 2q + k, \qquad \text{(I-22)}$$

where

$$q = 0,1,2,3\ \text{---}. \qquad \text{(I-23)}$$

Thus, dc components are obtained for $p = 2q = 0,2,4$ --- and fundamental harmonic ac terms for $p = 2q + 1 = 1,3,5,7$ ---. The contribution to a given harmonic decreases with increasing p for $\Delta E_{ac} < 0.1$ V, a condition always obeyed in ac polarography. At sufficiently small amplitudes($\Delta E_{ac} < 8/n$ mV), only the term corresponding to the lowest value of p need be considered. For p = 0, one obtains:

$$\int_0^t \psi_0(t-u)\,du/(\pi u)^{1/2} = 1/(1 + e^{j}). \qquad \text{(I-24)}$$

The solution for $\psi_0(t)$ is obtained most conveniently by application of the method of Laplace transformation to Eq. (I-24). Applying Eqs. (I-13) and (I-19) to the solution for $\psi_0(t)$, we get:

$$i_{dc}(t) = nFAC_0^{*}D_0^{1/2}/(1 + e^{j})(\pi t)^{1/2} \quad . \qquad \text{(I-25)}$$

This is well-known expression for the potentiostatic direct current at a planar electrode with a reversible process[7].

For p = 1, one has:

$$e^{-j}[1 - \int_0^t \psi_0(t-u)\,du/(\pi u)^{1/2}]\sin \omega t = (1 + e^{-j})\int_0^t \psi_1(t-u)\,du/(\pi u)^{1/2} \quad . \qquad \text{(I-26)}$$

Note that the integral equation for the small-amplitude fundamental harmonic contains a term in the dc component $\psi_0(t)$. This represents a general feature of the

theoretical method. As will be seen, the integral equation for the second-harmonic contains terms $\psi_1(t)$ and $\psi_0(t)$. In general, the integral equation for any higher-order term contains all the lower-order terms. For the reversible case, explicit solution of the lower-order terms($\psi_p(t)$) is not required, since the integral equations provide the required relationships. Thus, substitution of Eq. (I-24) in Eq. (I-26) eliminates $\psi_0(t)$, yielding:

$$\int_0^t \psi_1(t-u)du/(\pi u)^{1/2} = \sin \omega t/4\cosh^2 (j/2) . \quad \text{(I-27)}$$

However, for most electrode-reaction mechanisms, explicit solution for $\psi_0(t)$ is required to obtain a general solution for $\psi_1(t)$, solution of $\psi_0(t)$ and $\psi_1(t)$ is required for $\psi_2(t)$, etc. The need to obtain an explicit solution for the dc component presents the most serious obstacle to obtaining completely general ac polarographic wave equations for a particular kinetic scheme.

The form of Eq. (I-27) is such that $\psi_1(t)$ can contain only fundamental harmonic terms. Thus, we may write:

$$\psi_1(t) = A\sin \omega t + B\cos \omega t . \quad \text{(I-28)}$$

Substituting this relation in Eq. (I-27), employing the trigonometric identities:

$$\sin \omega(t-u) = \sin \omega t\cos \omega u - \cos \omega t\sin \omega u, \quad \text{(I-29)}$$

$$\cos \omega(t-u) = \cos \omega t\cos \omega u + \sin \omega t\sin \omega u, \quad \text{(I-30)}$$

applying the steady-state approximation($\int_0^t = \int_0^\infty$) [8] and the relations[9]:

$$\int_0^\infty \cos \omega u du/(\pi u)^{1/2} = \int_0^\infty \sin \omega u du/(\pi u)^{1/2}$$
$$= 1/(2\omega)^{1/2}, \qquad \text{(I-31)}$$

we obtain the result:

$$(A + B)\sin \omega t - (A - B)\cos \omega t =$$
$$[(2\omega)^{1/2}/4\cosh^2 (j/2)]\sin \omega t. \qquad \text{(I-32)}$$

The steady-state approximation neglects transient behaviour in the ac concentration profile. As shown by Berzins and Delahay[10], transients are negligible when $(\omega t)^{1/2} >> 1$, where t is time elapsed after application of the alternating potential.

Equating coefficients of sin ωt and cos ωt on both sides of Eq. (I-32), and solving for A and B, we obtain:

$$A = B = (2\omega)^{1/2}/8\cosh^2 (j/2). \qquad \text{(I-33)}$$

Application of the trigonometric identity:

$$a\sin \omega t + b\cos \omega t = (a^2 + b^2)^{1/2}\sin [\omega t + \cot^{-1} (a/b)], \qquad \text{(I-34)}$$

yields:

$$\psi_1(t) = [\omega^{1/2}/4\cosh^2 (j/2)]\sin (\omega t + \pi/4) \qquad \text{(I-35)}$$

Applying Eqs (I-13) and (I-19), one obtains as the solution for the small-amplitude fundamental harmonic current:

$$I(\omega t) = [n^2F^2AC_0^*(\omega D_0)^{1/2}\Delta E_{ac}/4RT\cosh^2 (j/2)]\times$$
$$\sin (\omega t + \pi/4) . \qquad \text{(I-36)}$$

One may proceed in a similar manner to obtain higher-order current components. Equation (I-21) has the form, for p = 2,

$$(e^{-j}/2)[1 - \int_0^t \psi_0(t-u)du/(\pi u)^{1/2}]\sin^2 \omega t -$$
$$[e^{-j}\int_0^t \psi_1(t-u)du/(\pi u)^{1/2}]\sin \omega t =$$
$$(1 + e^{-j})\int_0^t \psi_2(t-u)du/(\pi u)^{1/2} . \qquad \text{(I-37)}$$

Substituting Eqs. (I-24) and (I-27) in Eq. (I-37), rearranging, and applying the trigonometric identity:

$$\sin^2 \omega t = (1 - \cos 2\omega t)/2, \qquad \text{(I-38)}$$

we get

$$\int_0^t \psi_2(t-u)du/(\pi u)^{1/2} = [\sinh (j/2)/16\cosh^3 (j/2)]\times$$
$$(1 - \cos 2\omega t) . \qquad \text{(I-39)}$$

The form of Eq. (I-39) indicates that $\psi_2(t)$ is made up of dc and second-harmonic components, so that one can write:

$$\psi_2(t) = A_0(t) + A_2 \sin 2\omega t + B_2 \cos 2\omega t. \qquad \text{(I-40)}$$

Substituting Eq. (I-40) in Eq. (I-39) generates expressions for the dc and ac coponents[applying Eqs (I-29), (I-30), and (I-31) to the ac portion] given by the equation:

$$\int_0^t A_0(t-u)du/(\pi u)^{1/2} = \sinh (j/2)/16\cosh^3 (j/2) , \qquad \text{(I-41)}$$

and

$$(A_2 - B_2)\cos 2\omega t - (A_2 + B_2)\sin 2\omega t =$$
$$[\omega^{1/2}\sinh (j/2)/8\cosh^3 (j/2)]\cos 2\omega t , \qquad \text{(I-42)}$$

Solution of Eq. (I-41) is accomplished readily by the method of Laplace transformation and, after application of Eqs. (I-13) and (I-19), the dc component corresponding to $A_0(t)$ is shown to be:

$$I_2(dc) = n^3F^3AC_0^*D_0^{1/2}\Delta E_{ac}^2 \sinh (j/2)/$$

$$16R^2T^2(\pi t)^{1/2}\cosh^3 (j/2) . \qquad \text{(I-43)}$$

This represents the small-amplitude faradaic-rectification dc component flowing under the experimental conditions described. Addition of this term to the normal direct current[Eq. (I-25)] flowing in absence of alternating current yields an expression for the Fournier polarogram[11-13] within the framework of the planar-diffusion model. As will be pointed out below, the planar-diffusion model sometimes appears accurate ac components observed with a reversible process at a DME, but yields rather inaccurate expressions for the dc components. Influence of electrode growth and geometry must be considered in deriving the dc terms.

Proceeding as in the derivation of the fundamental harmonic component, one obtains solution for A_2 and B_2 in Eq. (I-42), corresponding to a second-harmonic component given by the equation:

$$I(2\omega t) = [2^{1/2}n^3F^3AC_0^*(\omega D_0)^{1/2}\Delta E_{ac}^2\sinh (j/2)/ 16R^2T^2\cosh^3 (j/2)]\sin (2\omega t - \pi/4) . \qquad \text{(I-44)}$$

One may solve the integral equation for large values of p to obtain expressions for third, fourth, etc., harmonics and larger amplitude contributions to all current components.[11,14].

The small amplitude expression given by Eq. (I-36) corresponds to a faradaic impedance(magnitude):

$$Z_f = 4RT\cosh^2 (j/2)/n^2F^2AC_0^*(\omega D_0)^{1/2}, \quad \text{(I-45)}$$

which is equivalent to a series RC circuit with:

$$R_f = 1/\omega C_f = 4RT\cosh^2 (j/2)/n^2F^2AC_0^*(2\omega D_0)^{1/2}. \quad \text{(I-46)}$$

Appendix II. The quasi-reversible ac polarographic wave[5,6]

Theoretical treatment of the ac polarographic wave kinetically controlled by both charge transfer and diffusion(the "quasi-reversible" case) requires minor modification in the mathematical formation of the reversible case. One deletes the assumption of nernstian behavior[Eq. (I-8)] and replaces it by the absolute rate expression[15]:

$$i(t)/nFAk_s = C_{Ox=0}\exp [(-\alpha nF/RT)(E(t) - E^\circ)] - C_{Rx=0}\exp [(1-\alpha)nF/RT](E(t) - E^\circ). \quad \text{(II-1)}$$

One substitutes the expression for surface concentrations[Eqs. (I-10) and (I-11)] in Eq. (II-1) and, proceeding as for the reversible case, one obtains Eqs. (2-2) and (2-3), where

$$F_1(t) = 1 + (\alpha e^{-j} - \beta)D^{1/2}\psi_0(t)/k_s e^{-\alpha j}, \quad \text{(II-2)}$$

$$G_1(\omega) = \{2/[1 + [1 + [(2\omega)^{1/2}/\lambda]]^2\}^{1/2}, \quad \text{(II-3)}$$

$$F_2(t) = [P^2 + L^2]^{1/2}, \quad \text{(II-4)}$$

$$G_2(\omega) = \{2/[1 + [1 + (2\omega^{1/2}/\lambda)]^2]\}^{1/2} , \qquad \text{(II-5)}$$

where

$$P = (\alpha^2/2)(e^{j/2} + 2e^{-j/2} + e^{-3j/2}) - (\alpha e^{-j/2} - \beta e^{j/2})\times$$
$$[2 + (2\omega)^{1/2}/\lambda][1 + (\alpha e^{-j} - \beta)D^{1/2}\psi_0(t)/k_s e^{-\alpha j}]/$$
$$[1 + [1 + [(2\omega)^{1/2}/\lambda]]^2] , \qquad \text{(II-6)}$$

$$L = (\alpha e^{-j/2} - \beta e^{j/2})[(2\omega)^{1/2}/\lambda][1 + (\alpha e^{-j} - \beta)D^{1/2}\times$$
$$\psi_0(t)/k_s e^{-\alpha j}]/[1 + [1 + [(2\omega)^{1/2}/\lambda]]^2] , \qquad \text{(II-7)}$$

where

$$\psi_0(t) = (k_s e^{-\alpha j}/D^{1/2}) e^{\lambda^2 t} \operatorname{erfc}(\lambda t^{1/2}) , \qquad \text{(II-8)}$$

where

$$\operatorname{erfc}(x) = 1 - \operatorname{erf}(x) = (2/\pi^{1/2})\int_x^\infty \exp(-u^2)du =$$
$$[\exp(-x^2)/\pi^{1/2}x][1 - 1/2x^2 + 1\times3/(2x^2)^2 -$$
$$1\times3\times5/(2x^2)^2 + \cdots\cdots] . \qquad \text{(II-9)}$$

2-5. References

1 D.E. Smith, Crit. Rev. Anal. Chem., 2(1971)247.

2 E.R. Brown, D.E. Smith and G.L. Booman, Anal. Chem., 40(1968)1411.

3 S. Vavricka, J. Kuta and L. Pospisil, J.Electroanal. Chem., 133(1982)299.

4 D.E. Glover and D.E. Smith, Anal. Chem., 43(1971)775.

5 D.E. Smith, in A.J. Bard(Ed.), Electroanalytical

Chemistry, Vol. 1, Dekker, New York, 1966, p. 1.

6 T.G. McCord and D.E. Smith, Anal. Chem., 40(1968)289.

7 P. Delahay, New Instrumental Methods in Electrochemistry, Wiley(Interscience), New York, 1954.

8 P. Delahay, in P. Delahay and C.W. Tobias(Ed.), Advances in Electrochemistry and Electrochemical Engineering, Vol. 1, Chap. 5, Wiley(Interscience), New York, 1961.

9 C.D. Hodgman(Ed.), Handbook of chemistry and Physics, 41st ed., Chemical Rubber Publishing Co., Cleveland, 1959, p.275.

10 T. Berzins and P. Delahay, Z. Elektrochem., 59(1955)792.

11 M. Senda and I. Tachi, Bull. Chem. Soc. Jpn, 28(1955)632.

12 M. Fournier, Comp. Rend., 232(1951)1673.

13 G.S. Buchanan and R.L. Werner, Australian J. Chem., 7(1954)239.

14 H. Matsuda, Z. Elektrochem., 61(1957)489.

15 S. Glasstone, K.J. Laidler and H. Eyring, The Theory of Rate Process, McGraw-Hill, New York, 1941, p.575.

Chapter 3. Kinetic analysis for the electrochemical reduction of chromium(VI) in alkaline solution

3-1. Introduction

As mentioned in general introduction, the analysis of the oxidation and reduction mechanisms of multivalent chemical species is a continuing problem. In paticular, many studies[1-7] have been published to date on the polarographic reduction of the chromium(VI) species. The polarographic study of chromium(VI) in neutral and alkaline solutions was first performed by Kolthoff and Lingane[1]. Tondeur et al.[2] studied double layer effects on this system, and Miller[3] investigated the dc polarography of this system in the presence of complexing agents.

Delahay et al.[4,5] also studied this system by employing dc polarography and chronopotentiometry. They suggested that chromium(IV) is an intermediate product of the reduction of chromium(VI) to chromium(III).

There have, however, been few reports[6] on its ac polarography and no report on the kinetics of this system.

In this chapter, the precise analysis of the

electrochemical reduction of chromium(VI) to chromium(III) in alkaline solution, already in use for the quantitative chemical analysis of chromium(VI)[1,7], was attempted by employing fundamental harmonic(1f) phase-selective ac polarography.

In general, 1f(0°) component of alternating current has been almost used for the quantitative analysis and other purpose(cf. Chap. 1). The ac polarogram of this chromium(VI) system at high frequency, especially in 1f(45°) component, was not a first derivative form of the dc polarogram. The non-linear phenomenon was investigated by a curve fitting calculation. The curve fitting analysis was performed by using the theoretical equations of Hung and Smith[8] for a stepwise reaction controlled by ac polarography.

3-2. Experimental

A stock solution of chromium(VI) was prepared from sodium chromate(VI), $Na_2CrO_4 \cdot 4H_2O$, and its concentration was determined gravimetrically with barium chloride[9].

The working electrode was a dropping mercury electrode; the capillary had a drop time of 4.25 s at -1.0 V in 1 M sodium hydroxide and the mercury flow was 1.769

mgs^{-1} at a height of 70 cm.

The typical compensation resistance of the iR compensator[10,11](cf. Chap. 2) was 75 Ω for the Zn(II)/Zn(Hg) and 60 Ω for the Cr(VI) system.

The theoretical and curve fitting calculations were performed by using an ACOS NEAC 1000 at the Computation Center, Osaka University.

3-3. Results and discussion

Figure 3-1 shows the ac polarograms, 1f(0°) and 1f(45°), of chromium(VI) in 1 M sodium hydroxide solution taken at various frequencies. 1f(0°) is the fundamental harmonic current at zero phase-angle. The dc polarogram is also included in the figure. It has been reported that in a neutral solution, the dc polarogram displays a small pre-wave and an irreversible main-wave[1-3]. The dc polarogram in 1 M sodium hydroxide in Fig. 3-1(A) does not show any pre-wave, but the ac polarogram at 15 Hz presents a small shoulder(S1 at -0.5 V) which precedes the main peak(M at -0.8 V) as shown in Fig. 3-1(B).

The involvement of the specific adsorption in the present system is not probable because; (1) both the diffusion of the dc polarogram and the peak current of M

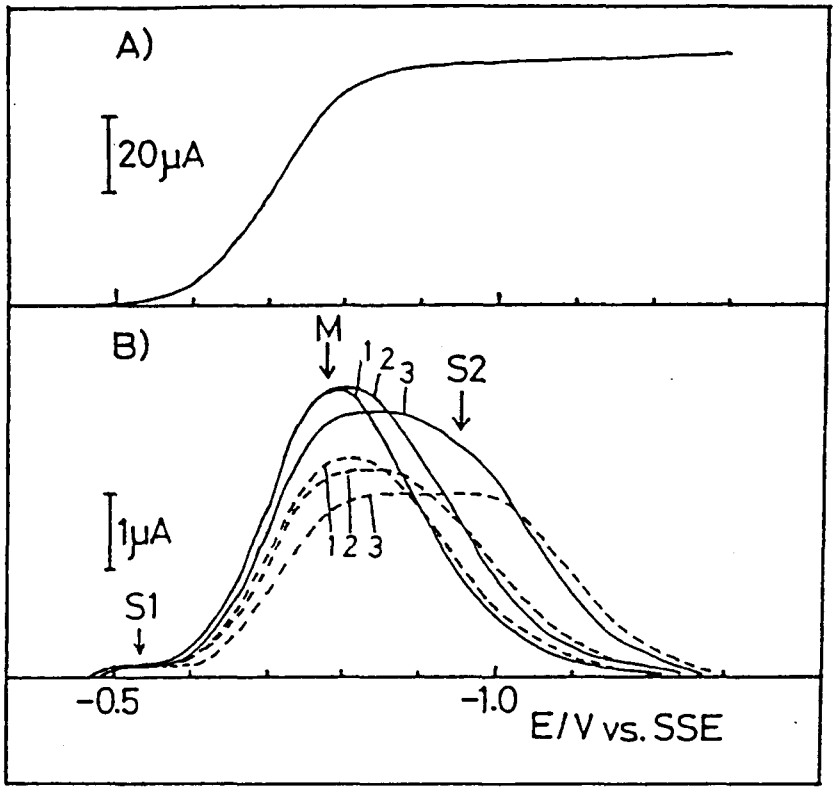

Fig. 3-1. Dc and ac polarograms for 5 mM Na_2CrO_4 in 1 M NaOH. (A) dc polarogram, (B) ac polarogram. Solid lines: 1f(0°); broken lines: 1f(45°); (1) 15 Hz, (2) 50 Hz, (3) 500 Hz, ΔE_{ac} = 5 mV(r.m.s.). M, S1, S2: see text for caption.

for 1f(0°) are proportional to the concentration of chromium(VI) in the range 0.2-5.0 mM(Fig. 3-2), (2) the shapes of polarograms of both 1f(0°) and 1f(90°) components do not change with the concentration, (3) the phase angle is less than 45°.

As the frequency increases, another shoulder(S2) appears in the 1f(0°) polarogram between -0.9 and -1.0 V. This shoulder(S2) is more clearly seen in 1f(45°) than in 1f(0°).

The comparison between the experimental polarograms and the theoretical curves for one-step reversible, irreversible and quasi-reversible process[12-14](cf. Chaps. 2 and 5) leads to the following conclusions. (1) The theory for reversible process($k_s >> 1$ cms^{-1}) predicts that the half-width of the ac polarogram is 90/n mV[12](n; the number of electrons transferred in the charge transfer step) for all frequencies, whereas that of the experimental polarograms is larger than 200 mV at low frequency. (2) The theory for an irreversible process[13]($k_s < 10^{-5}$ cms^{-1}) predicts polarograms similar in shape to that observed at low frequency, whereas the theoretical one has neither the shoulder S1 nor S2. (3) The theoretical polarogram for a quasi-reversible process[12,14] presents the shoulder S1 when $\alpha < 0.5$ and $k_s \simeq 10^{-4}$ cms^{-1}, whereas the shoulder S2 does not appear in any case of the theory.

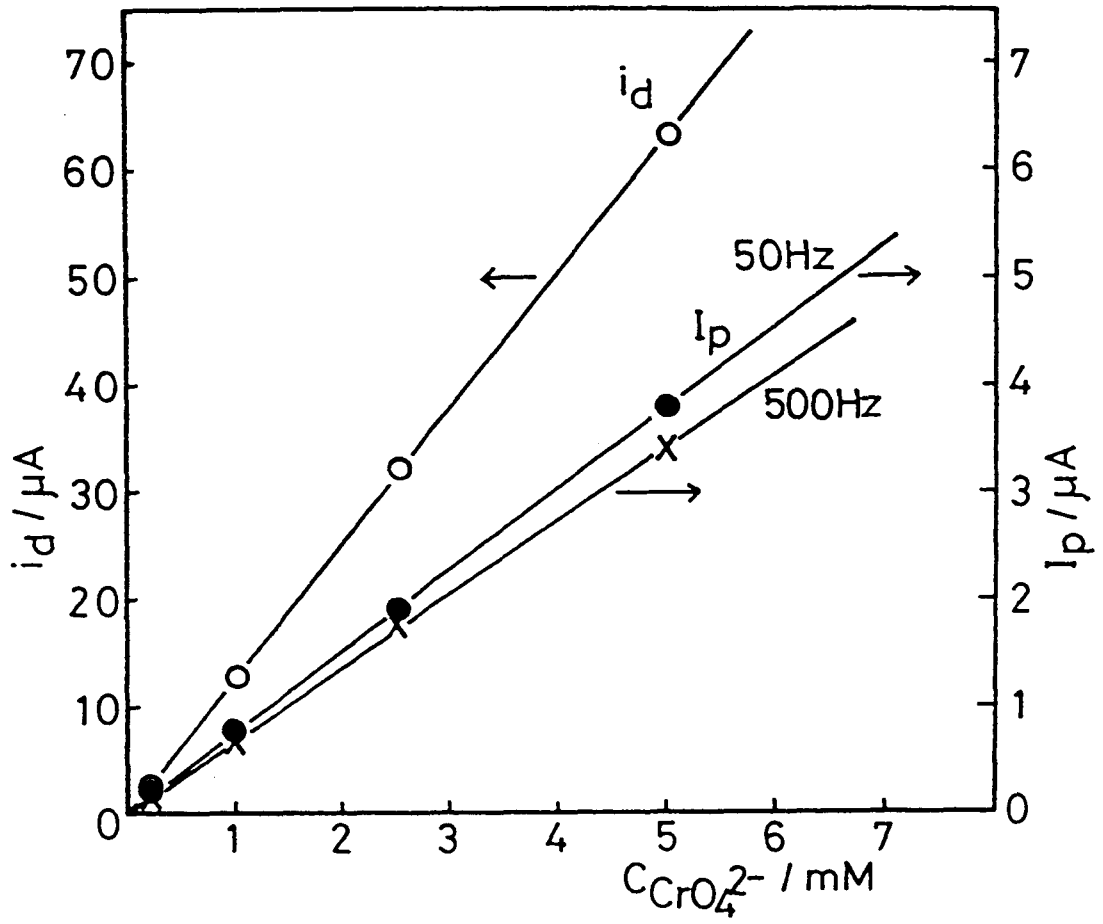

Fig. 3-2. Calibration curves for chromium(VI) in 1 M sodium hydroxide. (O) dc diffusion current(i_d); ac peak current (I_p): (●) 50 Hz, (X) 500 Hz, ΔE_{ac} = 5 mV(r.m.s.).

For the quasi-reversible two step(EE) mechanism, Hung and Smith have developed a theory based on the stationary plane diffusion model on the assumption of the Butler type equation for i-E relation[cf. Eq. (II-1) in Appendix II]. They have shown several theoretical polarograms in their paper which, however, are not similar to the experimental ones. Since their calculation was limited to the case of $k_s > 10^{-3}$ cms^{-1}, it is extended to the case of a slower rate. For the stepwise electrode reactions:

$$O + n_1e^- \rightleftharpoons Y , \tag{3-1}$$

$$Y + n_2e^- \rightleftharpoons R , \tag{3-2}$$

the fundamental harmonic alternating current is written as follows[8](cf. Appendix III):

$$I(\omega t) = I_{1f}\sin(\omega t + \phi), \tag{3-3}$$

where

$$I_{1f} = [2F^2AC_O^*\Delta E_{ac}(2\omega D_O)^{1/2}/RT][(Y^2 + Z^2)^{1/2}/Q], \tag{3-4}$$

where (see also Appendix III for Q, Y and Z)

$$Q = g_1(\omega, \lambda_i, j_i), \tag{3-5}$$

$$Y = g_2(\omega, \lambda_i, j_i, n_i), \tag{3-6}$$

$$Z = g_3(\omega, \lambda_i, j_i, n_i), \tag{3-7}$$

$$\phi = \cot^{-1}(Y/Z), \tag{3-8}$$

where

$$\lambda_i = [(k_{s,i}f_i)/D_i^{1/2}][\exp(-\alpha_i j_i) + \exp(\beta_i j_i)], \tag{3-9}$$

$$j_i = (n_iF/RT)(E_{dc} - E^r_{1/2,i}). \tag{3-10}$$

Y/Q and Z/Q in Eqs. (3-4)-(3-7) are the quantities

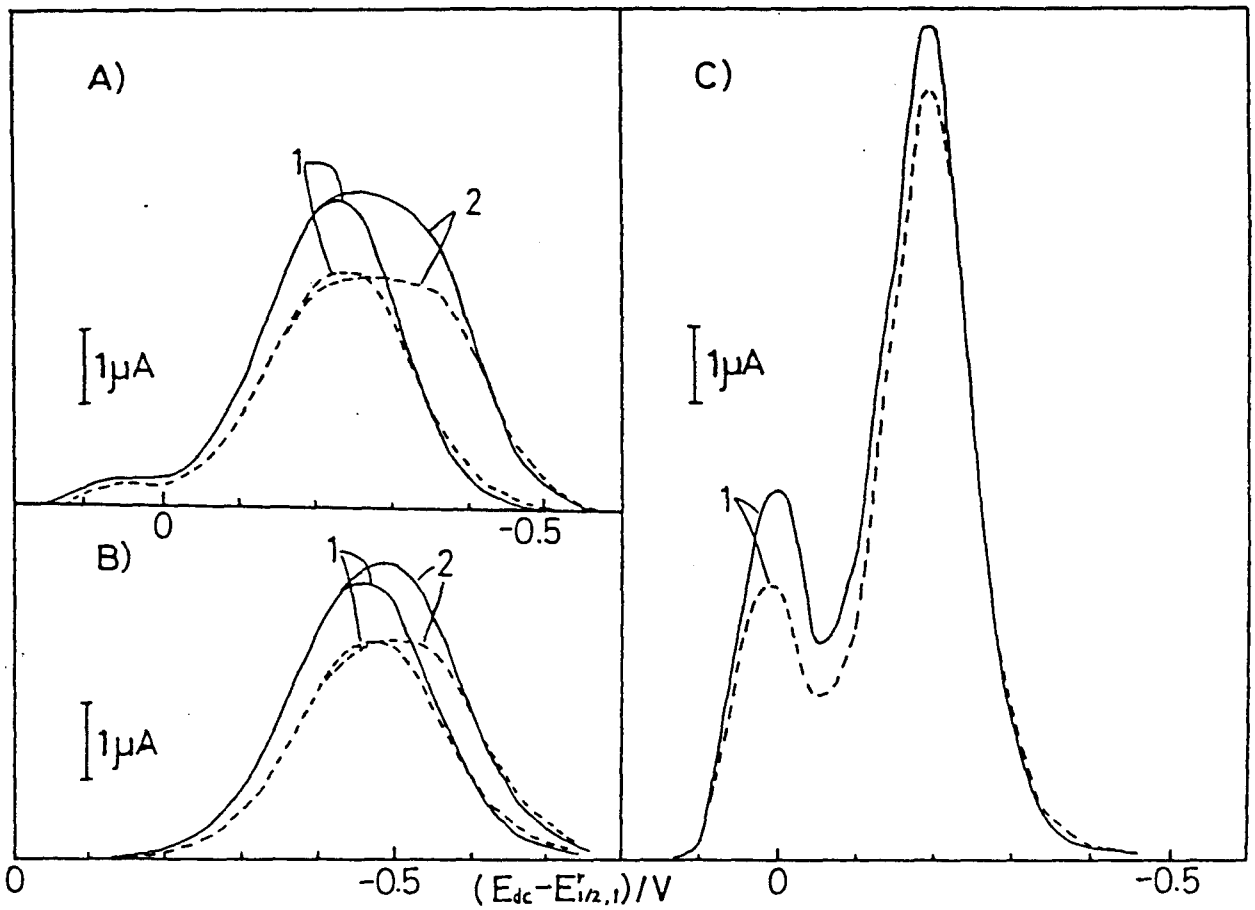

Fig. 3-3. Theoretical ac polarograms for two-step mechanism. Solid lines: 1f(0°); broken lines: 1f(45°); (1) 15 Hz, (2) 500 Hz, D_O = 9.61×10^{-6} cm^2s^{-1}(calculated from diffusion current for dc polarogram), $D_Y = D_R$ = 1×10^{-5} cm^2s^{-1}, A = 0.0327 cm^2, t = 4.25 s, ΔE_{ac} = 0.005 V, C_O^* = 5.0×10^{-3} M, T = 298 K. Values of n_1, n_2, α_1, α_2, $k_{s,1}$, $k_{s,2}$ and $(E^r_{1/2,1} - E^r_{1/2,2})$ are given in Table 3-1.

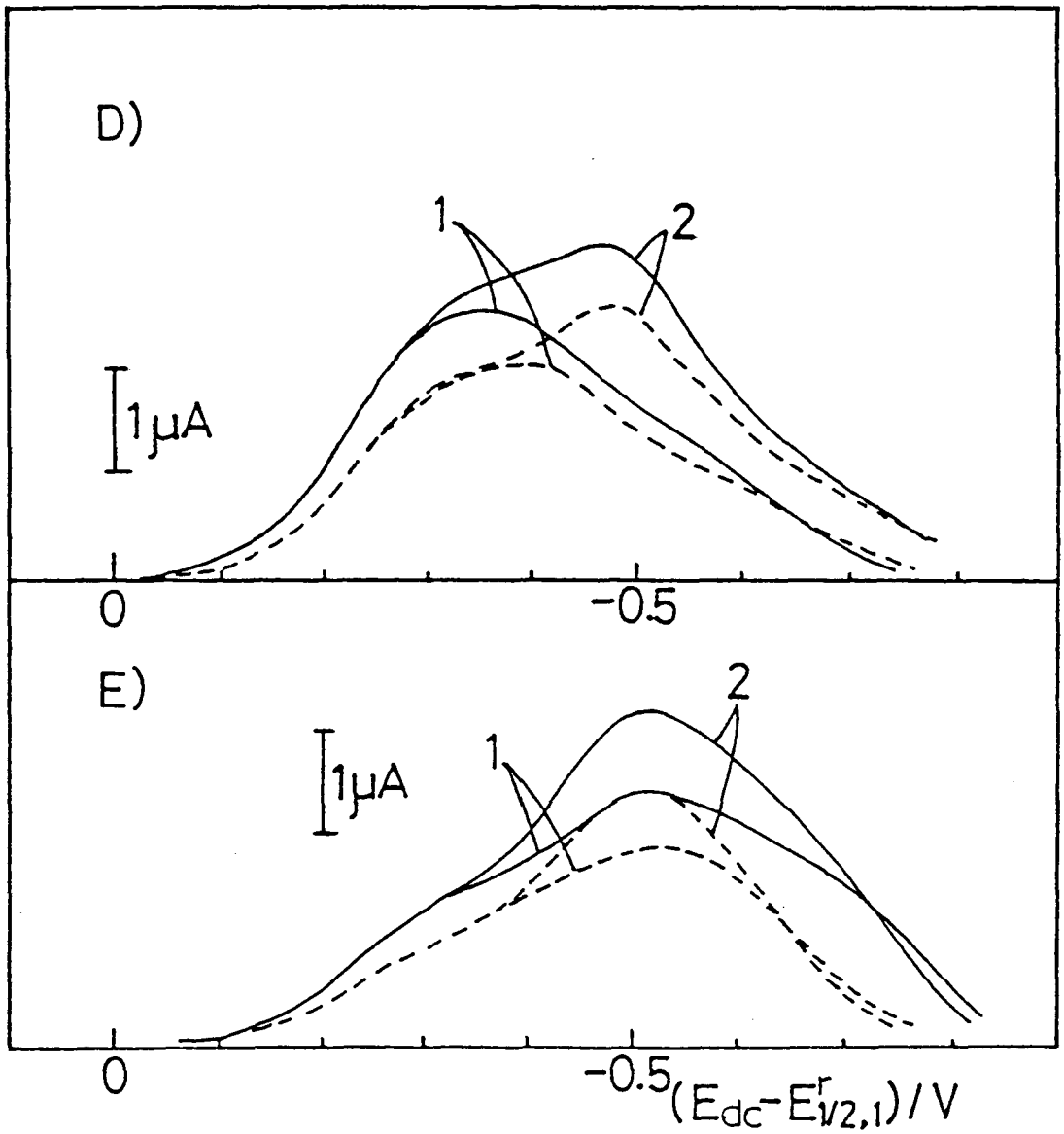

Fig. 3-3 (D) and (E).

Table 3-1. Parameters for the calculation.

Fig.	n_1	n_2	α_1	α_2	$k_{s,1}/cms^{-1}$	$k_{s,2}/cms^{-1}$	$E^r_{1/2,1}-E^r_{1/2,2}/V$
3-3 A	2	1	0.25	0.5	$1x10^{-4}$	$1x10^{-3}$	0.15
B	2	1	0.25	0.5	$1x10^{-6}$	$1x10^{-5}$	0.15
C	2	1	0.25	0.5	$1x10^{-3}$	$1x10^{-2}$	0.20
D	2	1	0.25	0.5	$1x10^{-5}$	$1x10^{-6}$	0.10
E	1	2	0.5	0.25	$1x10^{-5}$	$1x10^{-6}$	0.10

corresponding to the amplitude of sin ωt and cos ωt, respectively. The current $I_{1f}(\theta)$ at the phase-angle, θ is given by the following equation:

$$I_{1f}(\theta) = I_{1f}\cos(\phi - \theta). \qquad (3\text{-}11)$$

For the dc part of the theoretical calculation, the following approximation was used:

$$\exp(x^2)\operatorname{erfc}(x) \simeq (2/\sqrt{\pi})\int_{x}^{x+z} \exp(x^2 - u^2)du\,. \qquad (3\text{-}12)$$

A value of 10 for z in Eq. (3-12) is adequate to obtain a quasi-reversible theoretical ac polarogram[8].

The selected parameters in the calculation are n_1, n_2(number of electrons transferred in the first and the second heterogeneous charge transfer steps, respectively), α_1, α_2(transfer coefficients), $k_{s,1}$, $k_{s,2}$(heterogeneous rate constants) and $(E^r_{1/2,1} - E^r_{1/2,2})$(difference between the two reversible half wave potentials). Some of the typical theoretical polarograms obtained are shown in Fig. 3-3. The values of parameters used for the calculation are given in Table 3-1.

The following predictions can be derived from the calculations:

(1) α_1 and α_2 determine the width of the peak, as is the case for one step quasi-reversible process[10,13].

(2) The shoulder S1 appears only when $k_{s,1}$ is of the order of 10^{-4} cms^{-1} and α_1 is smaller than 0.5.

(3) The shape of the shoulder S2 changes according to

the ratio ($k_{s,1}/k_{s,2}$), the potential difference($E^r_{1/2,1} - E^r_{1/2,2}$) and the frequency.

The polarograms in Fig. 3-3(A) look quite similar to the experimental ones. In order to determine the kinetic parameters, a curve fitting procedure of the ac polarograms was performed by taking the values used for the polarograms in Fig. 3-3(A) as initial values. The flow chart for the procedure is given in Fig. 3-4. The FORTRAN programs have been written in quadruple precision. The curves were fitted by employing the gradient-expansion algorithm of Marquart[15]. Gans concluded[16] that the Marquart approach was a useful general purpose method for nonlinear least squares problems arising in data fitting. This method has already been used in the deconvolution of electrochemical data by Boudreau and Perone[17].

The curve fittings were performed for nineteen polarograms. The results are given in Table 3-2 together with the relevant experimental constants and related parameters. Figure 3-5 shows the best fit for the theoretical and experimental ac polarograms 1f(0°) and 1f(45°). The agreement is good if one considers that the theoretical calculation is based on a simple model of EE mechanism coupled with stationary plane diffusion. The change of shape of the 45° component with frequency matches the experimental results very well, probably because the

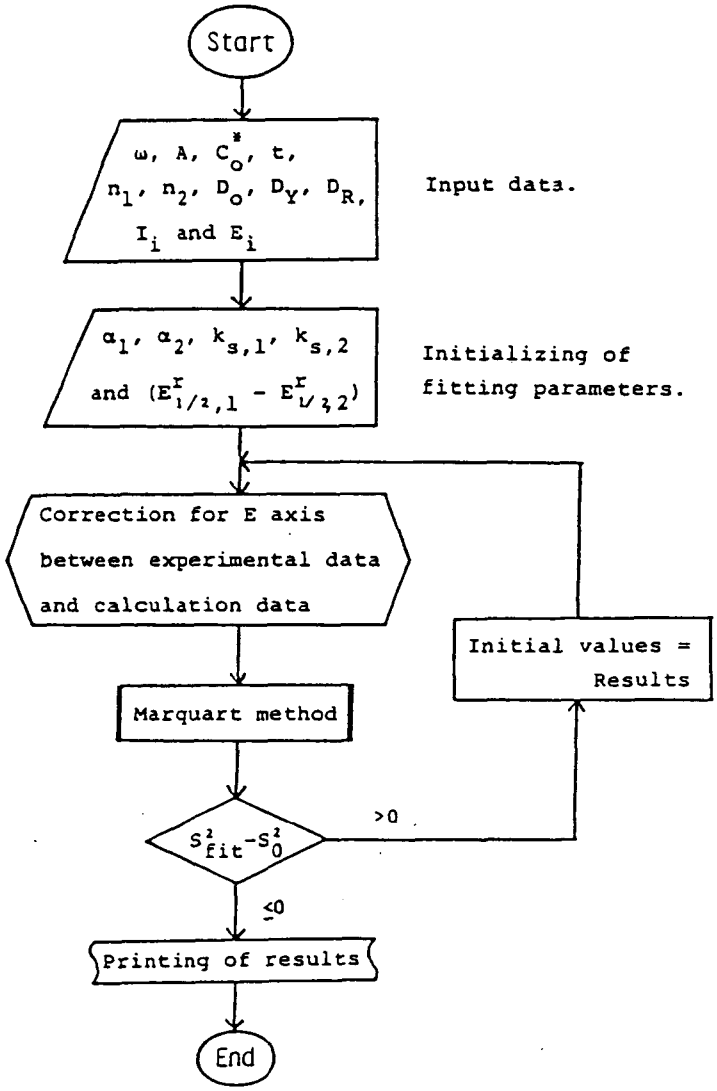

Fig. 3-4. Flow chart for curve fitting. I_i: experimental alternating current; E_i: experimental dc potential; $I(E_i)$: calculated alternating current; $S^2_{fit} = \sum[I_i - I(E_i)]^2$.

Table 3-2. Fitting parameters and other constants for curve fitting.

Parameter	9 Hz		15 Hz			30 Hz		50 Hz		
	0°	90°	0°	45°	90°	0°	90°	0°	45°	90°
α_1	0.19	0.22	0.19	0.19	0.17	0.19	0.17	0.18	0.18	0.18
α_2	0.63	0.84	0.54	0.50	0.51	0.52	0.47	0.54	0.53	0.52
$10^5 k_{s,1}$ /cms^{-1}	5.3	4.8	5.0	6.5	10.1	5.3	9.4	4.7	10.0	11.0
$10^3 k_{s,2}$ /cms^{-1}	1.8	0.3	1.9	2.2	1.2	2.3	7.2	1.9	1.4	2.3
$E^r_{1/2,1}-E^r_{1/2,2}$/V	0.18	0.26	0.20	0.21	0.17	0.20	0.21	0.21	0.19	0.27

Parameter	100 Hz		200 Hz		300 Hz		500 Hz			Average
	0°	90°	0°	90°	0°	90°	0°	45°	90°	
α_1	0.19	0.17	0.18	0.17	0.20	0.18	0.18	0.17	0.17	0.18±0.01
α_2	0.53	0.48	0.53	0.51	0.55	0.49	0.53	0.51	0.51	0.54±0.08
$10^5 k_{s,1}$ /cms^{-1}	4.7	9.8	6.0	10.0	2.1	12.0	6.0	10.1	10.1	7.5±2.9
$10^3 k_{s,2}$ /cms^{-1}	1.9	6.3	1.8	1.2	2.0	2.0	1.7	1.2	1.2	1.4±0.7
$E^r_{1/2,1}-E^r_{1/2,2}$/V	0.19	0.21	0.17	0.17	0.17	0.23	0.16	0.17	0.17	0.20±0.03

Other constants for curve fitting: $n_1 = 2$, $n_2 = 1$, $A = 0.0327$ cm^2, $t = 4.25$ s, $C_o^* = 5.0\times10^{-3}$ M, $D_o = 9.61\times10^{-6}$ cm^{2}s^{-1}, $D_Y = D_R = 1.0\times10^{-5}$ cm^{2}s^{-1}, $\Delta E_{ac} = 0.005$ V.

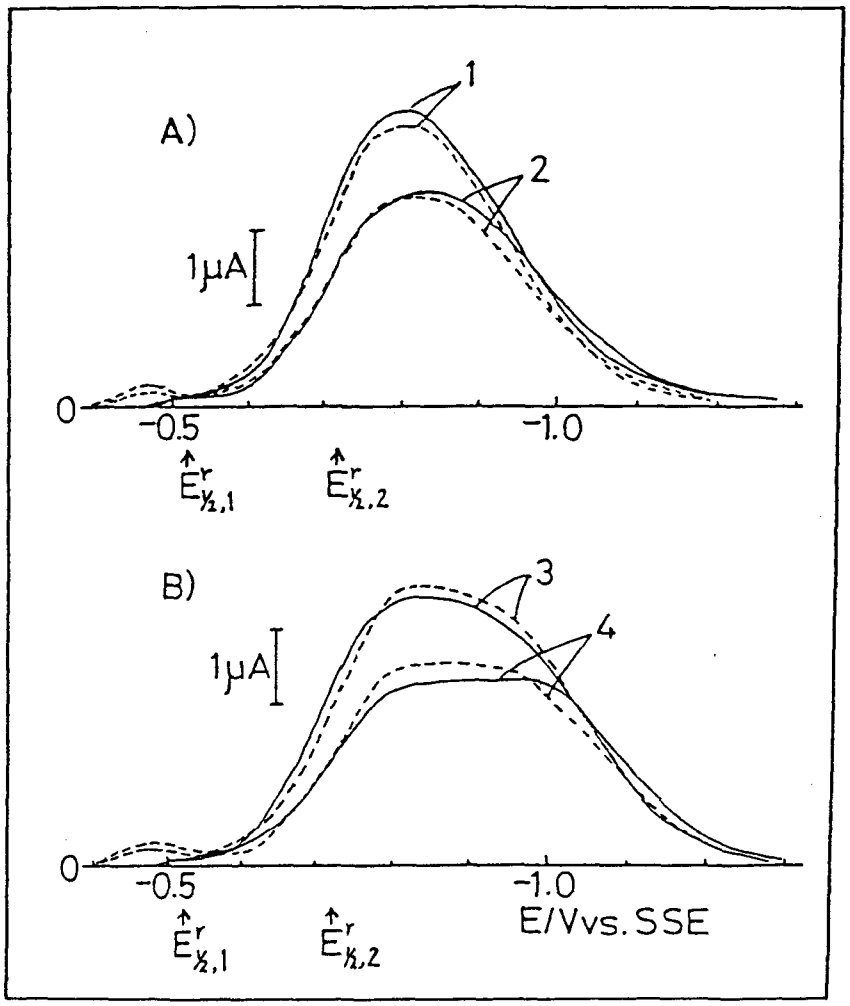

Fig. 3-5. Theoretical and experimented ac polarograms for 5 mM Na_2CrO_4 in 1 M NaOH. (A) 50 Hz, (B) 500 Hz; (1,3) θ = 0°, (2,4) θ = 45°; solid line: experimental; broken lines: theoretical. See Table 3-2 for fitting parameters and other constants.

first step is less reversible than the second, and that S2 is more emphasized in the 45° than in the 0° component. In other words, it is the 45° component which should be used to evaluate the relative rate constants, because its shape is the most sensitive to the ratio ($k_{s,1}/k_{s,2}$).

One can conclude that the electrochemical reduction of chromium(VI) to chromium(III) is controlled by the following stepwise process:

$$Cr(VI) + 2e^- \rightleftharpoons Cr(IV),$$

$$Cr(IV) + e^- \rightleftharpoons Cr(III),$$

and that the first reduction step of Cr(VI) to Cr(IV) is the rate determining step. The kinetic parameters for the Cr(VI) to Cr(III) reaction in 1 M sodium hydroxide solution are $k_{s,1} = (7.5\pm2.9)\times10^{-5}$ cms^{-1}, $k_{s,2} = (1.4\pm0.7)\times10^{-3}$ cms^{-1}, $\alpha_1 = 0.18\pm0.01$, $\alpha_2 = 0.54\pm0.08$, $E^r_{1/2,1} = -0.32$ V vs. NHE and $E^r_{1/2,2} = -0.52$ V.

The redox potential of $E° = -0.39$ V for $Cr(VI) + 3e^-$ $Cr(III)$ calculated from $E^r_{1/2,1}$ and $E^r_{1/2,2}$ may well be compared to the following standard redox potentials to estimate the electrogenerated Cr(III) species. When $[H^+] = 10^{-14}$ M[18],

$$CrO_4^{2-} + 8H^+ + 3e^- \rightleftharpoons Cr^{3+} + 4H_2O \qquad (-0.726 \text{ V}),$$

$$CrO_4^{2-} + 7H^+ + 3e^- \rightleftharpoons Cr(OH)^{2+} + 3H_2O \qquad (-0.526 \text{ V}),$$

$$CrO_4^{2-} + 6H^+ + 3e^- \rightleftharpoons Cr(OH)_2^+ + 2H_2O \qquad (-0.373 \text{ V}),$$

$$CrO_4^{2-} + nH_2O + 5H^+ + 3e^- \rightleftharpoons Cr(OH)_3\cdot nH_2O + H_2O \qquad (-0.133 \text{ V}).$$

Therefore, the Cr(III) could be in the form of $Cr(OH)_2^+$.

The so-called pre-wave in the dc polarogram in neutral or weak alkaline solutions has been studied by Tondeur et al.[2], who reported that its shape and current change with the supporting electrolytes. They have explained it in terms of double layer effects. The experiments indicated that the shoulder(S1) in 1f(0°) does not correspond to the so-called pre-wave, because the peak current in 2f(90°) corresponding to the S1 in 1 M sodium hydroxide decreases with frequency, while that of the pre-wave in sodium chloride is independent of frequency.

Appendix III. Alternating current polarogram with multi-step charge transfer(EE mechanism)

Q, Y and Z in Eqs. (3-4)-(3-7) can be written as follows[8]:

$$Q = g_1(\omega, \lambda_i, j_i) = 4[1 - (1 + e^{-j_1})(1 + e^{j_2})]^2/(1 + e^{-j_1})^2 \times (1 + e^{j_2})^2 + 4(2\omega)^{1/2}[(1 + e^{-j_1})(1 + e^{j_2}) - 1](\lambda_1 + \lambda_2)/(1 + e^{-j_1})(1 + e^{j_2})\lambda_1\lambda_2 + 4\omega(\lambda_1 + \lambda_2)^2/\lambda_1^2\lambda_2^2 + 2(2\omega)^{3/2} \times (\lambda_1 + \lambda_2)/\lambda_1^2\lambda_2^2 + (2\omega)^2/\lambda_1^2\lambda_2^2 \quad , \qquad \text{(III-1)}$$

$$Y = g_2(\omega, \lambda_i, j_i, n_i) = n_1^2 G_1(t)[(1 + e^{j_2} + n_2/n_1) \times$$

$$[(1 + e^{j_2})(1 + e^{-j_1}) - 1]/(1 + e^{-j_1})(1 + e^{j_2})^2 +$$
$$(2\omega)^{1/2}[n_1(1 + e^{j_2}) + n_2](\lambda_1 + \lambda_2)/n_1(1 + e^{j_2})\lambda_1\lambda_2 +$$
$$2\omega[\lambda_1 + \lambda_2[(n_2 + 2n_1(1 + e^{j_2})]/2n_1(1 + e^{j_2})]/\lambda_1\lambda_2^2 +$$
$$(2\omega)^{3/2}/2\lambda_1\lambda_2^2] + n_2^2G_2(t)[(1 + e^{-j_1} + n_1/n_2)[(1 + e^{j_2})\times$$
$$(1 + e^{-j_1}) - 1]/(1 + e^{-j_1})^2(1 + e^{j_2}) + (2\omega)^{1/2}[n_2(1 + e^{-j_1})$$
$$+ n_1](\lambda_1 + \lambda_2)/n_2(1 + e^{-j_1})\lambda_1\lambda_2 + 2\omega[\lambda_2 + \lambda_1[n_1 +$$
$$2n_2(1 + e^{-j_1})/2n_2(1 + e^{-j_1})]/\lambda_1^2\lambda_2] + (2\omega)^{3/2}/2\lambda_1^2\lambda_2] \quad , \tag{III-2}$$

$$Z = g_3(\omega, \lambda_i, j_i, n_i) = n_1^2G_1(t)[(1 + e^{j_2} + n_2/n_1)\times$$
$$[(1 + e^{j_2})(1 + e^{-j_1}) - 1]/(1 + e^{-j_1})(1 + e^{j_2})^2 +$$
$$(2\omega)^{1/2}[(1 + e^{j_2})(1 + e^{-j_1}) - 1]/(1 + e^{-j_1})(1 + e^{j_2})\lambda_2 +$$
$$\omega[n_1(1 + e^{j_2})\lambda_1 - n_2\lambda_2]/n_1(1 + e^{j_2})\lambda_1\lambda_2^2] + n_2^2G_2(t)\times$$
$$[(1 + e^{-j_1} + n_1/n_2)[(1 + e^{j_2})(1 + e^{-j_1}) - 1]/(1 + e^{-j_1})^2\times$$
$$(1 + e^{j_2}) + (2\omega)^{1/2}[(1 + e^{j_2})(1 + e^{-j_1}) - 1]/(1 + e^{-j_1})\times$$
$$(1 + e^{j_2})\lambda_1 + \omega[n_2(1 + e^{-j_1})\lambda_2 - n_1\lambda_1]/n_2(1 + e^{-j_1})\lambda_1^2\lambda_2] \quad , \tag{III-3}$$

where Gl(t) and G2(t) are expressed by the equations:

$$G_1(t) = [1/(1 + e^{-j_1}) + \psi_{2,0}(t)(1 + e^{-j_2})/\lambda_2(1 + e^{-j_1}) +$$
$$\psi_{1,0}(t)(\alpha_1 + \alpha_1e^{-j_2} - \beta_1e^{j_1})/\lambda_1]/(1 + e^{-j_2} + e^{j_1}) \quad , \tag{III-4}$$

$$G_2(t) = [1/(1 + e^{j_2}) - \psi_{1,0}(t)(1 + e^{j_1})/\lambda_1(1 + e^{j_2}) -$$
$$\psi_{2,0}(t)(\beta_2 + \beta_2e^{j_1} - \alpha_2e^{-j_2})/\lambda_2]/(1 + e^{-j_2} + e^{j_1}) \quad , \tag{III-5}$$

where

$$\psi_{1,0}(t) = [\lambda_1/(1 + e^{j_1})(\chi_- - \chi_+)][(\chi_- - \lambda_2)\times$$
$$\exp(\chi_-^2t)\operatorname{erfc}(\chi_-t^{1/2}) - (\chi_+ - \lambda_2)\exp(\chi_+^2t)\operatorname{erfc}(\chi_+t^{1/2})], \tag{III-6}$$

$$\psi_{2,0}(t) = [\lambda_1\lambda_2/(\chi_- - \chi_+)(1 + e^{j_1})(1 + e^{j_2})]\times$$
$$[\exp(\chi_+^2 t)\mathrm{erfc}(\chi_+ t^{1/2}) - \exp(\chi_-^2 t)\mathrm{erfc}(\chi_- t^{1/2})], \quad \text{(III-7)}$$

where

$$\chi_\pm = [\lambda_1 + \lambda_2 \pm [(\lambda_1 + \lambda_2)^2 - 4K]^{1/2}]/2, \quad \text{(III-8)}$$

$$K = \lambda_1\lambda_2[e^{j_2} + e^{-j_1} + e^{(j_2 - j_1)}]/(1 + e^{j_2})(1 + e^{-j_1}). \quad \text{(III-9)}$$

And D, f, and E in Eqs. (3-9) and (3-10) are obtained from the relations:

$$D_1 = D_O^{\beta_1} D_Y^{\alpha_1},\ D_2 = D_Y^{\beta_2} D_R^{\alpha_2},\ f_1 = f_O^{\beta_1} f_Y^{\alpha_1},\ f_2 = f_Y^{\beta_2} f_R^{\alpha_2},$$
$$\beta_i = 1 - \alpha_i, \quad \text{(III-10)}$$

$$E^r_{1/2,1} = E^\circ_1 - (RT/n_1F)\ln(f_Y/f_O)(D_O/D_Y)^{1/2}, \quad \text{(III-11)}$$

$$E^r_{1/2,2} = E^\circ_2 - (RT/n_2F)\ln(f_R/f_Y)(D_Y/D_R)^{1/2}. \quad \text{(III-12)}$$

On the other hand, the dc polarographic current is obtained from the following equation:

$$i_{dc}(t) = FAC_O^* D_O^{1/2}[n_1\psi_{1,0}(t) + n_2\psi_{2,0}(t)]. \quad \text{(III-13)}$$

3-4. References

1 J.J. Lingane and I.M. Kolthoff, J. Am. Chem. Soc., 62(1940)852.

2 J.J. Tondeur, A. Dombret and L. Gierst, J. Electroanal. Chem., 3(1962)225.

3 I.R. Miller, J. Electroanal. Chem., 15(1967)49.

4 T. Berzins and P. Delahay, J. Am. Chem. Soc., 75(1953)5716.

5 P. Delahay and C.C. Mattax, J. Am. Chem. Soc., 76(1954)874.

6 A. Saito, Nippon Kagaku Zasshi, 82(1961)718.

7 P.F. Urone, M.L. Drushel and H.K. Aanders, Anal. Chem., 22(1950)472.

8 H.L. Hung and D.E. Smith, J. Electroanal. Chem., 11(1966)425.

9 N.H. Furman(Ed.), Standard Methods of Chemical Analysis, Vol. 1, 6th ed., Van Norstrand, New York, 1962, Chap. 15.

10 D.E. Smith, Crit. Rev. Anal. Chem., 2(1971)247.

11 E.R. Brown, D.E. Smith and G.L. Booman, Anal. Chem., 40(1968)1411.

12 D.E. Smith in A.J. Bard(Ed.), Electroanalytical Chemistry, Vol. 1, Dekker, New York, 1966, p. 1.

13 D.E. Smith and T.G. McCord, Anal. Chem., 40(1968)474.

14 H. Matsuda, Z. Elektrochem., 62(1958)977.

15 P.R. Bevington, Data Reduction and Error Analysis for the Physical Sciences, McGraw-Hill, New York, 1969, p. 235.

16 P. Gans, Coord. Chem. Rev., 19(1976)99.

17 P.A. Boudreau and S.P. Perone, Anal. Chem., 51(1979)811.

18 G. Milazzo and S. Caroli, Tables of Standard Electrode Potentials, Wiley, Chichester, 1978, p. 258.

Chapter 4. On the polarographic reduction of nitrate ion in the presence of zirconium(IV)

4-1. Introduction

It is well known that nitrate ion produces polarographic waves in certain supporting electrolytes[1-5].

Tokuoka and Ruzicka[1,2] studied the polarography of nitrate ion in the presence of mono-, di- and trivalent cations. They suggested that the nitrate is reduced by splitting into its elementary ions(N^{5+} and O_3^{6-}) in the strong electric field existing in the proximity of the dropping mercury electrode(DME), high-valency cations serving to drag the anion close to the DME interface. Therefore, the DME interface should be investigated. For the effect of high-valence elements upon the polarographic reduction of the nitrate, zirconium(IV) as a tetravalent element has been selected. There is no agreement among previous investigators[6,7] on the mechanism of the reduction of nitrate ion in the presence of this element. Mechelynck and Mechelynck-David[6] concluded that, for the

reduction mechanism, Zr^{4+} ion acts as a catalyst through the reaction $ZrO^{2+} + 2H^{+} \rightleftharpoons Zr^{4+} + H_2O$ in the DME interface. Wharton[7] argued for a mechanism, in which the polarographic reduction of the nitrate ion is not catalytic but rather involves the reduction of distinct zirconium(IV)-nitrate complexes.

As mentioned in chapter 1, the 1f(0°) and 1f(90°) modes of the phase selective ac polarography are valid for a study on the specific adsorption of electrolyte ions on the DME .

In this chapter, therefore, the mechanism of the reduction of the nitrate in the presence of the zirconium(IV) ion was investigated by means of dc and phase-selective ac polarography. As the reduction products in this system have never been eatablished, they were studied by controlled-potential electrolysis(CPE) and by a qualitative and quantitative analysis. In order to investigate the vicinity of the electrode, the differential capacity was measured by ac polarography.

4-2. Experimental

Analytical-reagent grade chemicals were used as received. A stock solution of zirconium(IV) was prepared

from zirconium oxychloride octahydrate($ZrOCl_2 \cdot 8H_2O$), and its concentration was determined gravimetrically as zirconium oxide with cupferron (ammonium nitrosophenylhydroxylamine)[8]. The stock solution was allowed to age for at least two weeks prior to use, in order to eliminate the ageing effect of zirconium solution[7]. The stock solution of sodium nitrate was determined gravimetrically with nitron (3,4,6-triphenyl-2,3,5,6-tetraazabicyclo[2.1.1] hex-1-ene)[9].

The working electrode for dc and ac polarography was the DME; the mercury flow rate was 1.150 mgs^{-1} at a height of 70 cm and the drop time was 5.78 s in water at open circuit.

A hand-made coulomb counter[10] was used in the CPE coulometry. An H-type cell was used in the CPE. The working electrode was a mercury pool. The supporting electrolyte solution was degassed and pre-electrolyzed at -0.9 V vs. SSE(saturated silver chloride electrode[Ag/AgCl, sat.KCl]), and the solution was again pre-electrolyzed at -0.3 V after addition of the degassed nitrate solution. The sample solution was electrolyzed at -0.9 V until the current reached the base current of the pre-electrolysis.

The differential capacity was obtained by using phase-selective ac polarography(cf. Appendix IV). The

results of 0.1 M KCl solution was ±2.5 % of those of Grahame[11]. The electrocapillary maximum(ecm) was measured by a drop time method. The ecm of 0.1 M KCl solution was -0.508 V vs. NCE(-0.506 V according to Grahame[11]). The surface tention of 0.1 M KCl solution at the ecm was taken 426.7 mNm^{-1} at 25 °C[12].

Raman spectra were measured with a JASCO R 800, using 514.5 nm(Ar^{+}) laser as the excitation source.

Spectrophotometric measurements in the wave length range 200-900 nm were carried out with a HITACHI 228 spectrophotometer.

4-3. Results and discussion

4-3-1. Influence of solution composition on the dc polarographic waves

The dc polarograms of nitrate ion in the presence of zirconium(IV) salts were similar to those of Mechelynck and Mechelynck-David[6] and Wharton[7].

The first wave was observed between -0.7 and -1.1 V vs. SSE and the second was between -1.4 and -1.5 V. The dependence of i_d(dc plateau current) for the first and second waves on the concentration of sodium nitrate is

plotted in Fig. 4-1. Log(i_d/μA) for the first wave varies linearly with log($C_{NO_3^-}$/M) for the range 2.0×10^{-6} - 4.0×10^{-3} M and the slope is one. In the concentration range > 4.0×10^{-3} M, i_d is practically constant. The results indicate that the first wave is suitable for the quantitative analysis of nitrate in a wide concentration range.

As the concentration of nitrate(pH 2.93±0.02) increases, the second wave decreases and the i_d of the first wave is limited by the proton concentration. The protons around the DME are consumed and exhausted by the reduction of nitrate ions.

The i_ds of the first and second waves change linearly with the square root of the mercury height but the lines does not go through the origin. This suggests that both the polarographic reduction of the nitrate ion and that of the proton are controlled by a diffusion and a chemical reaction.

Figure 4-2(A) shows the change of the dc polarograms with the concentration of zirconium(IV). The dependence of i_d(the current at -1.2 V) on the concentration of zirconium(IV) is given in Fig. 4-2(B). For the first wave, at a low concentration of zirconium(IV), no plateau current is observed. As the concentration of zirconium(IV) increases, it is better defined. At a high concentration

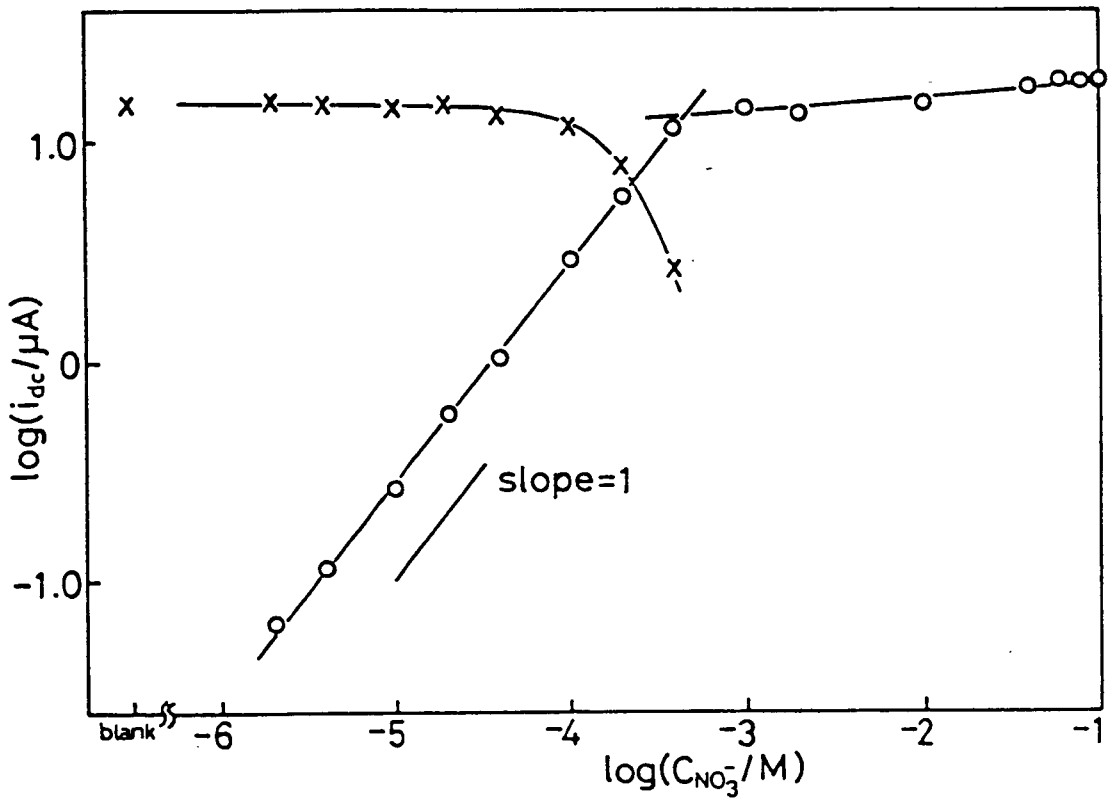

Fig. 4-1. The dependence of i_d on $C_{NO_3^-}$. x M $NaNO_3$ + y M $NaClO_4$ + 0.2 mM $ZrOCl_2$ + 1 mM $HClO_4$, x + y = 0.1, pH = 2.93±0.02, (O) 1st wave; (X) 2nd wave.

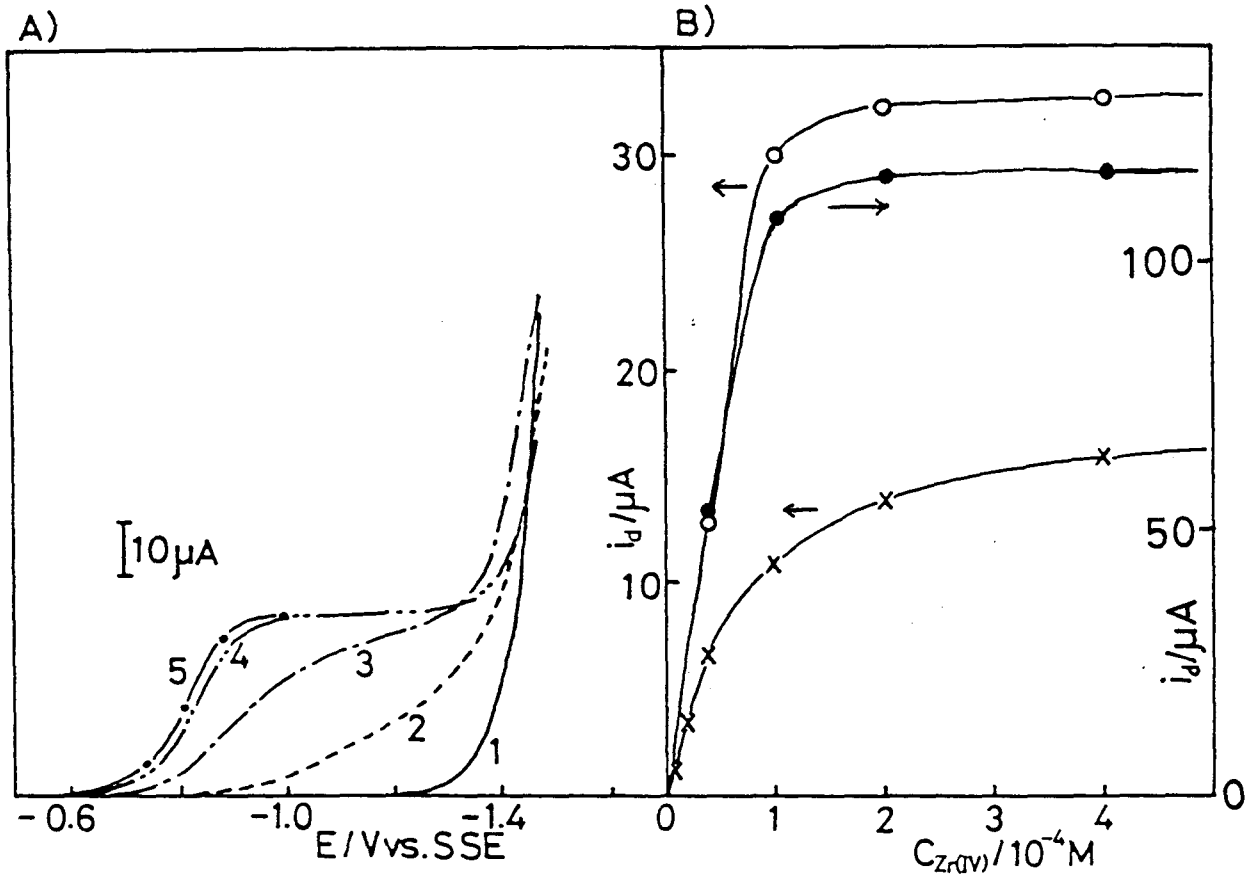

Fig. 4-2. (A) Dc polarograms of nitrate in the presence of various concentrations of zirconium(IV). 1 mM $NaNO_3$ + 0.01 M $HClO_4$ + 0.09 M $NaClO_4$; $C_{Zr(IV)}$: (1) 0, (2) 0.02, (3) 0.1, (4) 0.2, (5) 0.4 mM. (B) The dependence of i_d upon $C_{Zr(IV)}$. (X) 1 mM $NaNO_3$ + 1 mM $HClO_4$ + 0.1 M $NaClO_4$, pH = 2.95±0.05; (O) 1 mM $NaNO_3$ + 0.01 M $HClO_4$ + 0.09 M $NaClO_4$, pH = 2.02±0.02; (●) 0.05 M $NaNO_3$ + 0.01 M $HClO_4$ + 0.04 M $NaClO_4$, pH 2.02±0.03.

of zirconium(IV)(about 0.2 mM) the i_d levels off. These results suggest that for the reduction of nitrate, only a certain amount of zirconium(IV)(about 0.2 mM) is needed.

The dependence of i_d and $E_{1/2}$(halfwave potential) for the reduction of nitrate on pH in the bulk solution is given in Figs. 4-3(A) and (B), respectively. When the proton is in excess of the nitrate, both i_d and $E_{1/2}$ are practically independent of pH. When there is a proton deficiency for the reduction of nitrate, $\log(i_d/A)$ changes linearly with the pH(slope is -1) and the $E_{1/2}$ varies linearly with the pH(slope is about 120 mV). The positive slope($\delta E_{1/2}/\delta pH$) shows that the greater is the concentration of proton, the less is the nitrate reducible in the presence of zirconium(IV).

4-3-2. Total electrode reaction.

As n(the number of electrons in the charge transfer step) including the total electrode reaction has never been decided for this system, the CPE coulometry was employed. In the solution[(0.01 M $HClO_4$ + 0.09 M $NaClO_4$ + 1 mM $ZrOCl_2$)25 ml + (25 mM $NaNO_3$)1 ml] n was 5.8±0.4. After the CPE, the sample solution gave positive results with Tollens reagent and for the TTC(2,3,5-triphenyltetrazolium

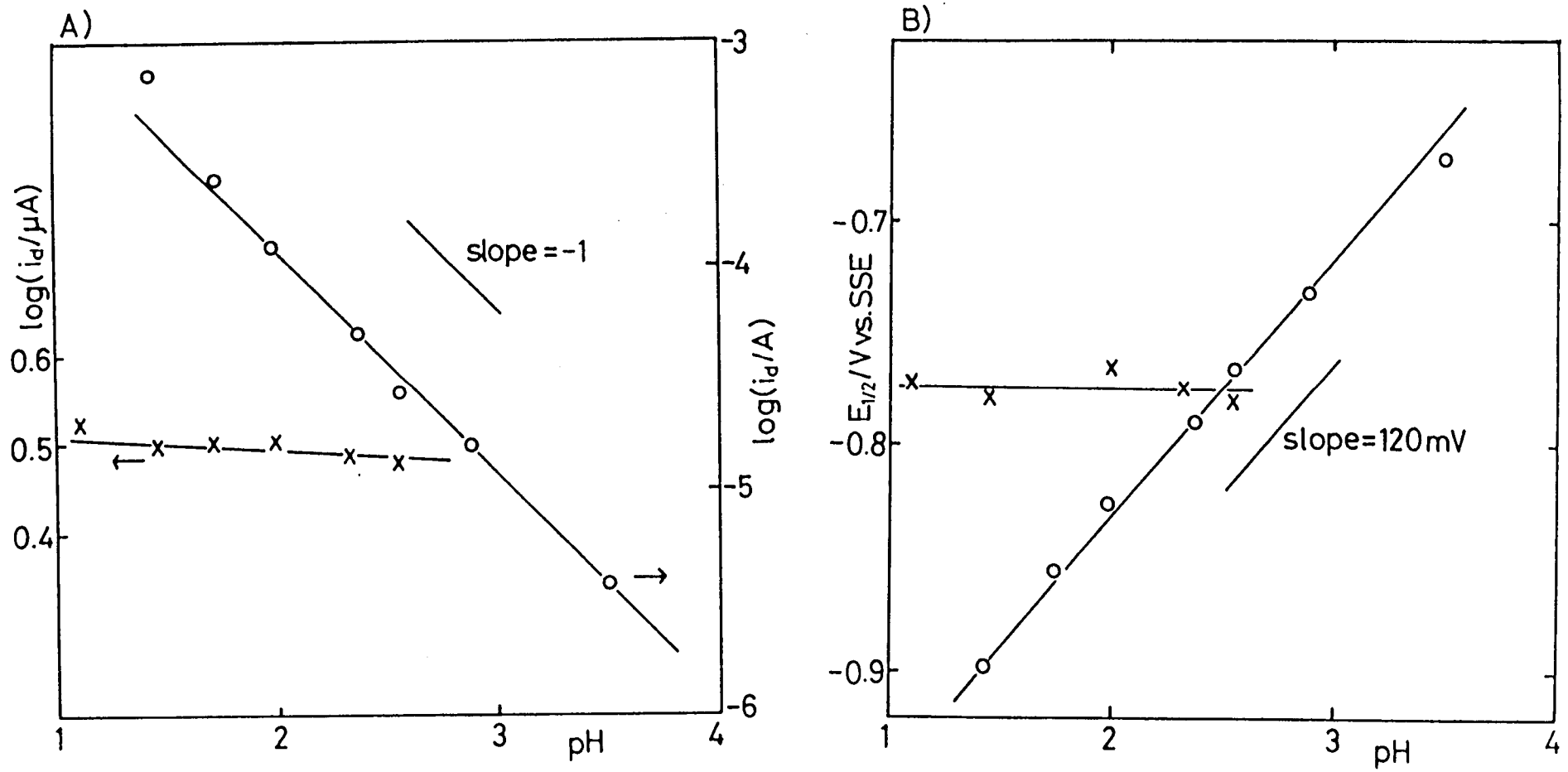

Fig. 4-3. The dependence of (A) i_d and (B) $E_{1/2}$ on pH. (O) 0.2 mM $ZrOCl_2$ + 0.05 M $NaNO_3$ + x M $HClO_4$ + y M $NaClO_4$, x + y = 0.05; (X) 1 mM $ZrOCl_2$ + 0.1 mM $NaNO_3$ + x M $HClO_4$ + y M $NaClO_4$, x +y = 0.1.

chloride) spot test[13]. The solution gave a negative result with Nessler's reagent. The results shows that hydroxylamine is in the solution after CPE and the ammonium ion is not(cf. in $LaCl_3$ and $CeCl_3$, the chief products were hydroxylamine and ammonia, n was 6.1-7.2[5]). The hydroxylamine in the solution after CPE was determined quantitatively by means of dc polarography at pH 6.3(with $K_2H_2PO_4$ + Na_2HPO_4 buffer)[14]. 92.4±0.4 % of the available nitrate ion changed to hydroxylamine in the CPE. Therefore, it is infered that the total reduction of nitrate in the presence of zirconium(IV) chiefly follows the reaction:

$$NO_3^- + 8H^+ + 6e^- \rightleftharpoons NH_2OHH^+ + 2H_2O \ .$$

4-3-3. The role of zirconium(IV).

The nitrate anion is reduced at more positive potentials (1.2-1.5 V) in the presence of a small amount of zirconium(IV)[Fig. 4-3(B)) than in only univalent cation supporting electrolyte[2].

Mechelynck and Mechelynck-David[6] asserted that Zr^{4+} ion was a catalyst for the reduction of nitrate. If the Zr^{4+} is produced by the reaction, $ZrO^{2+} + 2H^+ \rightleftharpoons Zr^{4+} + H_2O$, the lower is the pH, the more is the nitrate ion reducible; but Fig. 4-3(B) shows the contrary.

Wharton argued[7] that the reduction was not catalytic but rather involved the reduction of distinct zirconium(IV)-nitrate complexes. If such complexes are produced, a band will appear in Raman spectra, at about 750 cm^{-1} in addition to the band at 715 cm^{-1}(free solvated nitrate ion)[15,16]. In this system, however, the band assigned to the complexes in the bulk solution did not appear in any solution(0-0.01 M $HClO_4$ + 0-0.1 M $ZrOCl_2$ + 0.01-2 M $NaNO_3$). UV spectra were also measured. A band at about 300 nm for nitrate[17,18] did not change in shape or absorption maximum(301.4±0.7 nm) in any solution(0-0.01 M $HClO_4$ + 0-0.05 M $ZrOCl_2$ + 1-10 mM $NaNO_3$). Thus, evidence for complexes in the bulk solution in this system were not found from the Raman and UV spectra.

4-3-4. Electrode interface.

Complexes are not produced in the bulk solution. Only 0.2 mM zirconium(IV) is necessary for the reduction of the nitrate ion[Fig. 4-2(B)]. Considering these results, the zirconium(IV) may adsorb on the DME and largely change the double-layer capacity.

Accordingly, in order to obtain the differential capacity and the potential of the outer Helmholtz plane

(ϕ_2), the impedance in this system was measured by means of phase-selective ac polarography. The solution components were made up such that the ionic strength was constant and the activity coefficient was also constant. The differential capacity was analyzed by the same method as used by Grahame and Soderberg[19] ($\Gamma_{salt}^{ecm} = 0.0\ \mu Ccm^{-2}$, $(\partial E^{-}/\partial\mu)^{ecm} = 0.305$, $C_{+}^{ecm} = 9.59\ \mu Fcm^{-2}$ in the solution, 0.01 M HCl + 0.09 M NaCl + 0.2 mM $ZrOCl_2$)(cf. Appendix IV).

The differential capacity in the presence of zirconium(IV) changed a little from that in its absence (Fig. 4-4). No large capacity difference which might be assigned to strong adsorption was found. The differential capacity in the presence of the nitrate ion at more positve potentials than that at which the nitrate ion is reduced, was the same as that in its absence. The plot of ϕ_2 vs. the dc potential is given in Fig. 4-5. Though there is a difference in the distance of closest approach of the ions[20], ϕ_2 was calculated as a solution of 0.1 M MeCl(Me indicates univalent cation), because an aqueous solution of $ZrOCl_2 \cdot 8H_2O$ exhibits the same pH as a hydrochloric acid solution of the same concentration, $ZrOCl_2 + H_2O \rightleftharpoons ZrO(OH)^{+} + H^{+} + 2Cl^{-}$.

From the data of Grahame and Soderberg[19], it follows that the product of the cation charge and its concentration being equal, the higher the valence of the cation is(in

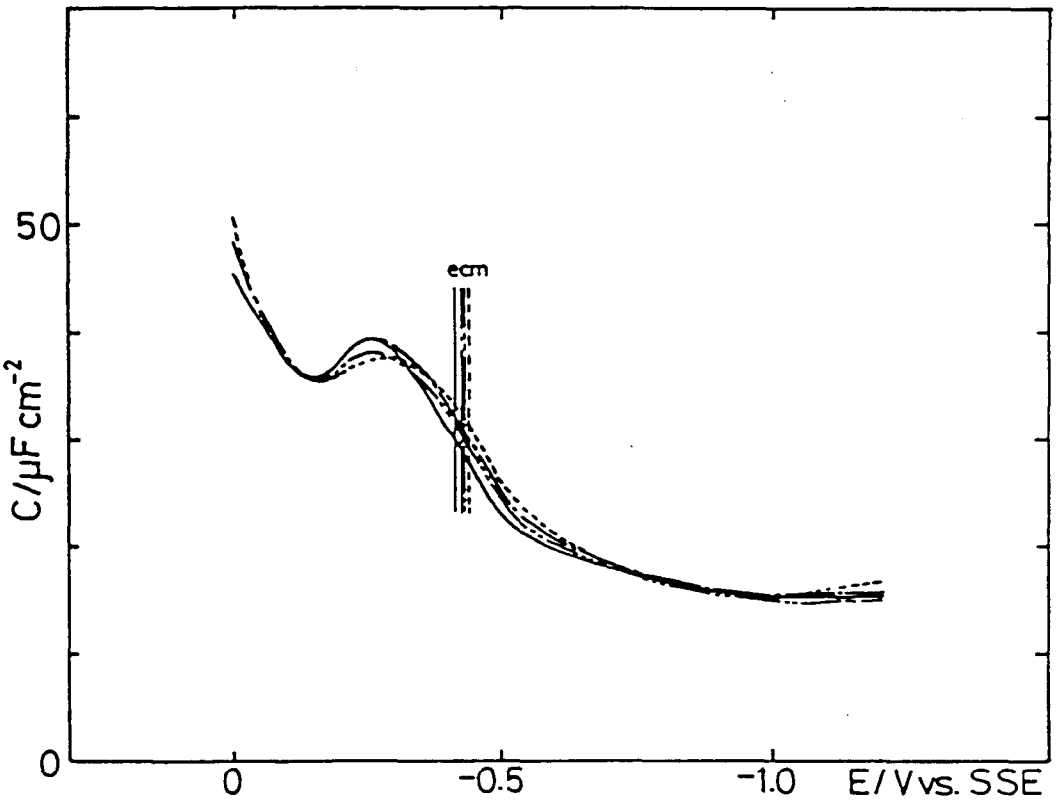

Fig. 4-4. The differential capacity of a solution containing various concentrations of zirconium(IV). $C_{Zr(IV)}$; (———) 0, (—·—) 2×10^{-5}, (— — —) 4×10^{-5}, (-----) 2×10^{-4} M in 0.01 M HCl + 0.09 M NaCl.

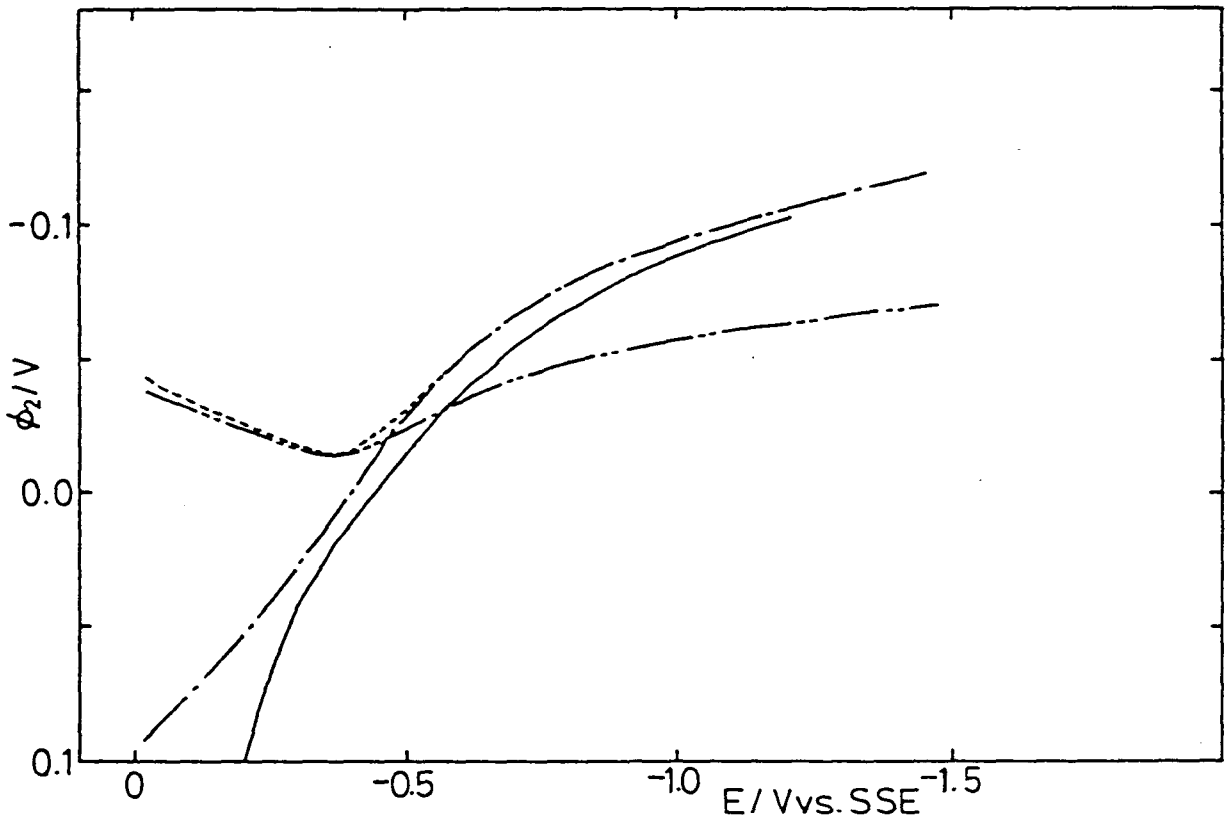

Fig. 4-5. Plots of ϕ_2 vs. dc potential. (1, ——) 0.2 mM $ZrOCl_2$ + 0.01 M HCl + 0.09 M NaCl, (2, - - - - -) 0.1 M KCl, (3, — - —) 0.1 M KF, (4, — · · —) 0.05 M $BaCl_2$; (2,3,4) data from ref. 19.

this system, if the species of zirconium(IV) is a polymer[21-25]), the nearer ϕ_2 comes to zero, even if the dc potential is far more negative than the ecm.

Therefore, the difference in ϕ_2 at the reduction potential of nitrate in the absence and presence of zirconium(IV) seems to be at most 0.10-0.15 V. On the other hand, the difference of the reduction potential of nitrate in the absence and presence of zirconium(IV) is 1.2-1.5 V. Consequently, the contribution of ϕ_2 to the difference of the reduction potential of nitrate is at most about 10 %. In other words, the mass transfer of nitrate ion to the vicinity of the electrode against the negative charge of electrode is not a very important process for the reduction of nitrate ion. Therefore, a large part of the difference of the reduction potential seems to be in the charge transfer step and/or in a chemical reaction step in the vicinity of the DME.

Figure 4-6 shows the relationship between the reduction potential of nitrate ion in the presence of various metal ions and the reduction potential of the metal ion to the metal[26]. It is thought that the metal ion acts as a intermediary for the charge transfer of the electrode to the nitrate ion. Therefore, the more the metal ion is reducible(that is to say, an electrochemical depolarizability), the more the nitrate ion in the presence

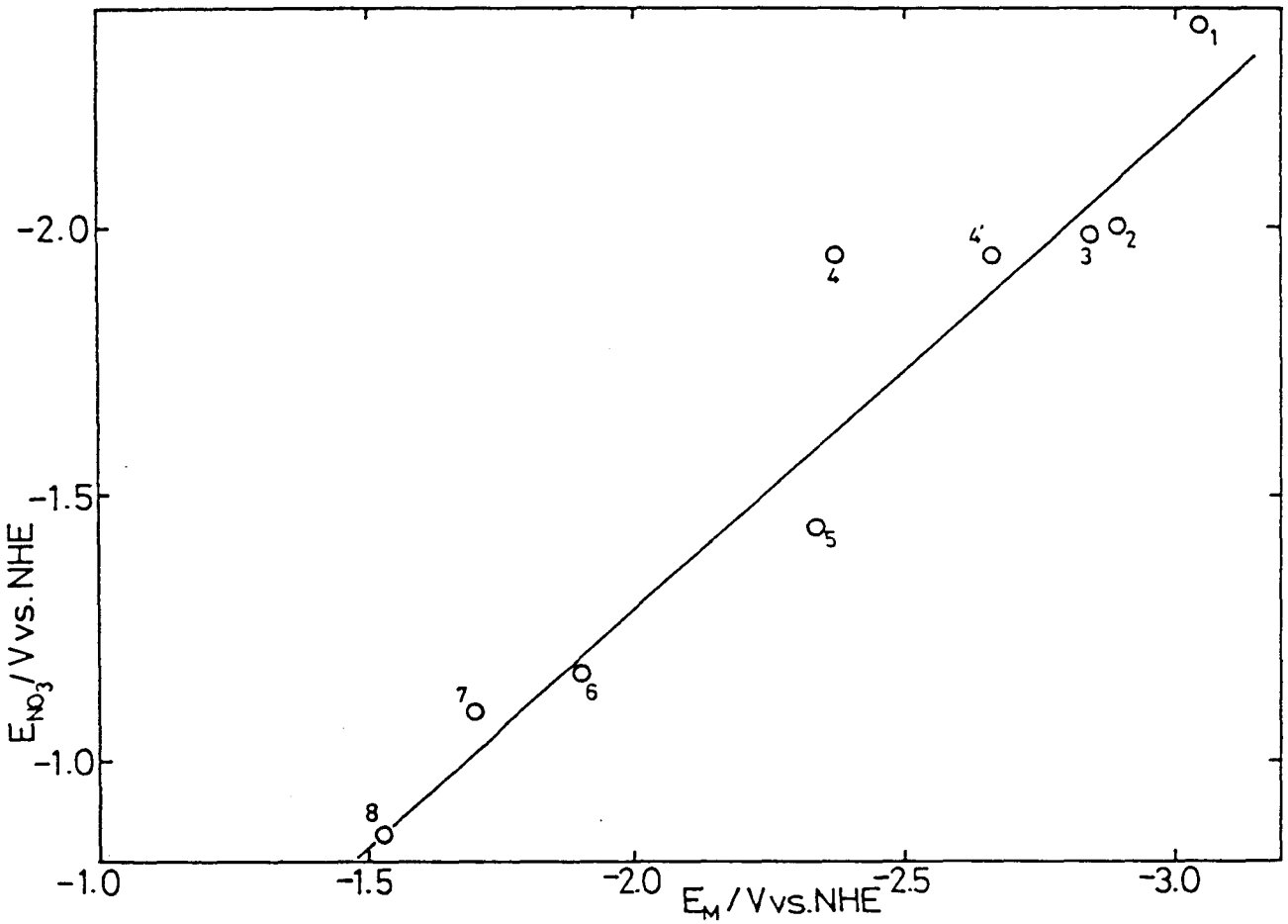

Fig. 4-6. Relationship between the reduction potential ($E_{NO_3^-}$) of nitrate ion in the presence of metal ion and that (E_M) of metal ion to metal. (1) Li(I), (2) Sr(II), (3) Ca(II), (4) Mg(II), (5) Ce(III), (6) Th(IV), (7) Hf(IV), (8) Zr(IV). $E_{NO_3^-}$ data from: (1)-(5) ref. 2; (6) 0.1 M $NaNO_3$ + 0.1 mM $Th(ClO_4)_4$ + 0.005 % gelatin; (7) 0.1 M $NaNO_3$ + 0.01 M $HClO_4$ + 0.2 mM $HfOCl_2$; (8) 0.05 M $NaNO_3$ + 0.05 M $NaClO_4$ + 0.2 mM $ZrOCl_2$. E_M data from ref. 26; (4') Mg(II)/Mg(I).

of the metal ion is also reducible.

Appendix IV. The method for obtaining the differential capacity from phase-selective ac polarographic data, and the relationship between the differential capacity and the potential of the outer Helmholtz plane[19].

The equivalent circuit for the impedance of solution-electrode interface is shown in Fig. IV-1. The impedance Z and admittance Y(=1/Z) of the circuit are as follows:

$$Z = R + L/(j\omega C) \qquad \text{(IV-1)}$$

and

$$Y = R/[R^2 + (1/\omega C)^2] - (1/\omega C)j/[R^2 + (1/\omega C)^2] \qquad \text{(IV-2)}$$

, respectively. The 0° and 90° components of the ac polarographic current at a given dc potential from Ohm's law(I=YE) relate to R and C by the equations:

$$I(0°) = \{R/[R^2 + (1/\omega C)^2]\}\Delta E_{ac}, \qquad \text{(IV-3)}$$

$$I(90°) = \{(1/\omega C)/[R^2 + (1/\omega C)^2]\}\Delta E_{ac}, \qquad \text{(IV-4)}$$

and solving for R and C, the relationships can be obtained:

$$R = \{I(0°)/[I(0°)^2 + I(90°)]\}\Delta E_{ac}\ , \qquad \text{(IV-5)}$$

$$C = \{[I(0°)^2 + I(90°)^2]/I(90°)\}(1/\omega\Delta E_{ac}). \qquad \text{(IV-6)}$$

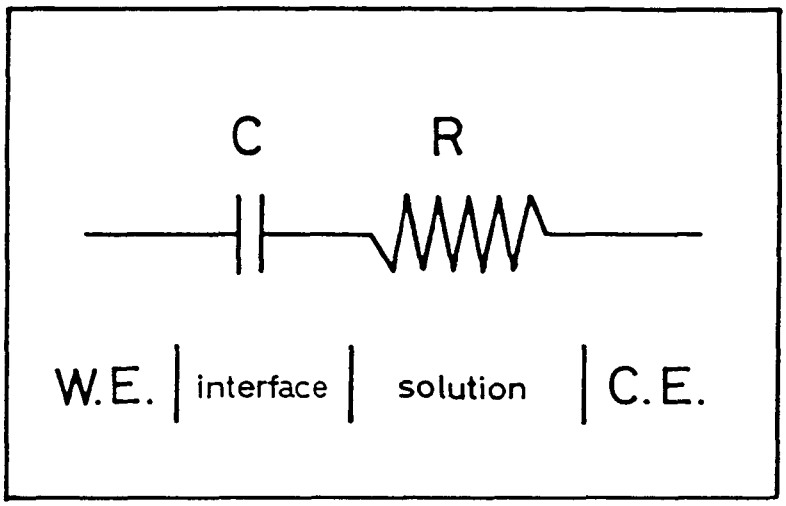

Fig. IV-1. The equivalent circuit of the electrochemical cell, in the case of the supporting electrolyte solution in the absence of a depolarizer.

From the drop time(t/s) at a given dc potential and the mercury flow rate(m/mgs^{-1}), the electrode area(A/cm^2) at the dc potential is given by the equation:

$$A = (4\pi)^{1/3}(3mt/\rho)^{2/3}\times 10^{-2}, \qquad \text{(IV-7)}$$

where ρ/gcm^{-3} is the density of mercury. And the differential capacity(C/Fcm^{-2}) is obtained from Eqs. (IV-6) and (IV-7).

The surface charge density(q/Ccm^{-2}) of the DME can be expressed by the equation:

$$q = \int_{E^{ecm}}^{E} C dE \ , \qquad \text{(IV-8)}$$

where E^{ecm} is the electrocapillary maximum, and the E^{ecm} is obtained by the measurement of the drop time.

On the other hand, q and C are expressed by the equations:

$$q = q_+ + q_-, \qquad \text{(IV-9)}$$

$$q_+ = -z_+F\Gamma_+, \ q_- = -z_-F\Gamma_- \ , \qquad \text{(IV-10)}$$

$$C = C_+ + C_-, \qquad \text{(IV-11)}$$

where $z_+(z_-)$ is the valence of cation(anion), $\Gamma_+(\Gamma_-)$ is the excess of cation(anion), $q_+(q_-)$ is the part of the total surface charge density attributable to the approach or departure of cation(anion) and $C_+(C_-)$ is the part of the total capacity attributable to the approach or departure of cation(anion).

C and C_+ have also relation to μ(the chemical

potential) and E(the dc potential) by the following equation:

$$z_+\nu_+F(\partial C/\partial\mu)_E = -dC_+/dE, \qquad \text{(IV-12)}$$

where ν_+ is the number of cations formed by the dissociation of one molecule of the electrolyte. Therefore, C_+ is obtained by the integration of Eq. (IV-12) as follows:

$$C_+ = \int (dC_+/dE)dE + k$$
$$= z_+\nu_+F\int_{E^{ecm}}^{E} (\partial C/\partial\mu)dE + C_+^{ecm}, \qquad \text{(IV-13)}$$

where

$$C_+^{ecm} = z_+\nu_+FC^{ecm}(\partial E/\partial\mu)^{ecm}. \qquad \text{(IV-14)}$$

And Γ_+ has relation to C_+ by the following equation:

$$z_+F(\partial\Gamma_+/\partial E)_\mu = -C_+. \qquad \text{(IV-15)}$$

Using the relation $z_+F\Gamma_+ = -q_+$, one can obtain on integration of Eq. (IV-15):

$$-q_+ = z_+F\Gamma_+ = \int_{E^{ecm}}^{E} C_+dE + z_+F\Gamma_+^{ecm}, \qquad \text{(IV-16)}$$

where the Γ_+^{ecm} is obtained from the following relationship:

$$(\partial\sigma/\partial\mu)^{ecm} = -\Gamma_{salt}^{ecm} = -\Gamma_+^{ecm}/\nu_+, \qquad \text{(IV-17)}$$

where σ is the interfacial tention of the mercury contact with the inert electrolyte.

For a 1:1 electrolyte, the potential of the outer Helmholtz plane ϕ_2 has relation to Γ_+ by the equation:

$$\phi_2 = -(2RT/z_+)\ln[(z_+F\Gamma_+/K) + 1], \qquad \text{(IV-18)}$$

where

$$K = (RT\varepsilon c/2\pi)^{1/2}, \qquad \text{(IV-19)}$$

where ε means the absolute value of the electronic charge, and c is the concentration of cation.

4-4. References

1 M. Tokuoka, Collect. Czech. Chem. Commun., 4(1932)444.

2 M. Tokuoka and J. Ruzicka, Collect. Czech. Chem. Commun., 6(1934)339.

3 L. Holleck, Z. Physik. Chem. (Leipzig)., 194(1944)140.

4 I.M. Kolthoff and J.J. Lingane, Polarography, 2nd. Ed., Interscience Publishers, New York, 1952, p.533.

5 J.W. Collat and J.J. Lingane, J. Am. Chem. Soc., 76(1954)4214.

6 Ph. Mechelynck and C. Mechelynck-David, Anal. Chim. Acta, 21(1959)432.

7 H.W. Wharton, J. Electroanal. Chem., 9(1965)134.

8 E.C. Olson and P.J. Elving, Anal. Chem., 26(1954)1747.

9 A. Hulanicki and M. Maj, Talanta, 22(1975)767.

10 K. Yokoi, T. Ozeki, I. Watanabe and S. Ikeda, J. Electroanal. Chem., 132(1982)191.

11 D.C. Grahame, J. Am. Chem. Soc., 71(1949)2975.

12 M.A.V. Devanathan and P. Peries, Trans. Faraday Soc., 50(1954)1236.

13 G.A. Snow, J. Chem. Soc., (1954)2594.

14 L. Meites, Polarographic Techniques, 2nd Ed., Wiley, New York, 1965, p.560.

15 D.E. Irish, G. Chang and D.L. Nelson, Inorg. Chem., 9(1970)425.

16 D.L. Nelson and D.E. Irish, J. Chem. Soc. Faraday Trans. 1., 69(1973)156.

17 D.Meyerstein and A. Treinin, Trans. Faraday Soc., 57(1961)2104.

18 E. Rotlevi and A. Treinin, J. Phys. Chem., 69(1965)2645.

19 D.C. Grahame and B.A. Soderberg, J. Chem. Phys., 22(1954)449; D.C. Grahame, Chem. Rev., 41(1947)441.

20 K.M. Joshi and R. Parsons, Electrochim. Acta, 4(1961)129.

21 G.M. Muha and P.A. Vaugham, J. Chem. Phys., 33(1960)194.

22 R.L. Angstadt and S.Y. Tyree, J. Inorg. Nucl. Chem., 24(1962)913.

23 W.P. Griffith and T.D. Wickins, J. Chem. Soc., (1967)675.

24 Y. Shiokawa, A. Sato and S. Suzuki, Bull. Chem. Soc. Jpn., 49(1976)2456.

25 R.E. Connick and W.H. Reas, J. Am. Chem. Soc.,

73(1951)1171.

26 Chemical Society of Japan(Ed.), Kagaku Binran, Kisohen(Databook of Chemistry, Fundamental Volume), 3rd ed., Maruzen, Tokyo, 1984, p.II-474(in Japanese).

Chapter 5. Studies on the behavior of the second derivative polarograms of Pb(II), Tl(I), Cd(II), In(III), Zn(II), Ni(II), Co(II) and Mn(II) in aqueous solutions

5-1. Introduction

As mentioned in Chapter 1, the ac polarographic studies focusing to the analytical aspect, has been reported by several authors[1-10]. The total alternating current polarograms for the reductions of various metal ions have been studied[6]. However, the phase selective mode, especially 2f mode, has never been applied to these systems.

In this chapter, the electrode reactions of several inorganic ions were studied by the ac polarographic analysis based on the phase selective second harmonic ac polarograms. The metal ions employed for the study were lead(II), thallium(I), cadmium(II), indium(III), zinc(II), cobalt(II) and manganese(II) in aqueous solution. The analytical results obtained from 2f mode were compared with those from 1f mode in several aspects, in order to evaluate reliabilities for the application for the chemical analysis.

The benefits of the potential usage of 2f mode is explored and discussed in the next chapter.

5-2. Experimental

Except for a indium(III) solution, stock solutions used for the polarographic measurements of copper(II), lead(II), cadmium(II), thallium(I), zinc(II), nickel(II), cobalt(II) and manganese(II) were prepared from the salts: $CuCl_2 \cdot 2H_2O$, $PbCl_2$, $CdCl_2 \cdot 21/2H_2O$, TlCl, $ZnCl_2$, $NiCl_2 \cdot 6H_2O$, $CoCl_2 \cdot 6H_2O$ and $MnCl_2 \cdot 4H_2O$, respectively. The indium(III) stock solution was prepared by dissolving a relevant amount of pure metal indium (99.99 %) in its equivalent hydrochloric acid solution.

5-3. Results and discussion

The phase selective fundamental and second harmonic ac polarograms of various metal ions in 1 M potassium chloride solution are given in Figs. 5-1 and 5-2, respectively.

The contributions of the charging current(base current) to the faradaic current in 1f(0°) and 2f(90°) components are less than those in 1f(90°) and 2f(0°)

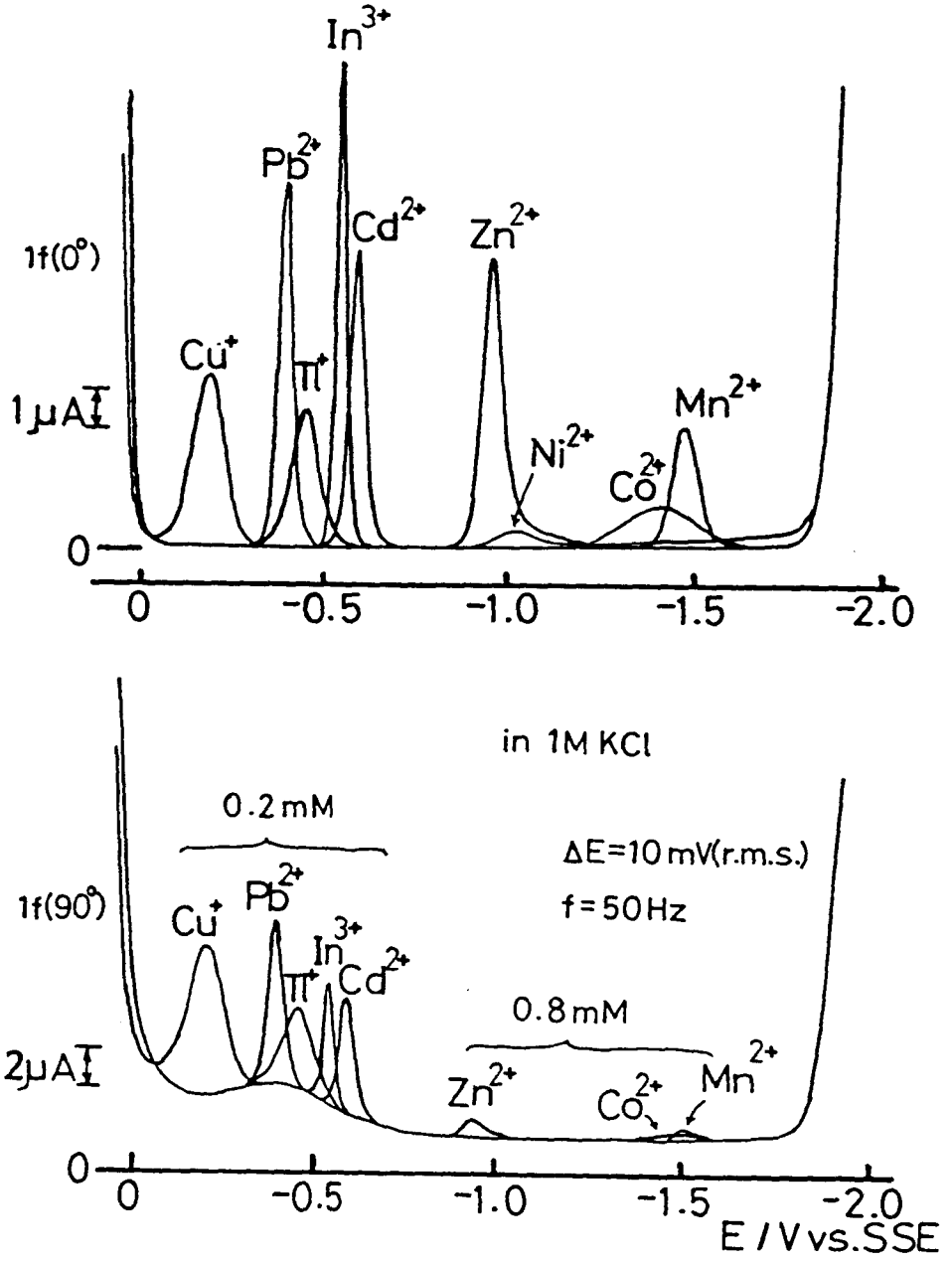

Fig. 5-1. Fundamental harmonic ac polarograms of various metal ions in 1 M potassium chloride. ΔE_{ac} = 10 mV(r.m.s.), f = 50 Hz. Upper: 1f(0°), lower: 1f(90°).

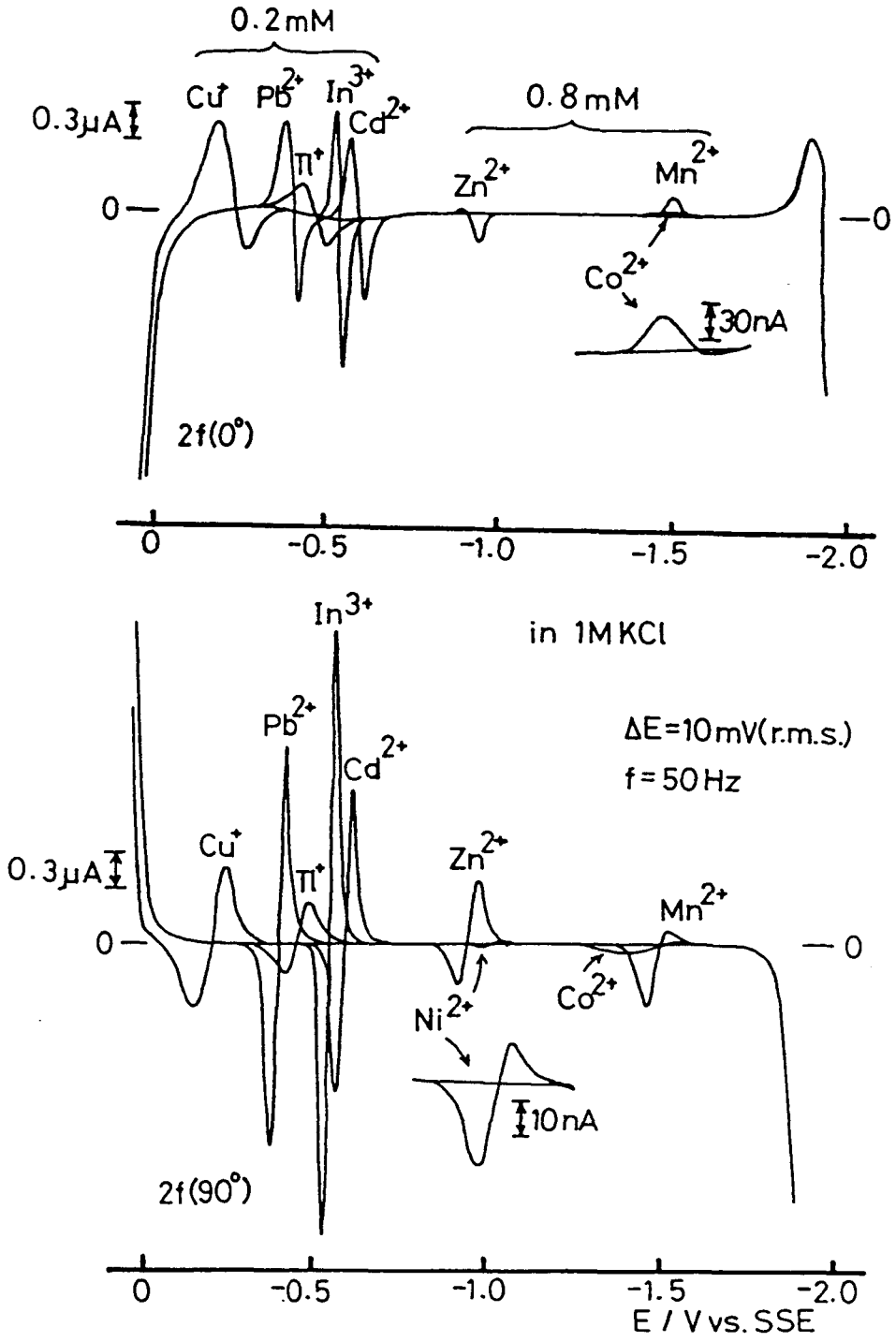

Fig. 5-2. Second-harmonic ac polarograms of various metal ions in 1 M potassium chloride. Upper: 2f(0°), lower: 2f(90°).

components, respectively. As compared with 1f and 2f modes, this contribution in 2f(0°) is far less than that in 1f(90°). Therefore, considering the detection limit, when the 2f mode is monitored, any phase angle component can be used for the trace analysis, while in 1f mode only 0° component can be utilized for the purpose. Such a flexibility on the selection of phase angle components monitored in 2f mode will provide a useful method when it is applied to the system in which a kinetics of redox process plays an important roll.

5-3-1. Systems of lead(II), cadmium(II) and thallium(I): reversible redox process

The systems of Pb(II)/Pb(Hg), Cd(II)/Cd(Hg) and Tl(I)/Tl(Hg) are well-known as the reversible process[11]. The polarogram of 1f mode has a shape of the first derivative wave of the dc polarogram, and that in 2f mode has a shape of the second derivative wave of the dc polarogram. When the system is reversible, the following relations are reasonably assumed: $(2\omega)^{1/2} \ll 1$ (in 1f mode) and $2\omega^{1/2} \ll 1$ (in 2f mode). And $F_1(t)G_1(\omega)$ in Eq. (2-4) become unity ($F_1(t)G_1(\omega) = 1$) and $F_2(t)G_2(\omega)$ in Eq. (2-5) is expressed identically by $\sinh (j/2)(F_2(t)G_2(\omega) =$

sinh (j/2)). The polarographic wave forms of 1f and 2f mode, therefore, can be expressed mathematically by $[\cosh^2(j/2)]^{-1}$ in Eq. (2-6) for 1f mode and by $[\sinh(j/2)][\cosh^3(j/2)]^{-1}$ in Eq. (2-7) for 2f mode, respectively. The half width of peak current in 1f mode is 90/n mV, and the difference between the potentials of two peaks in 2f mode is 68/n mV.

Eqs. (2-4)-(2-7) show that the current amplitude in 1f mode is proportional to ΔE_{ac}, while that in 2f mode is proportional to ΔE_{ac}^2. And these relationships for Cd(II) system are given in Figs. 5-3 and 5-4. When ΔE_{ac} become very large, these relationships are not approved any more. The results are understood from the fact that in Eq. (2-3) the second or its higher term in each bracket gives significant value when ΔE_{ac} is large.

The current amplitudes in both 1f and 2f modes are also proportional to $\omega^{1/2}$(or $f^{1/2}$)(Fig. 2-3) and to C_0^*.

In the reversible process, the phase angle ϕ_1 of 1f mode in Eq. (2-9) is $\pi/4$, and ϕ_2 of 2f mode in Eq. (2-10) is $-\pi/4$, which are independent of dc potentials. In both 1f and 2f modes, therefore, the current amplitude of 0° component is equal to that of 90° component(Fig. 2-3).

5-3-2. Systems of indium(III) and zinc(II): quasi-

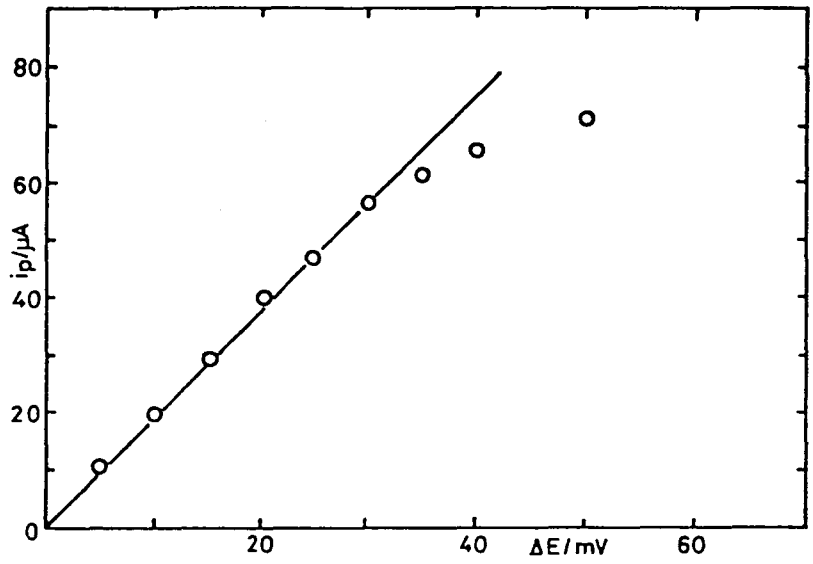

Fig. 5-3. Plots of i_p vs. ΔE_{ac} in 1f(0°). 0.2 mM cadmium chloride in 1 M potassium nitrate(pH2). f = 50 Hz.

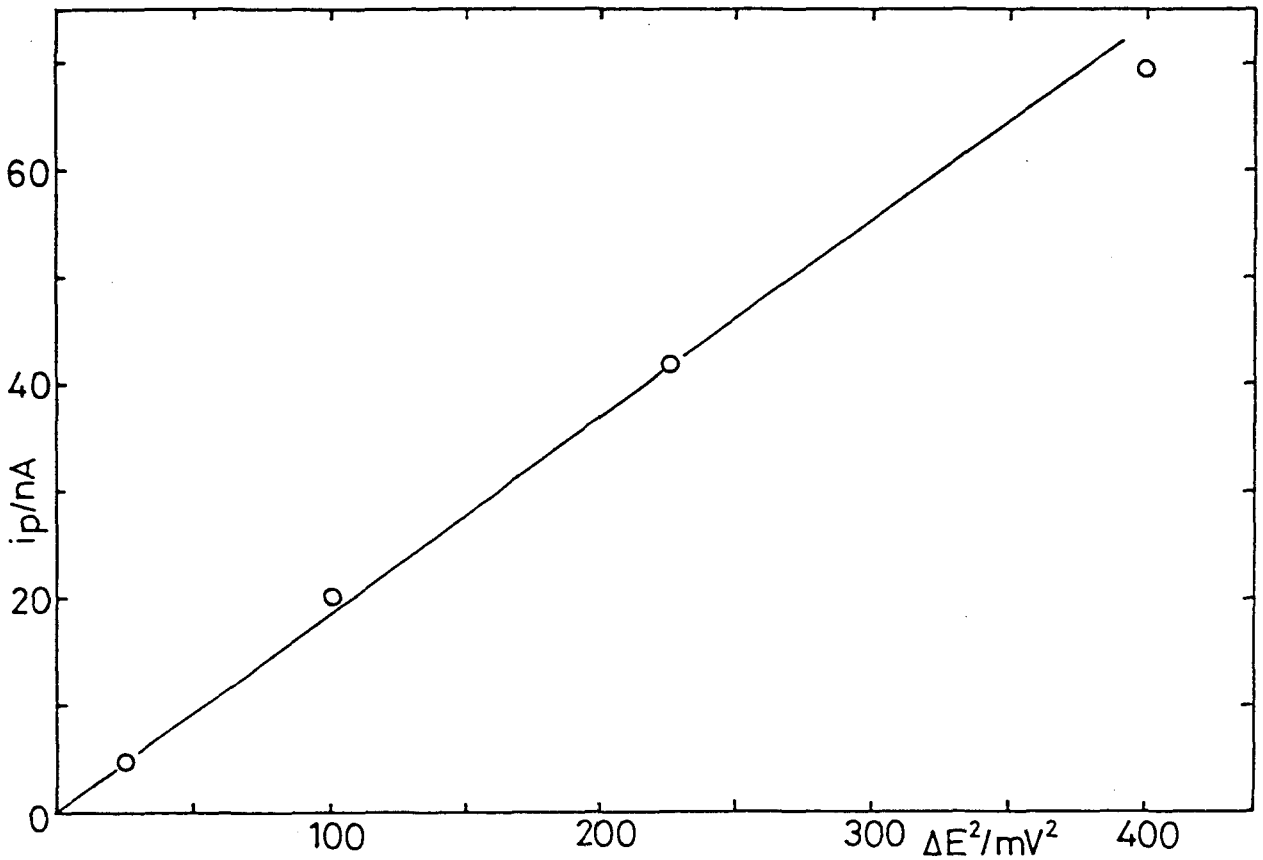

Fig. 5-4. Plots of i_p vs ΔE_{ac}^2 in 2f(90°). Other conditions are the same as Fig. 5-3.

reversible process

The systems of In(III)/In(Hg) and Zn(II)/Zn(Hg) in Figs. 5-1 and 5-2 are known as the quasi-reversible case[11]. A 1f polarogram does not correspond to a real first derivative form of the dc polarogram, and a 2f polarogram is also not a real second derivative form of the dc polarogram. In the quasi-reversible system, e.g., Zn(II) and In(III), the contributions to the current amplitudes of $F_1(t)G_1(\omega)$ in Eq. (2-4) and $F_2(t)G_2(\omega)$ in Eq. (2-5) are both less than unity($F_1(t)G_1(\omega) < 1$) and sinh (j/2) ($F_2(t)G_2(\omega) <$ sin (j/2)) , respectively. Therefore, the current amplitudes in 1f and 2f modes are not proportional to $\omega^{1/2}$. On the other hand, in case of the systems having the same n(number of electrons transfered) (e.g., Zn(II), Cd(II) and Pb(II)), the current amplitudes between these systems can be compared. And in the quasi-reversible Zn(II) system, the currents are both more diminished in their amplitudes than those in the reversible systems(Cd(II) and Pb(II)).

In the In(III) system, however, the current amplitude in 1f(0°), 2f(0°) and 2f(90°) components are larger than those of the reversible system(Cd(II) and Pb(II)). This is because the currents in 1f and 2f mode are both proportional to n^2 and n^3, respectively: in case of

In(III), n = 3, and in case of Cd(II) and Pb(II), n = 2.

The half-width in 1f mode is more than 90/n mV in the reversible process. The difference between the potentials of two peaks in 2f mode is also more than 68/n mV in the reversible process.

The phase angle ϕ_1 in 1f mode is not $\pi/4$(for reversible process) and changes from 0 to $\pi/4$ with E_{dc}, k_s (heterogeneous charge transfer rate constant), α (transfer coefficient) and f(frequency)[Eq. (2-8)]. The ϕ_2 in 2f mode is not $-\pi/4$(for reversible processes) but changes of 0 to 2π with E_{dc}, k_s, and f[Eq. (2-9)].

Figure 5-5 shows plots of cot ϕ_1 vs. the dc potential in the system Zn(II)/Zn(Hg). From this plots, the kinetic parameters, k_s and a can be obtained by the following equations[5]:

$$[E_{dc}]_{max} = E^r_{1/2} + (RT/nF)\ln(\alpha/\beta), \quad (5\text{-}1)$$

$$[\cot\phi_1]_{max} = 1 + (2\omega D)^{1/2}/k_s[(\alpha/\beta)^{-\alpha} + (\alpha/\beta)^{\beta}] \quad (5\text{-}2)$$

where $[E_{dc}]_{max}$ is a maximum at the dc potential of the plot, and $[\cot\phi_1]_{max}$ is a magnitude of it. The k_s in this work was 3.0×10^{-3} cms^{-1} and the was 0.29(cf. $k_s = 5.05\times10^{-3}$ cms^{-1} and $\alpha = 0.30$[11]).

Figure 5-6 shows a unusual shoulder at a less negative dc potential than a main peak in the Zn(II)/Zn(Hg) [12,13]. The unusual shoulder appears kinetically when the k_s is of the order of 10^{-3} cms^{-1}, while α is smaller than 0.5.

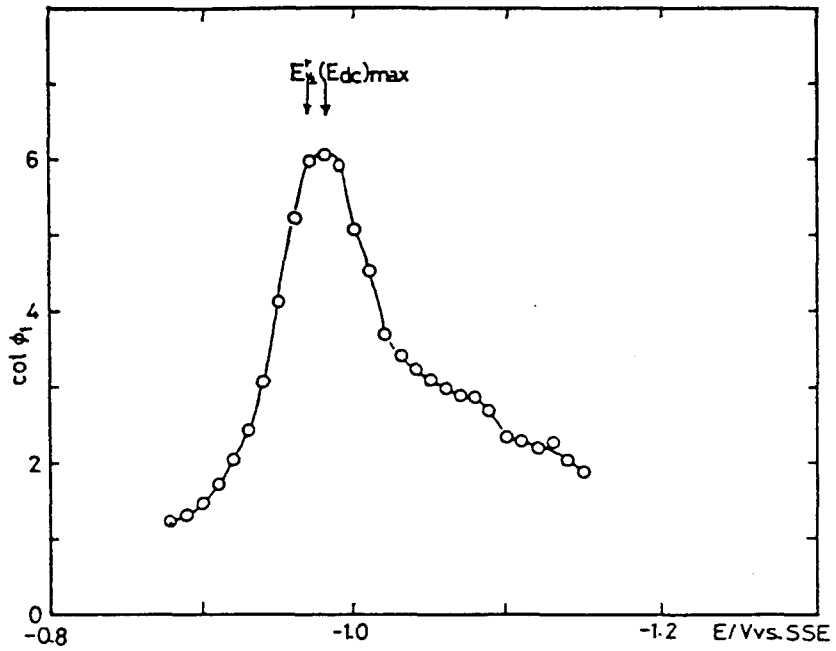

Fig. 5-5. The dependence of cot ϕ_1 on E_{dc} in the Zn(II)/Zn(Hg) system. ΔE_{ac} = 5 mV(r.m.s.), f = 10 Hz, D_O = 0.7×10^{-5} cm^2s^{-1}, D_R = 2.0×10^{-5} cm^2s^{-1}, $E^r_{1/2}$ = -0.9685 V, $[E_{dc}]_{max} - E^r_{1/2}$ = -11.5 mV.

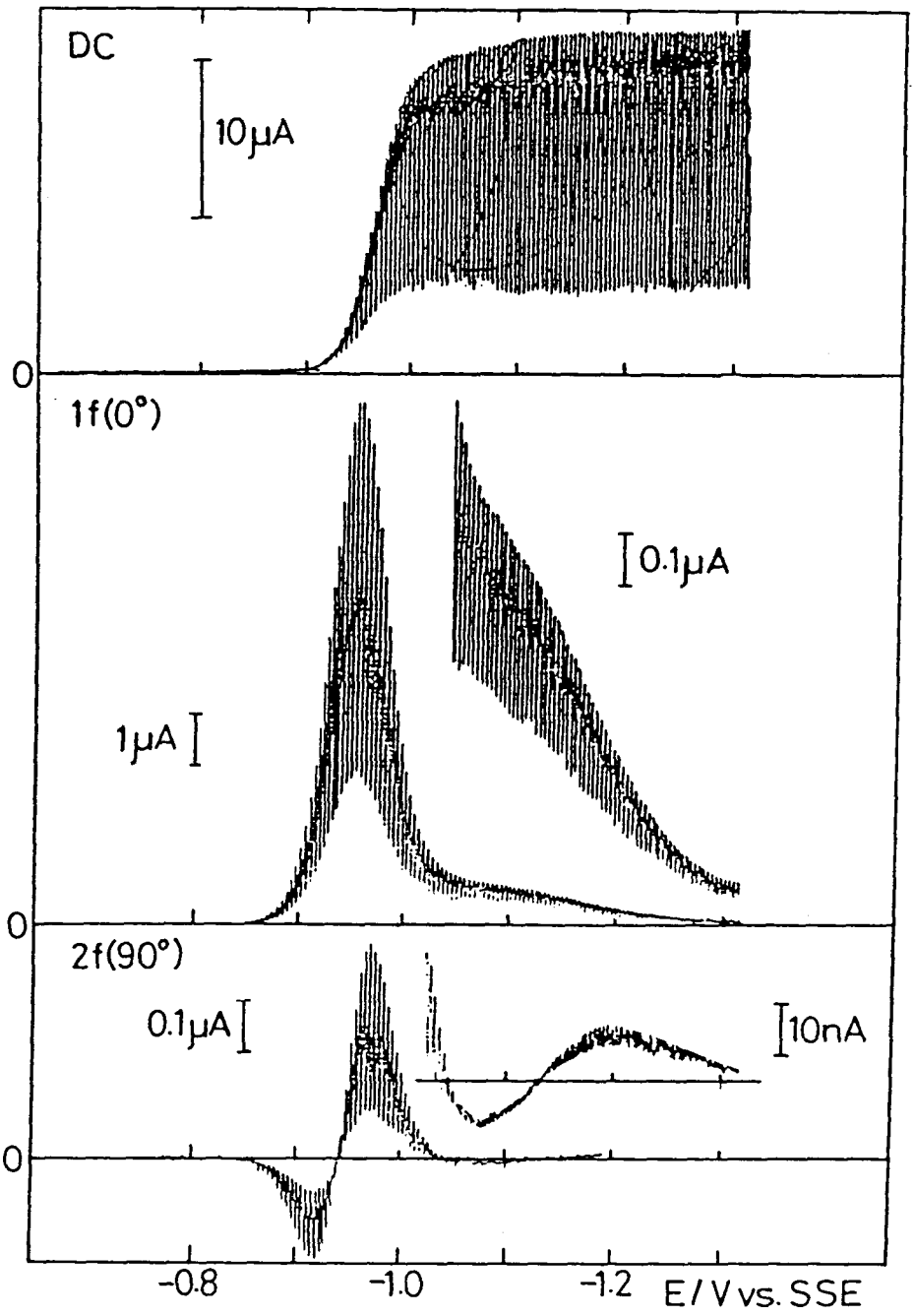

Fig. 5-6. Dc, fundamental(1f) and second-harmonic(2f) ac polarograms. 2 mM zinc chloride in 1 M potassium chloride(pH3). ΔE_{ac} = 5 mV(r.m.s.), f = 100 Hz.

Though the electrochemical charge transfer is one step, the two peaks are observed in 1f mode[14] and two maximum peaks and two minimum peaks are in 2f mode[18]. The unusual phenomenon in 2f mode has been known theoretically [15], but an experimental observation in 2f mode has not been reported.

This phenomenon is not observed in the dc polarography. And in 1f mode, this phenomenon is ill-defined, while that in 2f mode is well-defined(Fig. 5-6). In 2f mode, dependences of the currents for this phenomenon on the applied frequency are given in Fig. 5-7. The curve for the first anodic current shows a peak at a frequency($f \simeq 15$ Hz) and that for the second anodic current increases monotonously. Both first and second cathodic currents decrease monotonously. When in a certain system two-step currents are observed, the data of the dependence of 2f current on the applied frequency will give an indispensable proof for the decision of whether the two-step phenomenon is corresponding to a real two-step process or not.

5-3-3. Systems of nickel(II), cobalt(II) and manganese(II): irreversible process

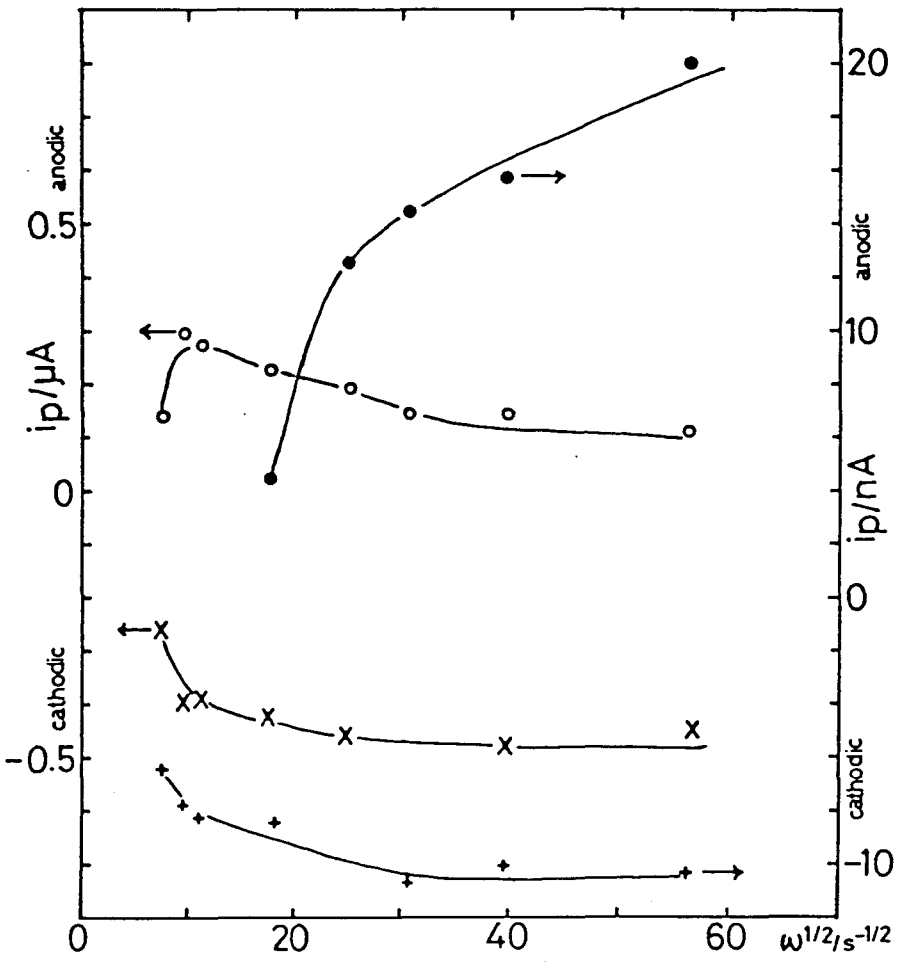

Fig. 5-7. Plots of i_p vs. $\omega^{1/2}$ of the Zn(II)/Zn(Hg) system. (o) first anodic peak, (x) first cathodic peak, (o) second anodic peak, (+) second cathodic peak. Other conditions are the same as Fig. 5-6.

In an irreversible system, a dc polarogram does not show a well-defined wave such as the reversible or quasi-reversible process, and the corresponding ac polarogram shows a broad peak[16]. In Figs. 5-1 and 5-2, the systems of Ni(II)/Ni(Hg), Co(II)/Co(Hg) and Mn(II)/Mn(Hg) are known as this category[11].

Theoretical expressions for the irreversible ac polarographic wave induced by very heterogeneous charge transfer[16] can be written as(cf. Appendix V):

$$I(\omega t) = [1.644\alpha n^2F^2AC_0^*(\omega D_0)^{1/2}\Delta E_{ac}/RTe^{-J}(1 + e^{1.091J})\times [1 + (1 + Q_1e^J)^2]^{1/2}]\sin [\omega t + \cot^{-1}(1 + Q_1e^J)], \quad (5\text{-}3)$$

where

$$J = (\alpha nF/RT)[E_{dc} - E^r_{1/2} - (RT/\alpha nF)\ln (1.349k_s t^{1/2}/D^{1/2})], \quad (5\text{-}4)$$

$$Q_1 = 1.907(\omega t)^{1/2}, \quad (5\text{-}5)$$

and

$$I(2\omega t) = [2.325\alpha n^3F^3AC_0^*(\omega D_0)^{1/2}\Delta E_{ac}^2(X^2 + Y^2)^{1/2}/4R^2T^2e^{-J}(1 + e^{1.091J})[1 + (1 + Q_2e^J)^2]^{1/2}]\times \sin (2\omega t + \phi_2), \quad (5\text{-}6)$$

where

$$Q_2 = \sqrt{2}\, Q_1 = 2.697(\omega t)^{1/2}, \quad (5\text{-}7)$$

$$X = \alpha[1 - 2[(2 + Q_1e^J)/[1 + (1 + Q_1e^J)^2]], \quad (5\text{-}8)$$

$$Y = 2\alpha[Q_1e^J/[1 + (1 + Q_1e^J)^2]], \quad (5\text{-}9)$$

$$\phi_2 = \cot^{-1}[[Y(Q_2e^J + 1) + X]/[Y - X(Q_2e^J + 1)]]. \quad (5\text{-}10)$$

The current amplitudes of the irreversible processes (Eqs. (5-3) and (5-6)) are far small and are about 1/10 or 1/100 of that of the reversible process(Eq. (2-6) and (2-7)). As a irreversible process has a very small k_s($< 10^{-5}$ cms^{-1}), the alternating currents for 1f and 2f mode become significant when E_{dc} is far negative from $E^r_{1/2}$(Eq. (5-4)). In the reversible process, α is far from 0.5 for the reversible process. In 2f mode, the polarographic shape is asymmetry for α and k_s.

Therefore, one can understand the reversibility for a certain system from the data of i_p vs. $\omega^{1/2}$, of the half width in 1f mode or of the difference between the potentials of the two peaks in 2f mode, and of the phase angle.

The system Cu(II)/Cu(Hg) in chloride solution are known as a two-step reaction(Cu(II) $\rightarrow$ Cu(I) $\rightarrow$ Cu(Hg)) [3]. Since the reduction potential for the reaction: Cu(II) $\rightarrow$ Cu(I), is more positive than that for the reaction: Hg $\rightarrow$ Hg_2Cl_2, the alternating current for Cu(II)/Cu(I) is not observed and only the current for Cu(I)/Cu(0) appears. The reaction is also accompanied with the adsorption of Cu(I) on the electrode. This can be proved from the fact that the phase angle in 1f mode is more than $\pi/4$.

Appendix V. The irreversible ac polarographic wave induced by very slow heterogeneous charge transfer[16]

Under irreversible conditions, Eq. (II-8) in Appendix II is reduced to an analytical expression:

$$\psi_0(t) = (7/3\pi)^{1/2}/\{\lambda t^{1/2}[1 + (1.349\lambda t^{1/2})^{-1.091}]\} \quad . \tag{V-1}$$

Substituting Eq. (V-1) in Eq. (II-2) and invoking the relationship:

$$e^{-\alpha j} >> 1 > e^{\beta j} >> e > e^{j}, \tag{V-2}$$

$$\alpha e^{j}\psi_0(t) >> 1, \tag{V-3}$$

and employing the relation:

$$1.349k_s e^{-\alpha j} t^{1/2} D^{-1/2} = e^{-J}, \tag{V-4}$$

where

$$J = (\alpha nF/RT)[E_{dc} - E^{r}_{1/2} - (RT/\alpha nF)\ln (1.349k_s t^{1/2}/D^{1/2})], \tag{V-5}$$

and algebraic rearrangement yields the results:

$$I(\omega t) = [1.644\alpha n^2 F^2 AC_0^{*}(\omega D_0)^{1/2}\Delta E_{ac}/RTe^{-J}(1 + e^{1.091J})\times [1 + (1 + Q_1 e^{J})^2]^{1/2}]\sin [\omega t + \cot^{-1}(1 + Q_1 e^{J})], \tag{V-6}$$

where

$$Q_1 = 1.907(\omega t)^{1/2}, \tag{V-7}$$

and

$$I(2\omega t) = [2.325\alpha n^3 F^3 A C_0^* (\omega D_0)^{1/2} \Delta E_{ac}^2 (X^2 + Y^2)^{1/2} / 4R^2T^2 e^{-J}(1 + e^{1.091J})[1 + (1 + Q_2 e^J)^2]^{1/2}] \times \sin(2\omega t + \phi_2), \quad (V\text{-}8)$$

where

$$Q_2 = \sqrt{2}\, Q_1 = 2.697(\omega t)^{1/2}, \quad (V\text{-}9)$$

$$X = \alpha[1 - 2[(2 + Q_1 e^J)/[1 + (1 + Q_1 e^J)^2]], \quad (V\text{-}10)$$

$$Y = 2\alpha[Q_1 e^J/[1 + (1 + Q_1 e^J)^2]], \quad (V\text{-}11)$$

$$\phi_2 = \cot^{-1}[[Y(Q_2 e^J + 1) + X]/[Y - X(Q_2 e^J + 1)]]. \quad (V\text{-}12)$$

5-4. References

1 I.M. Kolthoff and J.J. Lingane, Polarography, Interscience, New York, 1952.

2 P. Delahay, New Instrumental Methods in Electrochemistry, Interscience, New York, 1954.

3 M. Shinagawa, Polarografu Bunseki-ho(Polarographic Analysis), Kyoritsu, Tokyo, 1965(in Japanese).

4 R. Tamamushi, Denki Kagaku(Electrochemistry), Tokyo Kagaku Dojin, Tokyo, 1967(in Japanese).

5 Z. Galus, in G.F. Reynolds(Translation Ed.), Fundamentals of Electrochemical Analysis, Ellis Horwoood, Chichester, 1976.

6 T. Fujinaga and M. Maruyama(Eds.), Polarography Dai-isshu(First Series for Polarography), Nanko-do, Tokyo, 1962.

7 B. Breyer and H.H. Bauer, Alternating Current Polarography and Tensammetry, Wiley, New York, 1963.

8 D.E. Smith, in A.J. Bard(Ed.), Electroanalytical Chemistry, Vol. 1, Dekker, New York, 1966, p. 1.

9 B. Breyer, Pure Appl. Chem., 15(1967)313.

10 D.E. Smith, Crit. Rev. Anal. Chem., 2(1971)247.

11 R. Tamamushi, Kinetic Parameters of Electrode Reactions, 1972 supplement to Electrochim. Acta, 9(1964)963.

12 M. Senda, M. Senda and I. Tachi, Denki Kagaku, 27(1959)83.

13 B. Timmer, M. Sluyters-Rehbach and J.H. Sluyters, J. Electroanal. Chem., 14(1967)181.

14 H. Matsuda, Z. Elektrochem., 62(1958)977.

15 T.G. McCord and D.E. Smith, Anal. Chem., 40(1968)289.

16 D.E. Smith and T.G. McCord, Anal. Chem., 40(1968)474.

Chapter 6. Analytical application of second harmonic ac polarography

6-1. Introduction

As shown in Chap. 2, the nonlinear second expanded term of total alternating current is corresponding to the second harmonic alternating current. And the polarogram of 2f mode has the second derivative shape of dc polarogram. Compared with the current in 1f mode, that in 2f mode has little contribution from the charging current over the whole phase angle components(cf. Figs. 5-1 and 5-2). In the chemical analysis, therefore, 2f mode is more advantageous than 1f mode.

In this chapter, phase-selective second harmonic ac polarography is used to determine one of two species having similar reduction potentials without any preliminary separation, selective complexation[1,2], masking of certain electrode process[3], or using computer techniques[4-10].

The present technique is different from the methods used by Devay et al.[11] and Fajioli et al.[12] in that it utilizes the difference in the dependence of phase angle on

dc potential for two species, which results from the kinetics of two-electrode processes. As examples, two systems are chosen, i.e., in 1 M potassium chloride solution, indium(III) in the presence of excess of cadmium(II), and zinc(II) in the presence of excess of nickel(II).

6-2. Experimental

The working electrode was a dropping mercury electrode; the capillary had a drop time of 3.96 s at -1.0 V vs. Ag/AgCl in 1 M potassium chloride solution and the mercury flow was 2.025 mgs^{-1} at a height of 70 cm.

The phase angle of faradaic alternating current was determined by recording in-phase(0°) and quadrature(90°) components. The phase angle of the lock-in amplifier was calibrated by use of a dummy cell[13](cf. Chap. 2). Applied ac voltage (ΔE_{ac}) and frequency(f) were 5-10 mV(r.m.s.) and 15-200 Hz, respectively.

6-3. Results and discussion

For the simple electrode reaction, $Ox + ne^- \rightleftharpoons Red$,

where rate is controlled by diffusion and/or heterogeneous charge-transfer kinetics, the fundamental and second harmonic alternating currents are given by the well-known equations[14,15](see also Chap. 2):

$$I(\omega t) = I(\omega t)_{rev} F_1(t) G_1(\omega) \sin(\omega t + \phi_1), \quad (6\text{-}1)$$

$$I(2\omega t) = I(2\omega t)_{rev} F_2(t) G_2(\omega) \sin(2\omega t + \phi_2), \quad (6\text{-}2)$$

where

$$I(\omega t)_{rev} = (nF)^2 A C_0^* (\omega D_0)^{1/2} \Delta E_{ac} [4RT\cosh^2(j/2)]^{-1}, \quad (6\text{-}3)$$

$$I(2\omega t)_{rev} = (nF)^3 A C_0^* (2\omega D_0)^{1/2} \Delta E_{ac}^2 [16R^2T^2\cosh^3(j/2)]^{-1}, \quad (6\text{-}4)$$

$$\phi_1 = \cot^{-1}[1 + (2\omega)^{1/2}/\lambda], \quad (6\text{-}5)$$

$$\phi_2 = \cot^{-1}[[L(2\omega^{1/2}/\lambda + 1) + P]/[L - P(2\omega^{1/2}/\lambda + 1)]], \quad (6\text{-}6)$$

where

$$j = nF(RT)^{-1}(E_{dc} - E_{1/2}^r); \lambda = (k_s f_a/RT)(e^{-\alpha j} + e^{\beta j}). \quad (6\text{-}7)$$

In Eqs. (6-3) and (6-4), if n(number of electrons transfered in heterogeneous charge transfer step) for a system is 2 and that for another system is 3(and the both systems are reversible processes), the current amplitudes in 1f mode are in the ratio 4:9 and those in 2f mode are in the ratio 8:27, respectively. Therefore, when a chemical species(n = 3) is analyzed in the presence of excess of another species(n = 2), the 2f mode is more advantageous than the 1f mode.

Equations (6-5) and (6-6) show that the fundamental

and second harmonic current phase angles(ϕ_1 and ϕ_2) change with dc potential. But for a process which displays a reversible wave in the ac or dc polarographic sence ($2\omega^{1/2}/\lambda \ll 1$ or $\lambda t^{1/2} \gg 50$), the ϕ_1 and ϕ_2 values are $\pi/4$ and $-\pi/4$, respectively, and these are independent of dc potential. These phase angle relationships prove useful for separation of two species with similar redox potentials.

A mixed solution of cadmium(II) and indium(III) in 1 M potassium chloride(pH 3) was investigated as one such example. As the Cd(II)/Cd(Hg) system in 1 M potassium chloride behaves as a reversible process(k_s = 2.5±0.3 cms^{-1}, α = 0.65±0.03)[16], the phase angle of the system is 45° for 1f over the peak potential region and that for 2f is -45° at the more positive potential than the zero crossing potential and 135° at the more negative potential. In contrast, as the In(III)/In(Hg) system in 1 M potassium chloride behaves as a quasi-reversible process(k_s = (6±2)× 10^{-2} cms^{-1}, β = 0.9±0.1)[16], the phase angles of the system for both 1f and 2f are not constant but change with dc potential. Therefore, as expected from the above theoretical relation, when the phase angle of the lock-in amplifier is adjusted to 135° for 1f or to 45° for 2f, the alternating current only for indium(III) is detected without interference from cadmium(II).

The principle of the separation in 1f mode is explained by a vector illustration in Fig. 6-1. Namely, ϕ_1 for the reversible process(Cd(II)/Cd(Hg) system) is $\pi/4$ independent of dc potential, while that in the quasi-reversible process(In(III)/In(Hg) system) changes from 0 to $\pi/4$ with dc potential(Eq. (6-5)). Therefore, in the 135° component, the alternating current for the revesible process vanishes over the whole range of dc potential, while that for the quasi-reversible process remains.

Curves 1 and 2 in Fig. 6-2 were obtained individually for each of cadmium(II) and indium(III) at 0.2 mM concentrations in 1 M potassium chloride acidified to pH 3 with hydrochloric acid. The peak potential difference between them for 1f was 45 mV. Curve 3 is for the mixed solution of 0.2 mM cadmium(II) and 0.2 mM indium(III). The polarograms of the mixture(curve 3) for the 0° component of 1f and for the 90° component of 2f show overlapping of the components. In contrast, the 135° component of 1f and the 45° component of 2f for the mixture display simple peaks corresponding to a single electrode reaction, and peaks for only indium(III) are detected; those for cadmium(II) are eliminated. As the contribution of the charging current is less in the 45° component of 2f than in the 135° component of 1f($F/C > 50$ for 2f and $F/C \simeq 1$

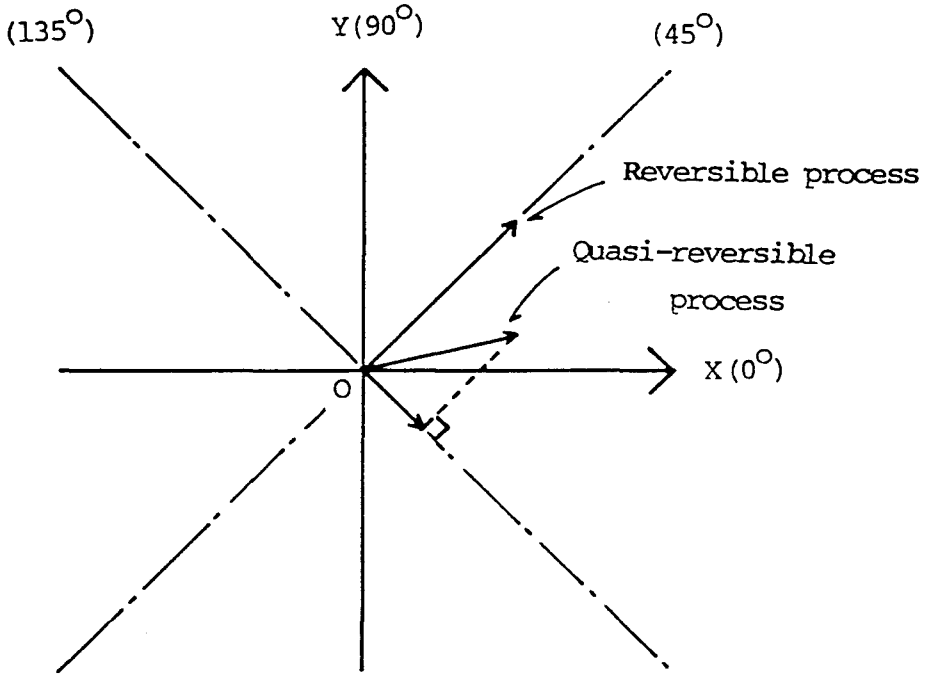

Fig. 6-1. Phase angle relationship between fundamental harmonic ac polarographic total currents and the current components at some phase angles.

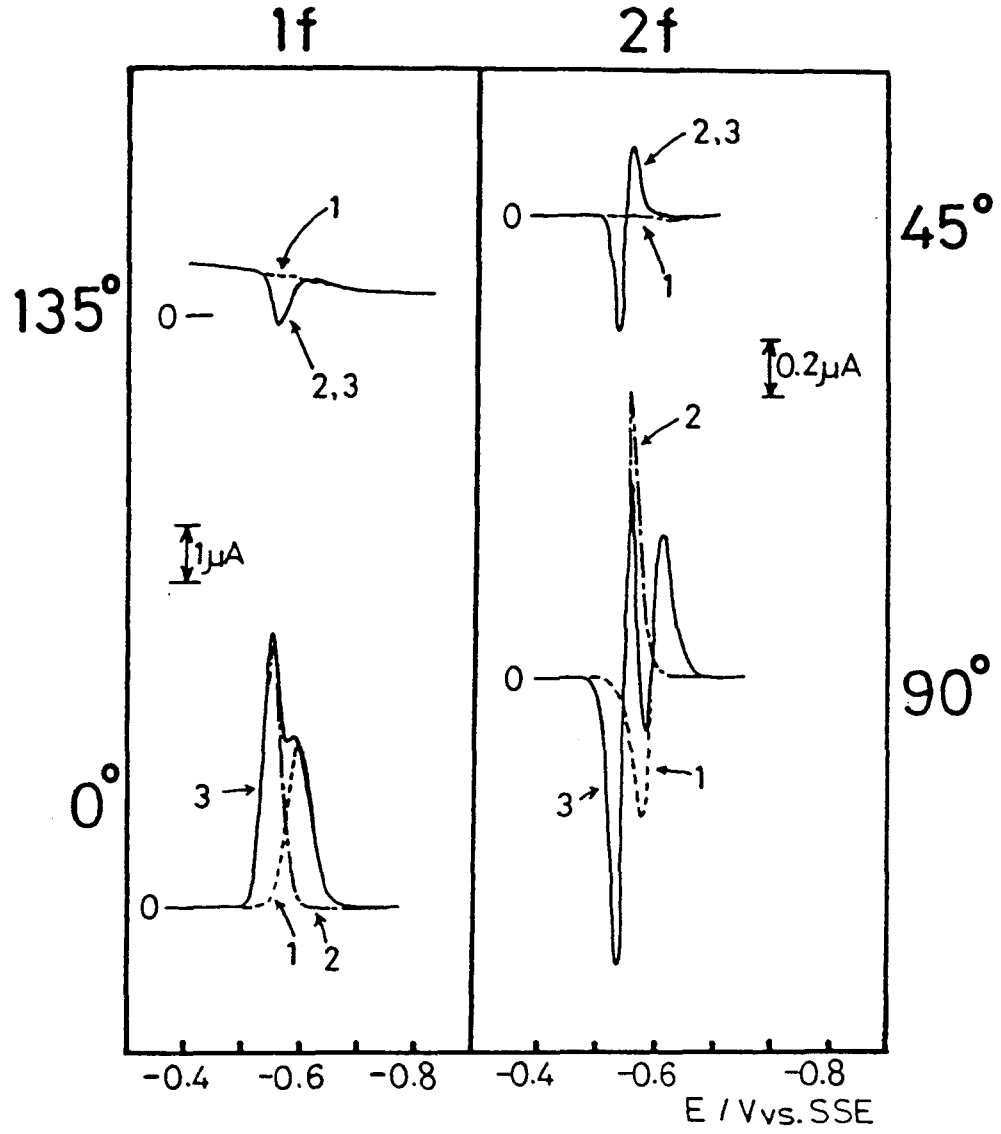

Fig. 6-2. Fundamental(1f) and second(2f) harmonic ac polarograms at various phase angles for cadmium(II), indium(III) and their mixture. (1) 0.2 mM Cd(II); (2) 0.2 mM In(III); (3) 0.2 mM Cd(II) + 0.2 mM In(III) in 1 M KCl(pH 3). ΔE_{ac} = 10 mV(r.m.s.), f = 25 Hz.

for 1f, where F is the faradaic current and C is the charging current), the 2f mode is superior to the 1f mode in this case.

The calibration curves of indium(III) in the presence and in the absence of 0.2 mM cadmium(II) for 2f are given in Fig. 6-3. The upper curve is for the 45° component and the lower is for the 90° component in the absence of cadmium(II). Peak current(I_p) for the 90° component was measured at -0.538 V for indium(III), because the peak at -0.570 V for indium(III) overlaps with the peak at -0.572 V for cadmium(II) when the concentration of indium(III) is low. The I_p for the 45° component is the sum of positive and negative peak currents. The I_p value for the 90° component in the presence of cadmium(II) deviates from the calibration curve even at the concentration ratio of $C_{In(III)}/C_{Cd(II)} = 1/5$, but that for the 45° component in the presence of cadmium(II) lies on the calibration curve up to a ratio of 1/50 when $C_{In(III)}$ is 4×10^{-6} M.

A mixed solution of zinc(II) and nickel(II) in 1 M potassium chloride was also investigated. Figure 6-4(A) shows the dependence of the phase angle of the alternating current upon dc potential for zinc(II) in 1 M potassium chloride, and Fig. 6-4(B) shows that for nickel(II). As the Zn(II)/Zn(Hg) system in chloride solution behaves as a quasi-reversible process in kinetics(k_s = (5.05±0.05)×

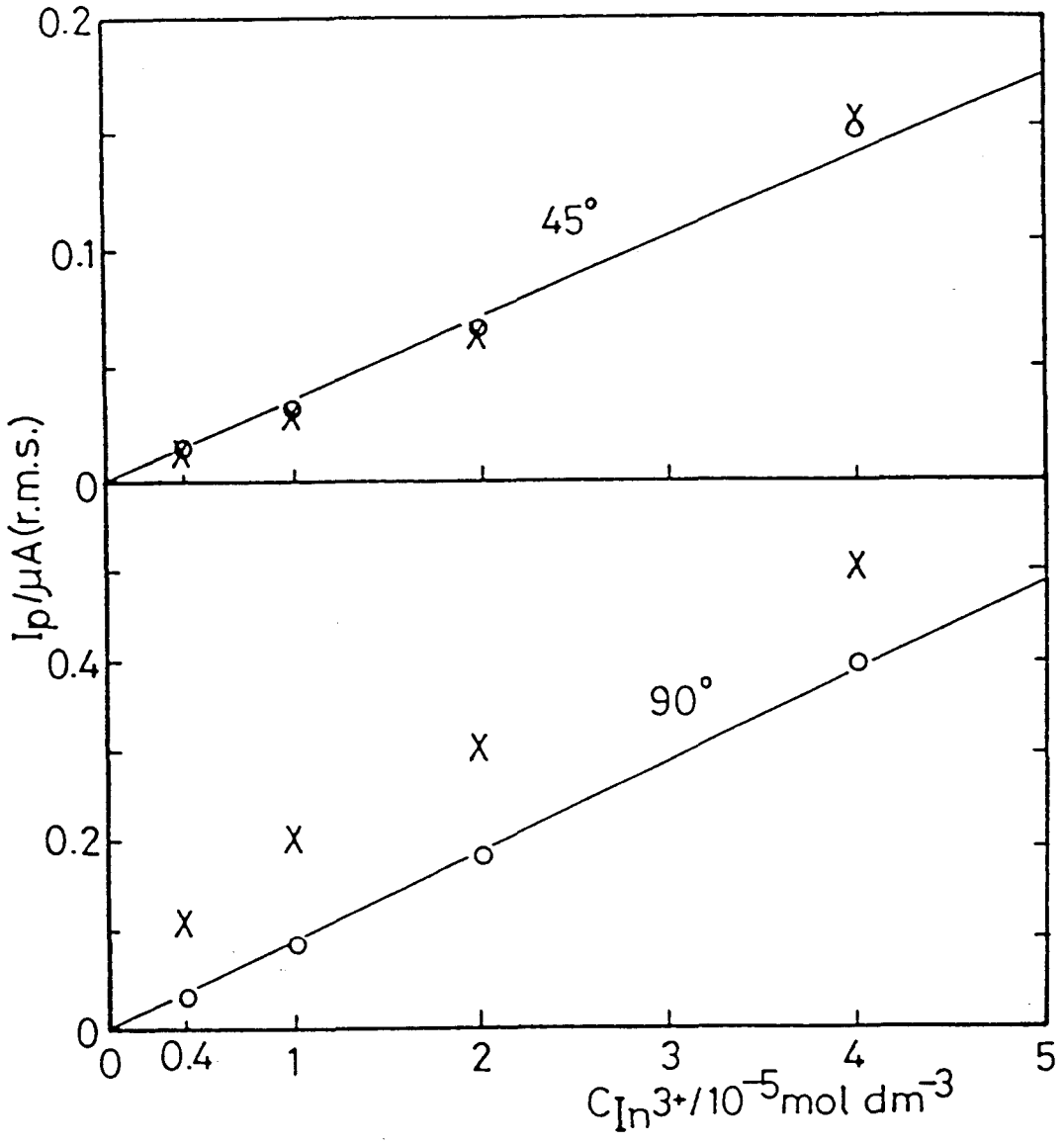

Fig. 6-3. Calibration curves for indium(III) in 1 M KCl(pH 3): (X) with 0.2 mM cadmium(II), and (O) without cadmium(II). The curves are for 45°(upper) and 90°(lower) components in the 2f mode. ΔE_{ac} = 10 mV(r.m.s.), f = 25 Hz.

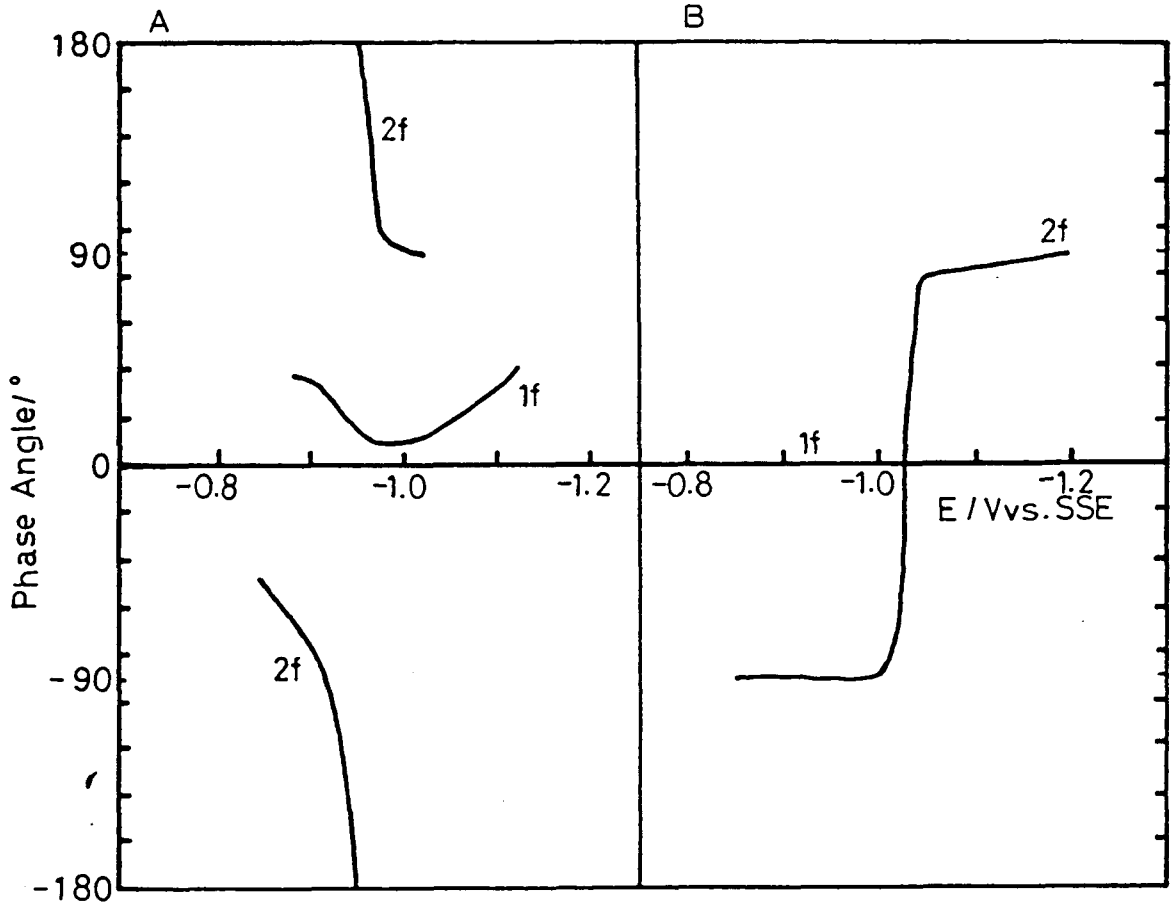

Fig. 6-4. The phase angle of fundamental(1f) and second(2f) harmonic currents for zinc(II) and nickel(II) in 1 M KCl. (A) 0.2 mM Zn(II); (B) 0.8 mM Ni(II). ΔE_{ac} = 5 mV (r.m.s.), f = 15 Hz.

10^{-3} cms^{-1}, α = 0.3±0.02)[16-18], the phase angle changes with dc potential. In contrast, the phase angle for nickel(II) in 1f is zero(k_s = 1.2×10^{-2} $cmlmol^{-1}s^{-1}$, $NiOH^+$ + $2e^-$ + Hg ⟶ Ni(Hg) + OH^- in 0.1 M KC1)[16]. The phase angle in 2f changes from -90° to +90° at the zero crossing potential. It has been suggested that the irreversibility of the Ni(II)/Ni(Hg) system in chloride solution is induced not by a very slow heterogeneous charge transfer reaction but other mechanisms[19-21].

The phase angle-potential relationships indicate that the current of 1f for nickel(II) vanishes when the phase angle of the lock-in amplifier is adjusted to 90°, and that the current of 2f vanishes when the phase angle is adjusted to 0°, while the currents of both modes for zinc(II) should be detected at these phase angles. Figure 6-5 shows ac polarograms of the 0° and 90° components for 1f and 2f. Curves 1 and 2 were obtained individually for each of 2 mM nickel(II) and 0.1 mM zinc(II). The peak potential difference between them for 1f was 65 mV. Curve 3 is for a mixed solution of 2 mM nickel(II) and 0.1 mM zinc(II).

Practically, the polarograms of the mixture(curve 3) for the 0° component of 1f and the 90° component of 2f show overlapping of the components and one cannot separate them well from each other. The 90° component in 1f and the 0° component in 2f for the mixture are almost the same as

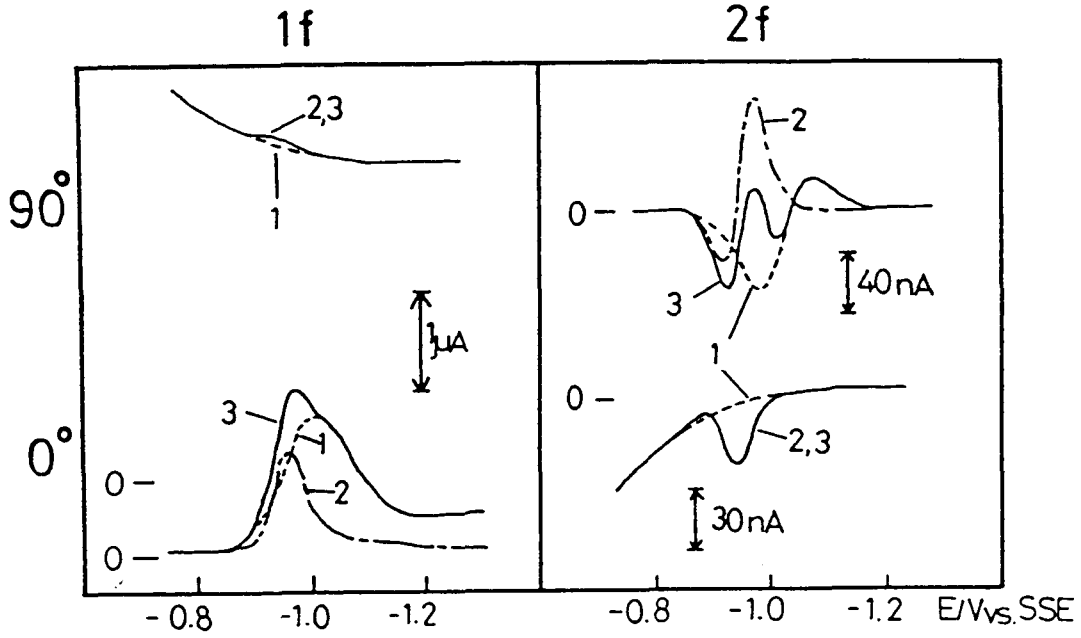

Fig. 6-5. Fundamental(1f) and second(2f) harmonic ac polarograms for zinc(II), nickel(II) and their mixture. (1) 2 mM Ni(II); (2) 0.1 mM Zn(II); (3) 2 mM Ni(II) + 0.1 mM Zn(II) in 1 M KCl. ΔE_{ac} = 10 mV(r.m.s.), f = 100 Hz.

those for zinc(II). The contribution of charging current to the whole current for the former is about 98% and that for the latter is about 10%. Therefore, the 2f mode is superior to the 1f mode for quantitative work.

Figure 6-6 shows the calibration curves obtained by the use of the 2f mode for zinc(II) in the presence and in the absence of 2 mM nickel(II) in 1 M potassium chloride. The upper curve is for the 0° component and the lower is for the 90° component. The I_p is measured by the same method as in the case of indium(III) and cadmium(II). When the ratio of $C_{Zn(II)}/C_{Ni(II)}$ is less than 1/5, the I_p for the 90° component in the presence of nickel(II) deviates from the calibration curve obtained in the absence of nickel(II). Yet the I_p values for the 0° component in the presence and in the absence of nickel(II) are equal even when the $C_{Zn(II)}/C_{Ni(II)}$ ratio is 1/100 at $C_{Zn(II)} = 2\times10^{-5}$ M.

The phase-selective second harmonic ac polarographic technique can be used to distinguish two species having similar peak potentials. The method presented, which utilizes phase angle detection, can be used even when the peak potentials are the same, provided that each electrochemical system has a different phase angle depending on its behavior as reversible, quasi-reversible or irreversible. When a given species reacts with the

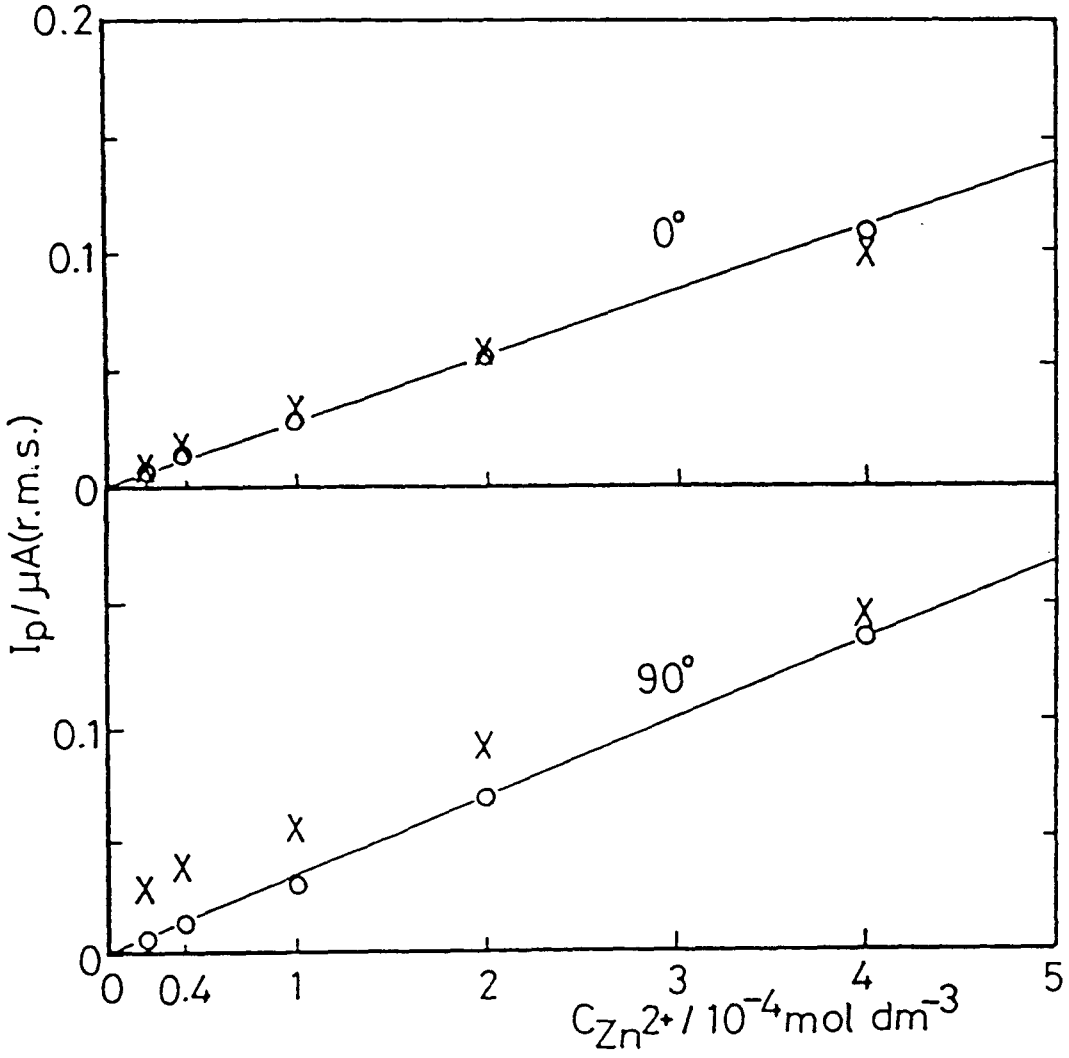

Fig. 6-6. Calibration curves for zinc(II) in 1 M KCl: (X) with 2 mM nickel(II), and (O) without nickel(II). The curves are for 0°(upper) and 90°(lower) components in the 2f mode. ΔE_{ac} = 10 mV(r.m.s.), f = 100 Hz.

electrode through two different electrode processes simultaneously, this method could be also applied to analyze the kinetics for each electrochemical reaction, provided that they give different phase angles.

6-4. References

1 I.M. Kolthoff and J.J. Lingane, Polarography, Interscience, New York, 1952.

2 K.M. Suyan, S.K. Shah and C.M. Gupta, Analyst, 104(1979)883.

3 E. Jacobsen and G. Tandberg, Anal. Chim. Acta, 47(1969)285.

4 I. Ruzic and M. Branica, J. Electroanal. Chem., 22(1969)243, 422.

5 I. Ruzic, J. Electroanal. Chem., 25(1970)144; 29(1971)440.

6 B.S. Grabaric, R.J. O'Halloran and D.E. Smith, Anal. Chim. Acta, 133(1981)349.

7 W.F. Gutknecht and S.P. Perone, Anal. Chem., 42(1970)906.

8 P.A. Boudreau and S.P. Perone, Anal. Chem., 51(1979)811.

9 A.M. Bond and B.S. Grabaric, Anal. Chem., 48(1976)1624.

10 J.J. Toman and S.D. Brown, Anal. Chem., 53(1981)1497.

11 J. Devay, T. Garai, L. Meszaros and B. Palagri-Fenyes, Hung. Sci. Instrum., 15(1968)1.

12 F. Fajioli, F. Dondi and C. Bighi, Ann. Chim. (Rome), 68(1978)111.

13 D.E. Glover and D.E. Smith, Anal. Chem., 43(1971)775.

14 D.E. Smith, in A.J. Bard(Ed.), Electroanalytical Chemistry, Vol. 1, Dekker, New York, 1966, p. 1.

15 T.G. McCord and D.E. Smith, Anal. Chem., 40(1968)289.

16 R. Tamamushi, Kinetic Parameters of Electrode Reactions, 1972 supplement to Electrochim. Acta, 9(1964)963.

17 T.G. McCord and D.E. Smith, Anal. Chem., 42(1970)126.

18 M. Hirota, Y. Umezawa and S. Fujiwara, Bull. Chem. Soc. Jpn., 48(1975)1053.

19 D.E. Smith and T.G. McCord, Anal. Chem., 40(1968)474.

20 C. Nishihara and H. Matsuda, J. Electroanal. Chem., 28(1970)17.

21 R. de Levie and A.A. Husovsky, J. Electroanal. Chem., 20(1969)181.

Chapter 7. Concluding remarks

The properties of the various phase angle components were precisely analyzed for the purpose of the analyses of electron transfer reaction kinetics and for the chemical analysis of inorganic ions in aqueous medium.

In the ac polarography, the total alternating current through the electrochemical cell can be expressed by power series. In the reversible process, the first term of the power series, 1f mode, is a real first derivative form of dc polarogram and the second term, 2f mode, is also that of 1f mode. In the quasi-reversible and irreversible process, however, 1f and 2f modes do not show the real derivative forms of dc and 1f, respectively. Therefore, this method gives useful informations in assessing the reaction kinetics of electrochemical process.

In the electrochemical reduction of chromium(VI) in alkaline solution, a characteristic electrochemical spectrum was observed by 1f(45°) component of the first derivative polarography. The spectrum and rate constant for the electron transfer of various steps of oxidation state was determined by the curve fitting method. From the results of

the analysis, it was proved that the rate determining step was the reduction of chromium(VI) to chromium(IV) in the total reaction of chromium(VI) to chromium(III) and that the final electrode reaction products would be $Cr(OH)_2^+$.

In the zirconium(IV)-nitrate ion system, the dc polarographic data for the reduction of nitrate ion suggested the contribution of adsorbed zirconium(IV). The differential capacity measurement by using 1f(0°) and 1f(90°), however, showed no evidence of its adsorption on the electrode. The role of zirconium(IV) in the reduction of nitrate was discussed. It was reasonably suggested that on the vicinity of the electrode, the zirconium(IV) might act as an intermediary role for charge transfer from the electrode to the nitrate ion.

The 2f mode in the phase selective ac polarography was investigted throughly for the purpose of the establishment of non-linear electrochemical method for chemical analysis. A new technique was proposed in analyzing two species having similar redox potentials by utilizing the difference in the electron transfer rates between them. The theoretical interpretation of the principle of this technique was attempted and applied in this analysis. Actually, it was successfully proved that the 2f(45°) and 2f(0°) were valid for the analyses of indium(III) in the presence of excess of cadmium(II) and of zinc(II) in the presence of nickel(II),

respectively.

Kinetic mechanisms of the reduction of multivalent ions, CrO_4^{2-} and NO_3^- were studied by means of phase selective voltammetric techniques. These electrochemical methods were also applied to quantitative analyses.

The information involved in various phase angle components will be useful for studies on reaction mechanisms, for understanding of properties of chemical species, and even for chemical analyses.

Acknowledgement

The author wishes to express his greatest gratitude to Professor Shigero Ikeda for his kind suggestion and support in coordinating this work.

The author also would like to express his hearty gratitude to Dr. Iwao Watanabe for valuable discussions and accurate instruction.

The author is indebted to many members of Ikeda Laboratory for their helpful advice and assistance.

The author is sincerely grateful to many members in Department of Chemistry, Faculty of Education, Akita University, especially to Dr. Akira Nakamura and Prof. Shigeki Matsuo, for their help and encouragement.

Papers relevant to the present study

1) Analytical application of second-harmonic a.c. polarography
N. Ogawa, I. Watanabe and S. Ikeda
Anal. Chim. Acta, 141 (1982) 123.

2) An ac polarographic study on the electrochemical reduction of chromium(VI) in alkaline solution
N. Ogawa, I. Watanabe and S. Ikeda
J. Electroanal. Chem., 177 (1984) 191.

3) On the polarographic reduction of nitrate ion in the presence of zirconium(IV)
N. Ogawa, H. Kodaiku and S. Ikeda
J. Electroanal. Chem., in press.